Università degli Studi di Sassari
Dipartimento di Agraria
Corso di Dottorato in Scienze Agrarie
Curriculum
Monitoraggio e controllo degli ecosistemi agrari e forestali in ambiente mediterraneo
XXXI CICLO

Investigation on lateral saturated soil hydraulic conductivity evaluated at different spatial scales in a Mediterranean hillslope

Dott. Roberto Marrosu

Coordinatore del Corso	Prof. Ignazio Floris
Referente di Curriculum	Prof. Alberto Satta
Docente Guida	Dott. Mario Pirastru
Docenti Tutor	Prof. Marcello Niedda
	Dott. Mirko Castellini

ANNO ACCADEMICO 2017-2018

This dissertation is dedicated to Maria, who has encouraged me,
loved and believed in me during the many years
leading to this research dissertation.

Acknowledgments

This work would not have been possible without the dedication and support of numerous people.

First of all, I would like to thank my advisor Dott. Mario Pirastru and my tutor Dott. Mirko Castellini for the efforts that they have made to guide me during the doctoral studies.

My deep gratitude goes out to Prof. Marcello Niedda for giving me the opportunity to join the doctoral programme. *"You are gone but your belief in me has made this journey possible"*.

I especially would like to acknowledge Simone di Prima who spent many hours planning, digging and discussing site instrumentation, data analysis and data interpretation.

I also want to thank Ph.D. Ana Helena Dias Francesconi for her English teaching and precious advises.

A huge thanks goes out to my colleagues and friends Maria Grazia Farbo, Maria Teresa Tiloca, Angela Scanu, Elisa Campus and last, but not least, Giovanni Ragaglia for the support, endless patience and encouragements in this hard period. Each of them has left a mark in my life and for this I offer my very sincere gratitude to everyone. I wish them all the success, happiness, and joy in life.

Thesis index

List of figures

List of tables

Introduction

The present research work focuses mainly on the estimation of the lateral saturated soil hydraulic conductivity, $K_{s,l}$, and on the quantification of lateral saturated subsurface flow generated in a Mediterranean hillslope. The $K_{s,l}$ is the key property governing groundwater flow and the runoff generation process by saturation excess in steep shallow soils of watersheds. The most common initiation mechanism of lateral saturated subsurface flow (also known as subsurface stormflow) in a hillslope is the transient saturation of a vertical soil profile portion (Weiler et al., 2005). A perched water table originates from infiltrating rainwater that is hindered from deep downward percolation by a soil-bedrock interface or another layer of low permeability beneath the soil surface. Once the water table is formed, the water starts to flow laterally in direction to the toe of the slope. The spatial-temporal dynamics of the water table are mainly driven by the downslope water transfer velocities in the soil. The $K_{s,l}$, thus, is the soil hydraulic property that mostly determines the lateral transmission rates of this saturated subsurface flow. As a consequence, the knowledge of reliable values of $K_{s,l}$ is a prerequisite for properly interpreting the soil hydrological dynamics related to subsurface flow. Consistent determinations of $K_{s,l}$ are important in studies evaluating the contribution of the subsurface stormflow to the volume of runoff discharge, or the transport of labile nutrients and pollutants from hillslope to the streams, surface reservoirs and aquifers (McGlynn and McDonnell, 2003; Tsuboyama et al., 1994; Zegre, 2003). Furthermore, subsurface flow is also reported as able to establish a positive pore water pressure in steep hillside (Montgomery and Dietrich, 2002; Schneider et al., 2014; Uchida et al., 2002, 2001, 1999; Wu and Sidle, 1995), which in turn can be a potential hydrological trigger for shallow landslides (Iverson, 2000; Montgomery et al., 1997; Schneider et al., 2014; Van Asch et al., 1999; Weiler et al., 2005). As these processes are intimately linked to the subsurface water flow velocities in the saturated soil, adequately $K_{s,l}$ characterizing is of great interest in hillslope hydrology.

Investigations on $K_{s,l}$ and on the lateral saturated subsurface flow process in general, have been undertaken mostly in watersheds of humid regions with steep slopes and shallow and conductive soils, where the subsurface flow often is acknowledged as the main mechanism of storm runoff production occurring on hillslopes. Conversely, in arid and semiarid regions this

process has received little attention, although recent studies have suggested that it plays a key role on hillslope hydrology even in these areas, including the Mediterranean ones (Maneta et al., 2008; Pirastru et al., 2014; van Schaik et al., 2014; Niedda et al., 2014). This was probably because in these environments lateral subsurface flow has traditionally been considered less important than surface hydrologic processes, since it is thought to occur only under certain extreme conditions (high rainfall depth and/or high antecedent soil moisture). Another reason is that measuring runoff in semiarid regions, compared to the humid temperate areas, faces more formidable challenges due to the particular climate features. In the former regions, in fact, the runoff producing events are rare and short-term; accordingly, time required for effectively characterizing runoff is relatively long-lasting, and occasions to make up for flawed monitoring strategy or equipment failures might be few and far between.

The $K_{s,l}$ is the most important parameter in many numerical models that simulate water flow processes both at hillslope and catchment scales (Dusek and Vogel, 2016; Hilberts et al., 2005). That models are used both for testing hydrological theories and for practical applications, such as assessing the effects of land-use or climate change scenarios on catchment hydrology. Successful numerical simulations require a good representation of the main processes affecting the dynamics of the hydrological system as well as reliable value estimates of model parameters. The $K_{s,l}$, as also pointed out by Flanagan and Nearing (1991), is generally one of the most sensitive parameters in predicting runoff. For this reason, efforts should be directed towards a proper identification of this soil property value. Despite the fact that a number of methods are available for estimating the $K_{s,l}$ in field and in laboratory, a common practice among modellers is to calibrate the parameter value without attempts to experimentally estimate it. The main reason is that it is difficult to obtain representative values of $K_{s,l}$ for large spatial scales (e.g., hillslope scale), which are generally those of practical interest for distributed model applications, due to the high spatial variability that the saturated hydraulic conductivity exhibits (Warrick, 1998). Because of this variability, the experimental estimate of the soil $K_{s,l}$ can vary over several orders of magnitude depending on the sampled soil volume in the individual measurement (Chapuis et al., 2005). For instance, Vepraskas and Williams (1995) compared hydraulic conductivities measured on three different kinds of sample that differed in volume, namely undisturbed detached cores (3.5×10^{-4} m^3), in situ columns (6.3×10^{-3} m^3), and in situ drain fields (6.8×10^{-1} m^3) and

found that mean conductivity increased by about one order of magnitude passing from the small soil cores to the columns. However, $K_{s,l}$ values obtained from the drain measurements did not significantly differ from the column ones. Chappell and Lancaster (2007) determined $K_{s,l}$ applying six field methods (i.e., slug test, constant- and falling-head borehole permeameter, ring permeameter, and two types of trench tests). The large-scale $K_{s,l}$ values determined by the trench percolation tests were, on average, 37 times larger than the conductivity values obtained by slug tests made in wells placed near the trenches. The large-scale influence of soil structure, macropore flow and soil heterogeneity, were considered the main factors leading to these $K_{s,l}$ discrepancies. In fact, when great soil volumes are investigated a number of short and initially discontinuous preferential flow features (macropores, cracks, soil pipes, and root channels) are included in the soil sample. When the soil is then saturated, the soil matrix provides the connection between these discrete preferential features, organizing them into a more complex network (Anderson et al., 2008; Sidle et al., 2001). Such circumstance promotes fast lateral transfer of water and, consequently, high $K_{s,l}$ values are determined through these measurements. Conversely, in investigations performed on small volume soil samples such complex mechanism of macropore network activation may not become completely effective and, therefore, $K_{s,l}$ values lower than those detected in large sized soil samples are generally found. This suggests possible limitations in the usability of $K_{s,l}$ determinations from small-size core-based laboratory methods and near-point field infiltrometric techniques to characterize large hydrological units such as the hillslopes. For the same reasons, model users should be cautious when using $K_{s,l}$ values measured in small soil samples without properly evaluating its representativeness for large-scale modelling (Pachepsky et al., 2014). For example, Grayson et al. (1992) found that the base flow coming out of the Wagga Wagga catchment in New South Wales could be most accurately simulated by the THALES model by using an average $K_{s,l}$ 10 times larger than the average measurement made with a disc permeameter. Wigmosta et al. (1994) found that the ‘‘effective’’ lateral $K_{s,l}$ determined by calibrating the DHSVM model on the Middle Fork Flathead River basin in north-western Montana was 100 times the vertical soil conductivity estimated from pedo-transfer functions. Vertessy et al. (1993) demonstrated that the TOPOG_Yield was not able to accurately simulate streamflow without using a lateral $K_{s,l}$ value roughly 10 times larger than the mean vertical K_s measured using

constant-head well permeameter. Once again, these discrepancies were attributed to the large-scale effects of macropore flow, which were not considered in the small-scale measurements. However, as Sherlock et al. (2000) suggested, calibrated $K_{s,l}$ values greater than the small-scale derived ones might also depend on compensations for the uncertainty of other calibrated hydrologic parameters in the model or could be linked to offsetting effects due to the simplified conceptual structure of the model. This indicates the need for identifying the most representative $K_{s,l}$ value of the soil through appropriate experimental methods. The scale of measurement should be comparable with the spatial discretization scale of the model, usually from tens to hundreds of meters of grid spatial resolution. Moreover, in order to elucidate scale-effects affecting the $K_{s,l}$ determination in hillslope soils, measurement techniques and strategies operating over a wide range of spatial scales have to be developed or improved.

Experiments that seem to have a great potential for properly characterizing the hydrologic properties of large (square meters) to very large areas (tens of square meters) consist of excavating open trenches or installing drains to collect and measure the saturated subsurface flow moving above a confining layer in a hillslope. The reason is that the intercepted outflow integrates the hydrological response of the hillslope soil, which mostly depends on the flow through soil macropores (Beven and Germann, 2013; Chappell, 2010). On the other hand, these methodologies are too costly, time-consuming and difficult to conduct, thus remaining rare in literature. Whipkey (1965) measured hillslope-scale lateral flow and calculated $K_{s,l}$ by a trench experiment in an isolated hillslope. The $K_{s,l}$ for the saturated soil was determined by using Darcy's law with reference to transient wetted cross-sectional area, the length of the saturated area, and the changes in hydraulic head over the entire saturated length. Similarly, Montgomery and Dietrich (1995) estimated the large-scale lateral $K_{s,l}$ based on the discharge from a gully cut which showed evidence of macropore flow. The authors observed that these determinations were comparable with the greatest conductivity obtained by falling-head tests in piezometers. Brooks et al. (2004) estimated the hillslope-scale $K_{s,l}$ as a function of the water table depth below the soil surface using drainage measurements performed on a 18-m wide isolated sloped land, reporting a hillslope-scale $K_{s,l}$ values 3.2–13.7 times greater than the available small-scale measurements.

Another possible way to determine representative $K_{s,l}$ for large areas is to perform drainage experiments in large-volume soil blocks (or monoliths) encased in situ with

impermeable material. For example, Day et al. (1998), who measured lateral water flow on a 3.38 m^3 soil block, sealed the vertical faces of the block using bentonite, sand, and lumber. Field procedures for evaluating the $K_{s,l}$ in large soil samples are also reported by Blanco-Canqui et al. (2002) and Mendoza and Steenhuis (2002). The latter developed and tested a device called "hillslope infiltrometer" by which the lateral drainage from each horizon of a layered soil was collected, and the specific lateral $K_{s,l}$ values of the soil horizons computed. Due to the increased exploited soil volume in the experimental approaches of Day et al.(1998), Blanco-Canqui et al. (2002) and Mendoza and Steenhuis (2002), an improved representation of the effects of soil heterogeneities compared with other near-point measurements would be expected. However, so far, only few cases of comparative analyses between $K_{s,l}$ measurements performed in small soil samples (near-point spatial scale) and those conducted in large volume soil blocks (plot scale) have been shown in literature (Blanco-Canqui et al., 2002). Furthermore, no comparative assessments of the $K_{s,l}$ determined at the plot scale and at the hillslope scale have been accomplished. Performing such comparisons could increase confidence in the measurements carried out by soil monolith approaches, like those of Day et al.(1998), Blanco-Canqui et al. (2002) and Mendoza and Steenhuis (2002), when these are used for large-scale applications.

2. Objectives and thesis outline

The main goal of the dissertation research was to investigate the changes of the lateral saturated soil hydraulic conductivity value estimations as a function of soil volume sampled with a given measurement technique. Indeed, different methods for the $K_{s,l}$ determination often yield substantially different $K_{s,l}$ values because this soil property is extremely sensitive to the sample size owing to heterogeneities of physical and hydrological soil characteristics. Comparing methodologically similar techniques, but dissimilar in involved measurement spatial scales, allows to better establish the usability of a given method for interpreting or modelling hydrological processes with reference to a specific scale of interest. By applying several methods involving diverse observational scales, the Ph.D. research is mainly aimed at gathering reliable $K_{s,l}$ estimates that are representative for the hillslope scale. Moreover, efforts are devoted to assessing the influence of the spatial scale of investigation on $K_{s,l}$ determinations at different soil depths. In fact, as reported by Ameli et al. (2016), the

knowledge of representative $K_{s,l}$ along the soil profile is an essential pre-requisite to consistently simulate the spatio-temporal hydrological dynamics in soils.

The dissertation is structured in four chapters, three of them report research works published in international peer-reviewed journals.

Chapter 1 contains the manuscript titled "Subsurface flow and large-scale lateral saturated soil hydraulic conductivity in a Mediterranean hillslope with contrasting land uses", which was published in *Journal of Hydrology and Hydromechanics* in 2017. The paper focuses on the lateral subsurface flow process characterization in two contiguous areas of a hillslope. An area was covered with natural maquis, the other one with grass. A continuous monitoring of the lateral saturated subsurface flow, collected at the footslope by drains, and of the water table levels, recorded in wells, was performed for two years. The investigation was mostly undertaken under natural rainfall regime, but also artificial rainfall experiments were carried out. Following the methodology introduced by Whipkey (1965) and Brooks et al. (2004) the hydrological data were used for computing $K_{s,l}$ values along the saturated soil profile. These values were considered representative for the large hillslope spatial scale, because the measured outflow by drains integrated the heterogeneous hydrological response of the hillslope soil. The specific objective of the research was to investigate the dependence of subsurface flow response from the soil use and to determine hillslope scale $K_{s,l}$ values of the two sampled areas.

Chapter 2 reports the paper entitled "Lateral saturated hydraulic conductivity of soil horizons evaluated in large-volume soil monoliths" that was published in *Water* in 2017. The manuscript explores the suitability of drainage experiments performed on large volume soil monoliths to determine representative $K_{s,l}$ values for macroporous steep soils. The monoliths had an average soil volume of 0.12 m³, thus the sampled soil sizes were larger than the commonly sampled sizes by laboratory and field techniques, but smaller when compared to large scale, controlled drain experiments. The study aimed to refine a field technique to determine spatially representative $K_{s,l}$ values of each soil horizon in the experimental hillslope. Specific objectives were: i) to investigate the $K_{s,l}$ variability along soil profile, and ii) to evaluate spatial representativeness of $K_{s,l}$ determined on monoliths at the studied site.

Chapter 3 reports the paper titled "In situ characterization of preferential flow by combining plot- and point-scale infiltration experiments on a hillslope", published in

Journal of Hydrology in 2018. The paper proposes a new experimental approach to determine reliable parameters describing the hydraulic properties of the soil in both matrix and preferential flow (or fast-flow) regions. For this purpose, it was considered the dual permeability approach (i.e., the concomitance of fast- and matrix- flow in soils) and was computed $K_{s,l}$ parameters for both flow regions. That was by coupling data from two kinds of infiltration experiments performed at the near-point (Beerkan method and modified cube method) and at plot spatial scale ($K_{s,l}$ measures by the soil monolith method). The aim was to quantify the related contribution of the soil matrix and of the macropore network to the total lateral saturated subsurface flow.

Chapter 4 provides a comprehensive comparison of all the $K_{s,l}$ determinations obtained at different spatial scales by each methodology employed during the research work. The objective was to identify scale dependency relations of $K_{s,l}$ as a function of the soil volume sampled by the applied measurement techniques. Moreover, in this part insights are given about the technique for attaining, with the most sustainable experimental effort, representative $K_{s,l}$ for the hillslope scale. Finally, concluding remarks of the dissertation research are outlined.

3. References

Ameli, A.A., Amvrosiadi, N., Grabs, T., Laudon, H., Creed, I.F., McDonnell, J.J., Bishop, K., 2016. Hillslope permeability architecture controls on subsurface transit time distribution and flow paths. Journal of Hydrology 543, 17–30. https://doi.org/10.1016/j.jhydrol.2016.04.071

Anderson, A.E., Weiler, M., Alila, Y., Hudson, R.O., 2008. Dye staining and excavation of a lateral preferential flow network. Hydrology and Earth System Sciences Discussions, European Geosciences Union 5, 1043-1065.

Beven, K., Germann, P., 2013. Macropores and water flow in soils revisited. Water Resources Research 49, 3071–3092. https://doi.org/10.1002/wrcr.20156

Blanco-Canqui, H., Gantzer, C.J., Anderson, S.H., Alberts, E.E., Ghidey, F., 2002. Saturated Hydraulic Conductivity and Its Impact on Simulated Runoff for Claypan Soils. Soil Science Society of America Journal 66, 1596–1062. https://doi.org/10.2136/sssaj2002.1596

Brooks, E.S., Boll, J., McDaniel, P.A., 2004. A hillslope-scale experiment to measure lateral saturated hydraulic conductivity. Water Resour. Res. 40, W04208. https://doi.org/10.1029/2003WR002858

Chappell, N.A., 2010. Soil pipe distribution and hydrological functioning within the humid tropics: a synthesis. Hydrological processes 24, 1567–1581.

Chappell, N.A., Lancaster, J.W., 2007. Comparison of methodological uncertainties within permeability measurements. Hydrological Processes 21, 2504–2514. https://doi.org/10.1002/hyp.6416

Chapuis, R.P., Dallaire, V., Marcotte, D., Chouteau, M., Acevedo, N., Gagnon, F., 2005. Evaluating the hydraulic conductivity at three different scales within an unconfined sand aquifer at Lachenaie, Quebec. Canadian Geotechnical Journal 42, 1212–1220.

Day, R.L., Calmon, M.A., Stiteler, J.M., Jabro, J.D., Cunningham, R.L., 1998. Water balance and flow patterns in a fragipan using in situ soil block. Soil science 163, 517–528.

Dusek, J., Vogel, T., 2016. Hillslope-storage and rainfall-amount thresholds as controls of preferential stormflow. Journal of Hydrology 534, 590–605. https://doi.org/10.1016/j.jhydrol.2016.01.047

Flanagan, D., Nearing, M., 1991. Sensitivity analysis of the WEPP hillslope profile model. Am. Soc. Agric. Eng. Paper.

Grayson, R.B., Moore, I.D., McMahon, T.A., 1992. Physically based hydrologic modeling: 1. A terrain-based model for investigative purposes. Water Resources Research 28, 2639–2658. https://doi.org/10.1029/92WR01258

Hilberts, A.G.J., Troch, P.A., Paniconi, C., 2005. Storage-dependent drainable porosity for complex hillslopes. Water Resources Research 41:W06001. https://doi.org/10.1029/2004WR003725

Iverson, R., M., 2000. Landslide triggering by rain infiltration. Water Resour. Res. 36, 1897–1910. https://doi.org/10.1029/2000WR900090

Maneta, M., Schnabel, S., Jetten, V., 2008. Continuous spatially distributed simulation of surface and subsurface hydrological processes in a small semiarid catchment. Hydrological Processes 22, 2196–2214. https://doi.org/10.1002/hyp.6817

McGlynn, B.L., McDonnell, J.J., 2003. Role of discrete landscape units in controlling catchment dissolved organic carbon dynamics. Water Resources Research 39. https://doi.org/10.1029/2002WR001525

Mendoza, G., Steenhuis, T.S., 2002. Determination of hydraulic behavior of hillsides with a hillslope infiltrometer. Soil Science Society of America Journal 66, 1501–1504.

Montgomery, D.R., Dietrich, W.E., 2002. Runoff generation in a steep, soil-mantled landscape. Water Resources Research 38(9), 1168. https://doi.org/10.1029/2001WR000822

Montgomery, D.R., Dietrich, W.E., 1995. Hydrologic Processes in a Low-Gradient Source Area. Water Resources Research 31, 1–10. https://doi.org/10.1029/94WR02270

Montgomery, D.R., Dietrich, W.E., Torres, R., Anderson, S.P., Heffner, J.T., Loague, K., 1997. Hydrologic response of a steep, unchanneled valley to natural and applied rainfall. Water Resources Research 33, 91–109. https://doi.org/10.1029/96WR02985

Niedda, M., Pirastru, M., Castellini, M., Giadrossich, F., 2014. Simulating the hydrological response of a closed catchment-lake system to recent climate and land-use changes in semi-arid Mediterranean environment. Journal of Hydrology 517, 732–745. https://doi.org/10.1016/j.jhydrol.2014.06.008

Pachepsky, Y.A., Guber, A.K., Yakirevich, A.M., McKee, L., Cady, R.E., Nicholson, T.J., 2014. Scaling and Pedotransfer in Numerical Simulations of Flow and Transport in Soils. Vadose Zone Journal 13. https://doi.org/10.2136/vzj2014.02.0020

Pirastru, M., Niedda, M., Castellini, M., 2014. Effects of maquis clearing on the properties of the soil and on the near-surface hydrological processes in a semi-arid Mediterranean environment. Journal of Agricultural Engineering 45, 176–187. https://doi.org/10.4081/jae.2014.428

Schneider, P., Pool, S., Strouhal, L., Seibert, J., 2014. True colors–experimental identification of hydrological processes at a hillslope prone to slide. Hydrology and Earth System Sciences 18, 875–892. https://doi.org/10.5194/hess-18-875-2014

Sherlock, M.D., Chappell, N.A., McDonnell, J.J., 2000. Effects of experimental uncertainty on the calculation of hillslope flow paths. Hydrological Processes 14, 2457–2471.

Sidle, R.C., Noguchi, S., Tsuboyama, Y., Laursen, K., 2001. A conceptual model of preferential flow systems in forested hillslopes: evidence of self-organization. Hydrological Processes 15, 1675–1692. https://doi.org/10.1002/hyp.233

Tsuboyama, Y., Sidle, R.C., Noguchi, S., Hosoda, I., 1994. Flow and solute transport through the soil matrix and macropores of a hillslope segment. Water Resources Research 30, 879–890. https://doi.org/10.1029/93WR03245

Uchida, T., Kosugi, K., Mizuyama, T., 2002. Effects of pipe flow and bedrock groundwater on runoff generation in a steep headwater catchment in Ashiu, central Japan. Water Resources Research 38. https://doi.org/10.1029/2001WR000261

Uchida, T., Kosugi, K., Mizuyama, T., 2001. Effects of pipeflow on hydrological process and its relation to landslide: a review of pipeflow studies in forested headwater catchments. Hydrological Processes 15, 2151–2174. https://doi.org/10.1002/hyp.281

Uchida, T., Kosugi, K., Mizuyama, T., 1999. Runoff characteristics of pipeflow and effects of pipeflow on rainfall-runoff phenomena in a mountainous watershed. Journal of Hydrology 222, 18–36. https://doi.org/10.1016/S0022-1694(99)00090-6

Van Asch, T.W.J., Buma, J., Van Beek, L.P.., 1999. A view on some hydrological triggering systems in landslides. https://doi.org/10.1016/S0169-555X(99)00042-2

van Schaik, N.L.M.B., Bronstert, A., Jong, S.M. de, Jetten, V.G., Dam, J.C. van, Ritsema, C.J., Schnabel, S., 2014. Process-based modelling of a headwater catchment in a semi-arid area: the influence of macropore flow. Hydrological Processes 28, 5805–5816. https://doi.org/10.1002/hyp.10086

Vepraskas, M.J., Williams, J.P., 1995. Hydraulic Conductivity of Saprolite as a Function of Sample Dimensions and Measurement Technique. Soil Science Society of America Journal 59, 975–981. https://doi.org/10.2136/sssaj1995.03615995005900040003x

Vertessy, R.A., Hatton, T.J., O'Shaughnessy, P.J., Jayasuriya, M.D.A., 1993. Predicting water yield from a mountain ash forest catchment using a terrain analysis based catchment model. Journal of Hydrology 150, 665–700. https://doi.org/10.1016/0022-1694(93)90131-r

Warrick, A.W., 1998. Spatial variability. In: D. Hillel, Editor. Environmental Soil Physics, San Diego: Academic Press, 655–675

Weiler, M., McDonnell, J.J., Meerveld, I.T., Uchida, T., 2005. Subsurface Stormflow, in: Encyclopedia of Hydrological Sciences. American Cancer Society. https://doi.org/10.1002/0470848944.hsa119

Whipkey, R.Z., 1965. Subsurface stormflow from forested slopes. Hydrological Sciences Journal 10, 74–85.

Wigmosta, M.S., Vail, L.W., Lettenmaier, D.P., 1994. A distributed hydrology-vegetation model for complex terrain. Water Resources Research 30, 1665–1679. https://doi.org/10.1029/94WR00436

Wu, W., Sidle, R.C., 1995. A Distributed Slope Stability Model for Steep Forested Basins. Water Resources Research 31, 2097–2110. https://doi.org/10.1029/95WR01136

Zegre, N.P., 2003. The hillslope hydrology of a mountain pasture: The influence of subsurface flow on nitrate and ammonium transport. Virginia Polytechnic Institute and State University.

CHAPTER 1

Subsurface flow and large-scale lateral saturated soil hydraulic conductivity in a Mediterranean hillslope with contrasting land uses

Mario Pirastru[1], Vincenzo Bagarello[2], Massimo Iovino[2], Roberto Marrosu[1], Mirko Castellini[3], Filippo Giadrossich[1], Marcello Niedda[1]

[1] Dipartimento di Agraria, Università degli Studi di Sassari, Viale Italia 39, 07100, Sassari, Italy
[2] Dipartimento di Scienze Agrarie e Forestali, Università degli Studi di Palermo, Viale delle Scienze, 90128, Palermo, Italy
[3] Consiglio per la ricerca in agricoltura e l'analisi dell'economia agraria – Unita di ricerca per i sistemi colturali degli ambienti caldo-aridi (CREA–SCA), Via Celso Ulpiani 5, 70125, Bari, Italy

Published in: *J. Hydrol. Hydromech., 2017, 65(3), 297-306.*

https://doi.org/10.1515/johh-2017-0006

Abstract. The lateral saturated hydraulic conductivity, $K_{s,l}$, is the soil property that mostly governs subsurface flow in hillslopes. Determinations of $K_{s,l}$ at the hillslope scale are expected to yield valuable information for interpreting and modeling hydrological processes since soil heterogeneities are functionally averaged in this case. However, these data are rare since the experiments are quite difficult and costly. In this investigation, that was carried out in Sardinia (Italy), large-scale determinations of $K_{s,l}$ were done in two adjacent hillslopes covered by a Mediterranean maquis and grass, respectively, with the following objectives: i) to evaluate the effect of land use change on $K_{s,l}$, and ii) to compare estimates of $K_{s,l}$ obtained under natural and artificial rainfall conditions. Higher $K_{s,l}$ values were obtained under the maquis than in the grassed soil since the soil macropore network was better connected in the maquis soil. The lateral conductivity increased sharply close to the soil surface. The sharp increase of $K_{s,l}$ started at a larger depth for the maquis soil than the grassed one. The $K_{s,l}$ values estimated during artificial rainfall experiments agreed with those obtained during the natural rainfall periods. For the grassed site, it was possible to detect a stabilization of $K_{s,l}$ in the upper soil layer, suggesting that flow transport capacity of the soil pore system did not increase indefinitely. This study highlighted the importance of the experimental determination of $K_{s,l}$ at the hillslope scale for subsurface modeling, and also as a benchmark for developing appropriate sampling methodologies based on near-point estimation of $K_{s,l}$.

Keywords: subsurface runoff, drain, pore connectivity, sprinkling experiments, land use change, maquis.

1. Introduction

Lateral saturated subsurface flow is the dominating runoff generation mechanism in most hillslopes or catchments of the humid temperate climates (Weiler et al., 2005) but it also occurs in many semiarid regions (Newman et al., 1998; Niedda and Pirastru, 2013; Van Schaik et al., 2008).

The most suitable approach for studying the mechanisms that govern the subsurface response of vegetated hillslopes consists of excavating open trenches or installing drains to intercept and measure directly the saturated subsurface flow moving above an impeding layer. The reason is that the measured outflow integrates the heterogeneous hydrological response of the soil in the hillslope, which can be governed by flow through the spatially and temporally variable soil macropores (Beven and Germann, 2013; Chappel, 2010). The primary role of the macropores in determining timing, peak and volume of the generated subsurface flow has been demonstrated in different large-scale investigations, that were primarily carried out in humid or temperate climates (Anderson et al., 2009; Dusek et al., 2012; Jost et al., 2012; Uchida et al., 2004). For example, Anderson et al. (2009) found that the hydraulic connectivity of the preferential flow network at the hillslope scale was an important factor governing subsurface flow, and they were able to determine relationships between lateral flow, hillslope length and various storm indicators. Uchida et al. (2004) found that hillslope discharge during storms was mainly due to macropore flow, which was strongly related to the cross-sectional area of the upslope saturated layer.

In semi-arid regions, subsurface processes have traditionally been considered less important than surface flow for discharge production. However, models which explicitly simulate lateral saturated subsurface flow in hillslopes (Maneta et al., 2008; Niedda and Pirastru, 2015; Van Schaik et al., 2014) suggest that subsurface flow plays a key role on catchment-scale hydrology even in semi-arid regions. In any case, little information is still available about the dominant mechanism of subsurface flow generation in many semiarid environments, including the Mediterranean ones. For these regions, there is the need to sample subsurface flow in natural hillslopes and to establish sources of spatial and temporal variability.

The lateral saturated hydraulic conductivity, $K_{s,l}$, is the soil property that mostly governs

lateral water transport in hillslopes and it is a key parameter in many numerical models that simulate hydrological processes both at the hillslope (Dusek and Vogel, 2016; Hillbert et al., 2005) and catchment (Maneta et al., 2008; Matonse and Kroll, 2013; Niedda et al., 2014) scales. For example, $K_{s,l}$ has to be known to estimate soil erosion with the modified Morgan-Morgan-Finney model by Morgan and Duzant (2008). The $K_{s,l}$ data used for modeling purposes should be determined in agreement with the considered flow direction. In fact, anisotropy can determine saturated conductivity differing, even greatly (four orders of magnitude or more), with the considered direction (e.g., Bathke and Cassel, 1991; Beckwith et al., 2003; Bouma and Dekker, 1981; Dabney and Selim, 1987). This circumstance is relevant for interpreting soil hydrological processes (Montgomery and Dietrich, 1995).

A variety of approaches can be found in the literature to determine $K_{s,l}$. For example, approximate criteria, based on soil textural characteristics alone (e.g., $K_{s,l}$ = 2100 mm h^{-1} for a sandy loam soil according to Morgan and Duzant, 2008), can be used. However, these values should be used with caution, being unverified. Various experimental techniques have been applied for small-scale estimates of $K_{s,l}$. These techniques include constant- and falling-head borehole permeameter techniques specifically developed for radial flow (Reynolds, 2010; 2011) and measurements on soil monoliths (Baxter et al., 2003; Blanco-Canqui et al., 2002; Chappell and Lancaster, 2007). Other methodologies have been developed with the specific objective to sample large to very large (dozens of m^2) areas, but only a few investigations of such a type can be found in the literature (Brooks et al., 2004; Chappell and Lancaster, 2007; Montgomery and Dietrich, 1995). The $K_{s,l}$ determinations obtained with large-scale experiments can be expected to allow an improved representation of heterogeneity effects on the hillslope hydrological response as compared with near-point measurements. The scarcity of large-scale investigations is due to the fact that the experiments are expensive and difficult to conduct. Brooks et al. (2004) determined the hillslope-scale $K_{s,l}$ as a function of the water table depth below the soil surface using drainage measurements performed on a 18 m wide isolated sloped land. These authors found that $K_{s,l}$ increased abruptly near the surface, due to the activation of flow in the near-surface macropores of biological origin. The reported hillslope-scale estimation of $K_{s,l}$ was 3.2–13.7 times greater than the available small-scale measurements. Montgomery and Dietrich (1995) estimated the large scale $K_{s,l}$ based on the discharge from a gully cut which showed evidence of macropore flow. Their determinations

were comparable with the greatest conductivity obtained by falling-head tests in piezometers. Chappell and Lancaster (2007) applied six field methods (i.e., slug test, constant- and falling-head borehole permeameter, ring permeameter, as well as two types of trench tests) to determine $K_{s,l}$. The large-scale $K_{s,l}$ values determined by the trench percolation tests were, on average, 37 times larger than the mean conductivity obtained by slug tests made in piezometers adjacent to the trenches.

Greater values of $K_{s,l}$, even by several orders of magnitude as compared with those determined at the point-scale, can be found when hydrological models are calibrated using the observed hydrologic response of the catchment (Blain and Milly, 1991; Chappell et al., 1998; Grayson et al., 1992). These discrepancies were generally attributed to the large-scale effects of macropore flow. However, Sherlock et al. (2000) also suggested that the differences between the measured and calibrated hydraulic conductivities could be linked to offsetting effects of the conceptual simplifications of the applied hydrological model, as well as to error effects of the other parameters involved.

In summary, our experimental knowledge of lateral subsurface flow processes in semi-arid environments is still incomplete notwithstanding that there are signs that these processes can be relevant even in these environments. Large-scale experiments are rare in general although they represent an efficient way to obtain directional soil hydraulic properties functionally averaging local heterogeneities.

This study focuses on the lateral subsurface flow processes in a hillslope with a different vegetation cover in the semiarid Mediterranean climate. A continuous monitoring of the lateral saturated subsurface flow and of the water table levels was carried out for two years in two contiguous areas, one covered with natural maquis and the other covered with grass established after the maquis clearing. The specific objective was to determine the subsurface flow response and the lateral saturated soil hydraulic conductivity of the two sampled hillslopes under both natural and artificial rainfall.

2. Material and Methods

2.1. Site description

The study was performed in the Baratz Lake catchment (Giadrossich et al. 2015; Niedda et al., 2014; Pirastru and Niedda, 2013), in North-West Sardinia, Italy. The climate is semiarid Mediterranean, with a mild winter, a warm summer and a high water deficit between April and September. The mean annual temperature is 15.8 °C and the mean relative humidity is 78.7%. The minimum and maximum mean daily temperatures are 3 °C and 29 °C, respectively. The average annual precipitation is about 600 mm, and this falls almost all from autumn to spring. The potential evapotranspiration is around 1000 mm year^{-1}.

The experimental area was on the steep side of a hill (Figure 1.1). It has a mean elevation of 63 m a.s.l. and it is about 60 m long. The sloped surface is roughly planar, faces north and has a mean gradient of 30%. In the upper part, the incoming overland and subsurface flows are diverted by the ditches alongside a road. At the foot, the hillslope is drained by the incised stream of the main river of the catchment area.

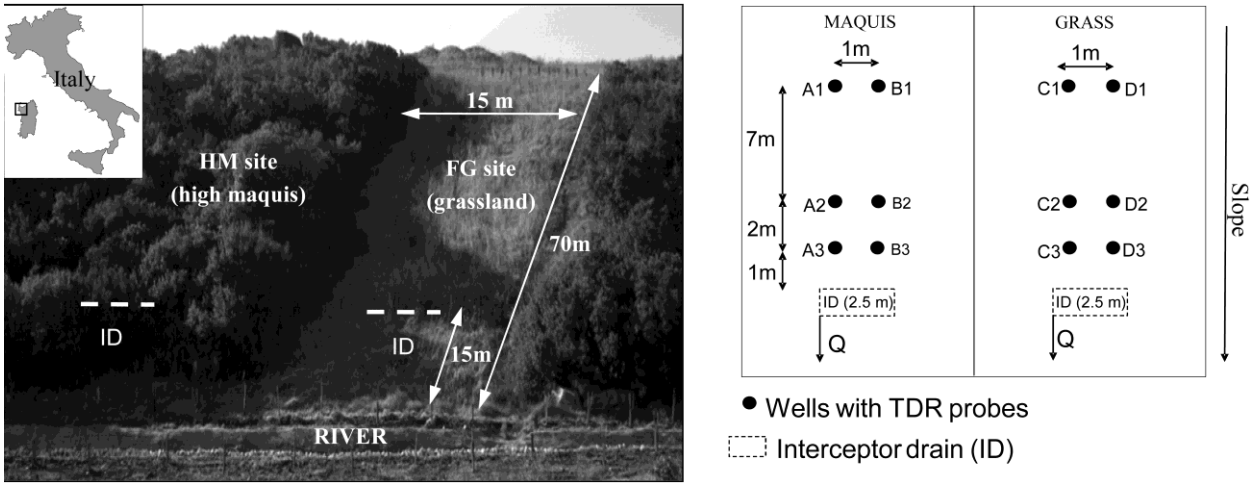

Fig. 1.1. View of the experimental hillslope, with location of the interceptor drains (ID) and spatial disposition of the piezometers at the FG and HM sites. The setup is not to scale.

Two adjacent sites in the hillslope were selected for the research. One site is covered with a well-developed Mediterranean maquis (hereafter named HM site). It consists of a very dense growth of evergreen trees and shrubs with a height of 2–4 m composed by

Myrtus Communis L., *Arbutus unedo L.*, *Erica arborea L.*, *Phillirea latifolia L.* and *Pistacia lentiscus L.* A litter at least 10 cm thick overlies the mineral soil at this site.

The other site is an unmanaged area covered with spontaneous grass (hereafter named FG site). This area developed about 15 years ago, after maquis clearing and mouldboard ploughing to create a 15 m wide firebreak.

The soil in the hillslope is Lithic Haploxerepts. It is about 0.4–0.5 m deep and overlies a grayish, altered substratum of Permian sandstone, which is very dense. This impeding layer limits deep water percolation. The soil texture is sandy-loam according to the USDA standards.

Field observations at the sites indicate that macropores due to grass or tree roots and animal burrows are mainly present near the surface. Detailed information about the hydraulic characteristics of the soils in the HM and FG sites are reported in Castellini et al. (2016) and Pirastru et al. (2014).

2.2. Measurement of lateral subsurface flow

Continuous hydro-meteorological data were collected at the experimental site from January 2014 to December 2015. The gross rainfall was measured every 5 minutes by a tipping bucket rain gauge (0.2 mm of resolution) in an automatic weather station 500 m away from the studied hillslope. The lateral saturated subsurface flow above the impeding layer was collected by two 2.5 m long French drains that were installed 15 m from the slope foot, as shown in Figure 1.1. At the FG site, the drain was installed centrally to the grassed area, and at the HM site it was about 10 m far from the lateral maquis border. Outflow from each drain was routed in a plastic box which outlet is a 60° V-notch weir. The water head over the V-notch was measured by a stand-alone pressure transducer every 5 minutes, and related with the flow rate by the weir formula. The outgoing flow from the box dropped into an automated tipping bucket (about $2 \cdot 10^{-3}$ l/tip), thus providing a more accurate measure of the flow rate when this was smaller than 0.4 l min^{-1}.

Twelve piezometers were hand-drilled until the impeding layer was reached (Figure 1.1). On each hillslope, six wells were grouped in two adjacent transects positioned upslope and perpendicular to the drain. Within a transect, three wells were spaced at a distance of 1, 3 and 10 m from the drain. As a convention, the transects were denoted by the letters from A to D

and the wells in each transect were progressively numbered from the top to the bottom (Figure 1.1). Each well had a diameter of 80 mm and it was screened by 0.3 m above the top of the impeding layer. The depth of the soil, as documented when drilling the wells, ranged from 0.35 to 0.45 m at the FG site, and from 0.38 to 0.44 m at the HM site. The wells were equipped with automated TDR probes (Campbell Scientific Inc. CS216 Water Content Reflectometers, two-rod model, 0.3 m rod-length and 32 mm spacing), standing vertically in the wells, whose output was recorded every 5 minutes. As the probe rods were short compared to the soil thickness, they were periodically moved up or down in the wells to maintain them always partially submerged. The relationship between the TDR output and the percentage of rod submergence was calibrated in the laboratory. This relationship, with the reference depth of the probe, was used to determine water table depths. These data were validated through manual measurements of water table depths collected in the field during site visits. The mean absolute error between the values of water level estimated by the calibrated TDR output and those measured manually in the field was less than 1 cm, and this error was considered negligible for the purposes of the investigation.

On April 2014, artificial rainfall was applied once at the FG site and twice at the HM site. In each site, a network of irrigation sprinklers was arranged in an area about 12 m long and 8 m large, located immediately upslope of the interceptor drain and including all the monitoring wells. At the HM site, irrigation water was applied below the trees to exclude interception by tree canopy.

In this site, a steady rainfall of 40 mm h^{-1} was applied for about 2.75 h on April 1. This irrigation was mainly made with the aim of increasing the soil moisture of the irrigated plot to a level comparable to that observed at the FG site. Two days after, a steady rainfall of 60 mm h^{-1} was applied for 2.7 hours at both the FG and HM sites.

2.3. Estimation of the lateral saturated soil hydraulic conductivity

The observed groundwater levels and the drained subsurface flow were used to estimate the lateral saturated soil hydraulic conductivity, $K_{s,l}$ [L T^{-1}], according to Childs (1971) and Brooks et al. (2004). In particular, Childs (1971) presented a solution to groundwater flow to a transverse ditch or tile line over a sloping impermeable bed. Brooks et al. (2004) applied the Childs (1971) solution to compute $K_{s,l}$ at an isolated sloping plot 35 m long and 18 m wide.

Assuming that the groundwater flow lines are parallel to the bed, following the Dupuit-Forchheimer approximation, flow of water per unit width of the drain, q [L^2T^{-1}], can be modelled by means of the Darcy's law:

$$q = -K_{s,l}T\left(\frac{dZ}{ds}\right) \quad (1)$$

where T [L] is the thickness of the saturated layer, measured perpendicular to the impermeable bed, Z [L] is the water table elevation from an arbitrary datum, and s [L] is the distance along the hillslope. In this investigation, q, T, and dZ/ds were measured during field monitoring or determined using simple geometry. In this way, Eq. (1) can be solved directly to obtain a relation between $K_{s,l}$ and the water table depth below the soil surface.

3. Results

3.1. Natural rainfall

Cumulative rainfall was 550 mm in 2014 and 528 mm in 2015. For the analysis, rainfall events were considered distinct if they were separated by at least 6 hours without rain, and events with less than 3 mm in six hours were disregarded. About eighty events, ranging in depth from 3.2 to 91 mm, occurred between January 2014 and December 2015. At the FG site, subsurface flow was observed during 80% of these events, mainly occurring during the autumn and spring periods. The maximum and the mean outflow volumes were about 3.6 m^3 and 1.3 m^3, respectively, and the maximum outflow rate was 11.7 l min^{-1}. At the HM site, drainage was less frequent than at the FG site and the collected water volumes were scarce. In particular, the drain intercepted subsurface flow for 40% of the rain events. The maximum and the mean collected water volumes were 0.3 and 0.05 m^3, respectively, and the maximum outflow rate was 2 l min^{-1}. Therefore, only few information about $K_{s,l}$ were obtained for the maquis soil. Considering the weak hydrological response of the HM site under natural rainfall, the hydraulic characterization of this site was only based on the artificial rainfall experiments.

At the FG site, a water table developed in autumn and spring only as a consequence of the greatest rainfall events. In winter, with high rainfall and low evapotranspiration, a water table steadily formed in the hillslope and, due to the high soil wetness, even small rainfall

events caused piezometer responses. Figure 1.2 shows a boxplot of the observed water table depths at the FG site. On the contrary, the piezometer responses were almost absent at the HM site throughout the monitored period. For consistency of the analysis, only periods when all instruments were simultaneously functioning were considered. Lack of data was due to malfunctioning of some device or to water level fluctuations greater than those measurable by the TDR probes. Data from all instruments were simultaneously available for the 80% of the time during the period of occurrence of drain outflow.

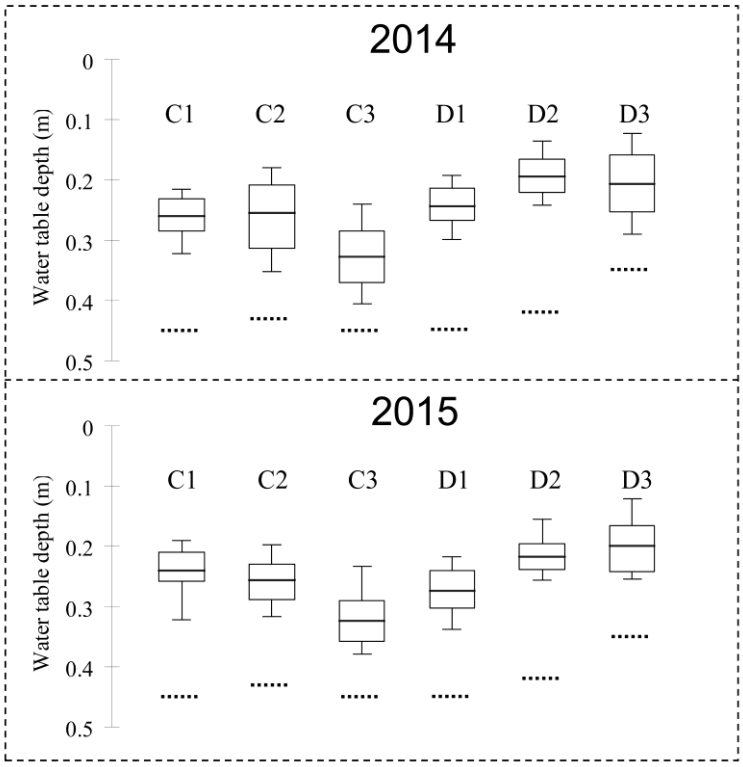

Fig. 1.2. Boxplots of the water table depth in each well at the FG site for the years 2014 and 2015. Only periods of natural rainfall are considered in the analysis. The boxes determine the 25th and 75th percentiles, the whiskers are the 10th and 90th percentiles, the horizontal lines within the boxes indicate the means. The dashed lines indicate the depth of the impeding layer as documented during well drilling.

The water table in the C3 well was the deepest on both years whereas the water levels in the D2 and D3 wells were the closest to the soil surface. The observed similarity between the two years of observation suggests that there was a temporal stability in the groundwater spatial dynamics in the hillslope. The piezometer responses were consistent between wells

located at the same elevation in the hillslope. On both years, the lowest Spearman correlation coefficients, ρ, were detected with reference to the water levels in the C2 and D2 wells (ρ = 0.81 in 2014 and ρ = 0.92 in 2015) whereas the highest ρ values were obtained for the C3 and D3 wells (ρ = 0.96 and 0.95, respectively).

Figure 1.3 shows a boxplot of the hydraulic gradients, *dZ/ds*, estimated from the water levels in the wells located 1 and 3 m far away the drain along the two established transects. The gradients used for $K_{s.l}$ calculation (Eq.1) were computed as the arithmetic mean of the hydraulic gradients along the two transects near the drain. Only the wells near the drain were considered in order to have a more accurate estimate of the gradients that effectively drove the drain response. Figure 1.3 shows the statistical spread of the *dZ/ds* values. Generally, the hydraulic gradients were close to the topographic gradient, and deviations from this latter did not exceed 5% in most cases.

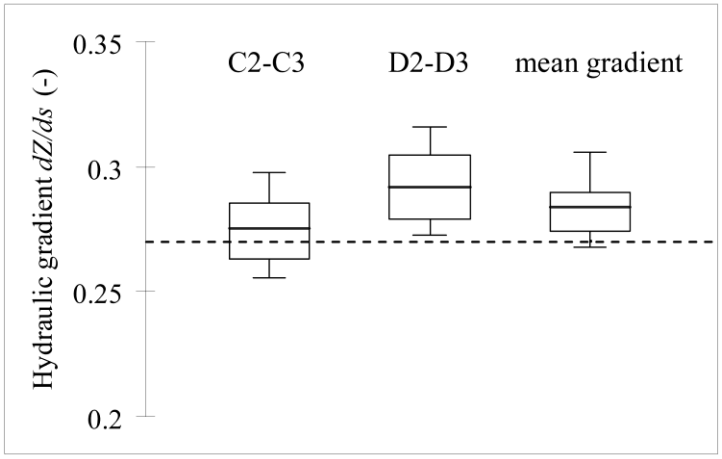

Fig. 1.3. Boxplot of the hydraulic gradient, *dZ/ds*, values measured near the drain at the FG site for the years 2014 and 2015. The statistical spread of mean hydraulic gradient used in Eq. (1) is also showed. The boxes determine the 25th and 75th percentiles, the whiskers are the 10th and 90th percentiles, the horizontal lines within the boxes indicate the means. The dashed line indicates the local topographic gradient.

The relationship between water table depth and outflow was investigated in detail by checking the hydrological response of the hillslope during a sequence of distinct rainfall events. Figure 1.4b shows the response of the drain and the water levels in the three wells of transect C for the period from February 2 to February 5, 2014. Data from a single transect were considered for this analysis due to the detected consistence between well data for the

two transects and also because similar results to those reported in Figure 1.4b were obtained by either considering transect D or averaging the two transects (data not shown). Lateral subsurface flow was almost absent on February 2, when 5 mm of rainfall caused a large fluctuation of the water table close to the C3 well but levels in the C1 and C2 wells varied by only a few centimeters. Seven and 8 mm of rainfall fell on February 3 and 4, respectively. The water level in the C3 well fluctuated and peaked, with a behavior similar to that observed for the previous event. For the C1 and C2 wells, water levels closer to the soil surface were observed. Both amount and peak of the outflow showed a variation between events larger than the variation in fallen rain. Therefore, a rise in water level in the C3 well alone was not enough to collect significant subsurface runoff volumes. Instead, the water table rise close to the soil surface in the drained area was a necessary condition for generation of considerable subsurface flow. A possible physical interpretation of this finding is that higher water levels increased hydraulic connectivity of the soil pore system.

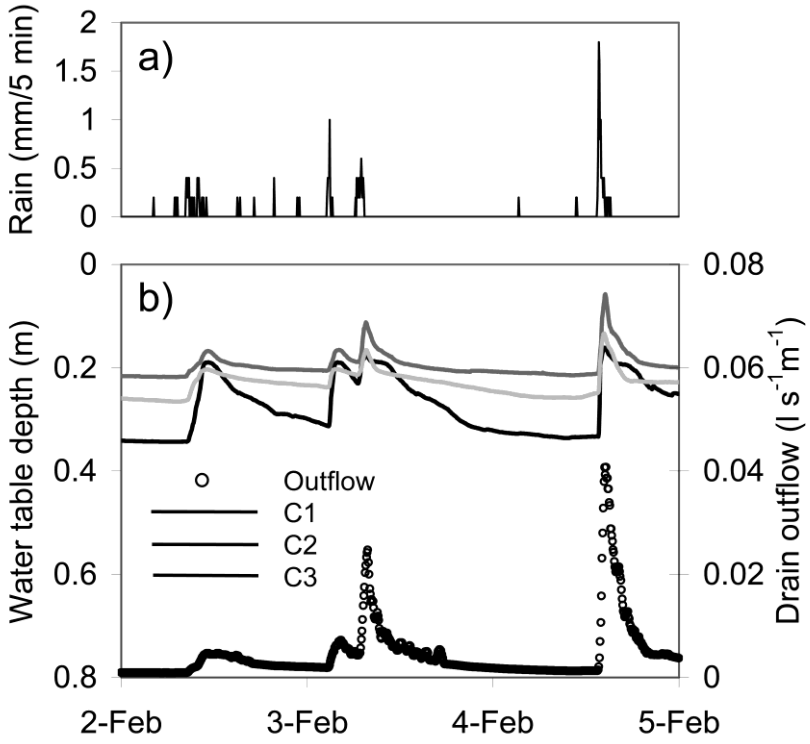

Fig. 1.4. a) Observed rainfall and b) observed drain outflow at the FG site and observed water table depths in the wells C1, C2 and C3 during the natural rainfall events occurring from 2 to 5 February 2014.

The time correspondence between water table level fluctuations and drain outflow response was also detected when peaks in both drain outflow and water table rise were well identifiable (Figure 1.4b). In general, the increase of water table started simultaneously in all wells and the time when levels peaked also coincided among wells. The drain outflow dynamics closely followed the water table dynamics. In fact, outflow started to increase when water table began to respond, and the outflow and water table levels peaked at the same time.

To establish the best estimate of the saturated layer thickness, T, to be used in Eq. (1), an estimate of the water table depth, WTD, at a given elevation along the hillslope was obtained by averaging the two water level values and the correlation between q and WTD was checked. The lowest correlation between q and WTD ($\rho = 0.86$) was found for the 2014 data and the wells farther away from the drain (C1 and D1). The highest correlation was obtained by considering the closest wells to the drain (WTD_3, i.e., the average of the C3 and D3 well levels), since ρ was close to 0.93 on both years. Therefore, WTD_3 was used for the calculation of T in Eq. (1).

Taking into account the similarity of the relationships between q and WTD_3 for the two monitored years, a single $q(WTD_3)$ relationship was developed by considering the $q(WTD_3)$ data of both years. This relationship was clearly non-linear (Figure 1.5). Above the depth of about 0.17 m (small thickness of the saturated layer), q varied by 2×10^{-4} l $s^{-1}m^{-1}$ per centimeter of WTD fluctuation. Below this depth (thicker saturated layer), q variation per unit change in water table depth was 25 times greater. This result suggested that $K_{s,l}$ greatly increased in the upper soil layer.

The highest estimated $K_{s,l}$ values were close to 3000 mm h^{-1} for a WTD of about 0.1 m (Figure 1.6a). Similar results (i.e., $K_{s,l}$ = 3600 mm h^{-1}) were obtained by Montgomery and Dietrich (1995) in a soil presenting the evidence of macropore flow. The rate of change of $K_{s,l}$ with WTD increased by more than one order of magnitude in the passage from small (i.e., $WTD \geq 0.17$ m) to large saturated soil layers. Figure 1.6b shows that the $K_{s,l}$ data were more prone to uncertainty (higher coefficients of variation, CV) for small water table levels (high WTD values). This result was a consequence of the relatively poor correlation between q and WTD for the high WTD values (Figure 1.5). A low correlation between the trench outflow and the water table depth for low subsurface flow regimes was also observed in other experimental hillslopes (Anderson et al., 2009; Uchida et al., 2004). The observed trend of $K_{s,l}$

as a function of WTD_3 was satisfactorily modelled by an exponential function (Figure 1.6a). This model is in agreement with the assumption of many hydrological models, such as TOPMODEL (Ambroise et al., 1996), that the soil transmissivity exponentially increases with the thickness of the saturated soil layer.

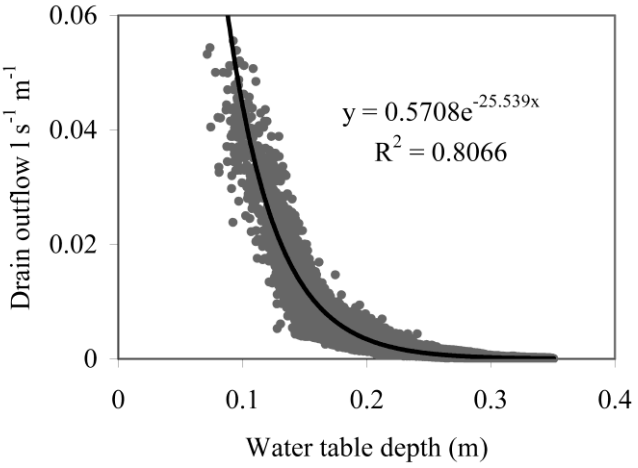

Fig. 1.5. Water flow per unit width of drain, q, vs. water table depth, WTD_3, values measured in the C3 and D3 wells of FG site for the natural rainfalls occurring in 2014–2015 years. The fitted exponential curve is also showed.

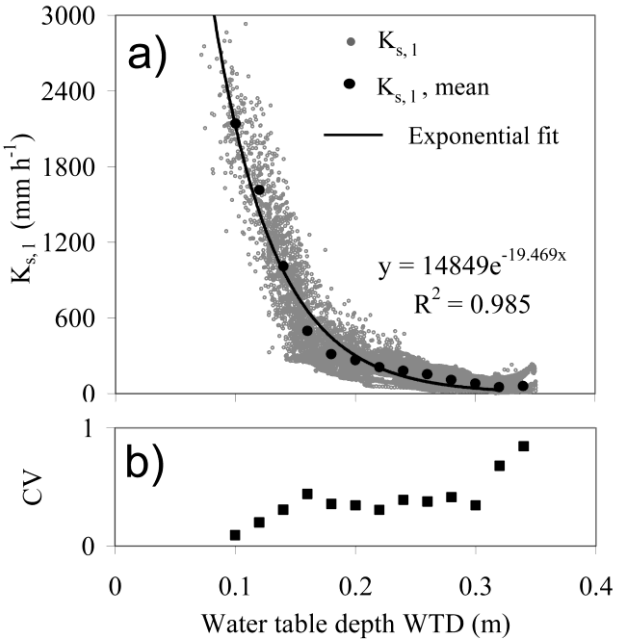

Fig. 1.6. a) Lateral saturated hydraulic conductivity, $K_{s,l}$, vs. water table depth values, WTD_3, for the natural rainfall occurring in 2014–2015 years. Average values of $K_{s,l}$ computed for selected water table depths are shown, together with the fitted exponential curve. b) Coefficients of variation (CV) of $K_{s,l}$ for selected water table depths.

3.2.Sprinkling experiment

At the HM site, the first sprinkling experiment (rainfall intensity = 40 mm h^{-1}) was carried out on an initially dry soil. The drain took about one hour to respond to the rainfall input. The outflow increased throughout the duration of the experiment, until $q = 0.085$ l s^{-1} m^{-1} was reached at the end of the experiment (Figure 1.7). The total collected water volume was 1.6 m^3 and the runoff coefficient was 0.5. Surface runoff did not occur during the experiment.

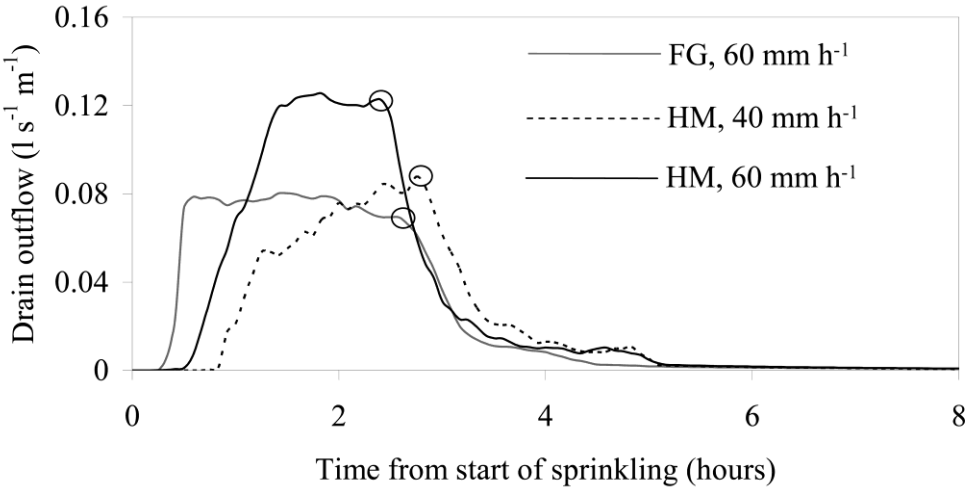

Fig. 1.7. Time series of the drain outflow observed during the sprinkling experiments in the FG and HM sites; circles indicate the end of water supply.

The second, more intense (rainfall intensity = 60 mm h^{-1}) sprinkling experiment was carried out while the drain was slowly leaking. The drain responded about 30 minutes after irrigation started. Subsurface flow increased for an hour up to a steady rate of about 0.12 l s^{-1} m^{-1}, which did not vary during the subsequent hour. The collected subsurface water volume was 2.25 m^3, which represented about 51% of the total supplied water volume. Surface runoff generated during this experiment, and its water volume was about 8% of the supplied water volume.

The two sprinkling experiments at the HM site yielded similar $q(WTD_3)$ relationships (Figure 1.8a). A complete saturation of the soil layer was never achieved, being 0.08 m the minimum reached water table depth. For a water table depth greater than about 0.25 m the drain response was almost absent while above this depth the outflow was highly responsive to

changes in water table level. The $K_{s,l}(WTD_3)$ data points, fitted with an exponential function (Figure 1.8b), closely resembled the $q(WTD_3)$ relationship (Figure 1.8a). During the steady outflow phase, a mean $K_{s,l}$ value of 3750 mm h^{-1} was computed for WTD = 0.1 m.

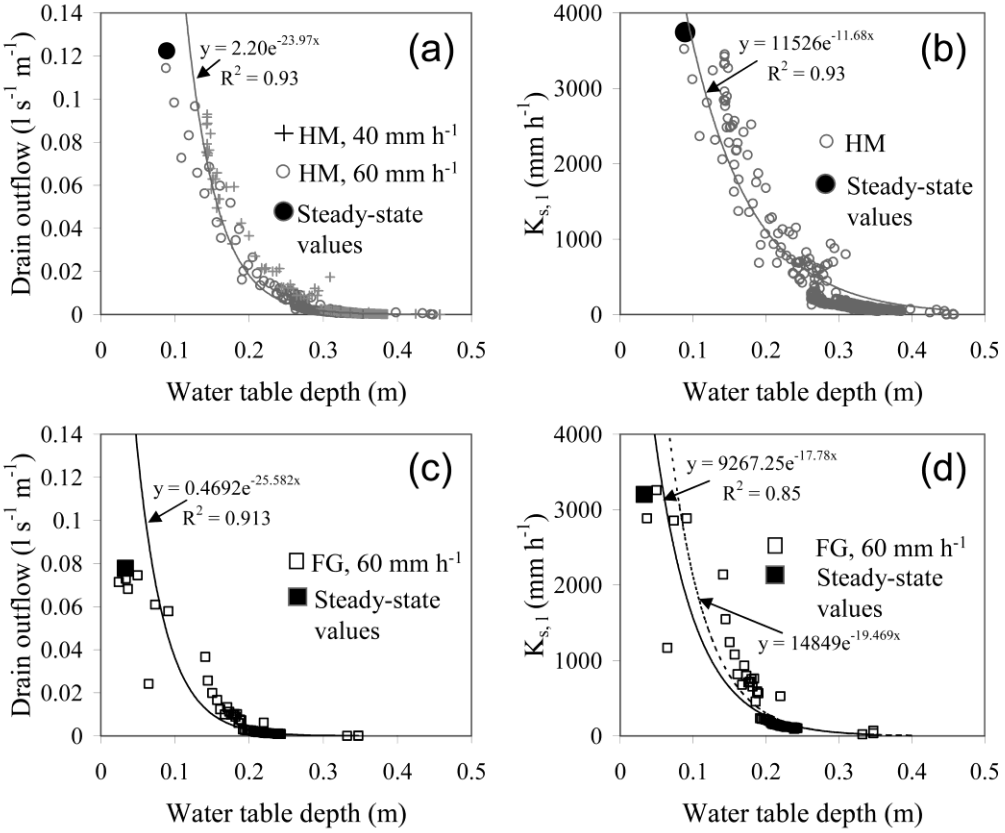

Fig. 1.8. a) Water flow per unit width of drain, q, vs. water table depth, WTD_3, values measured in the HM site during the transient and steady-state phases of the sprinkling experiments; b) lateral saturated hydraulic conductivity, $K_{s,l}$, vs. WTD_3 estimated for the sprinkling experiments in the HM site; c) q vs. WTD_3 values measured in the FG site during the transient and steady-state phases of the sprinkling experiment; d) $K_{s,l}$ vs. WTD_3 estimated for the sprinkling experiment in the FG site. The continuous lines are the exponential functions fitted to the $q(WTD_3)$ and $K_{s,l}(WTD_3)$ data estimated for the sprinkling experiments at the HM and FG sites. The dashed line in the Figure 1.8d is the exponential function fitted to the $K_{s,l}(WTD_3)$ data determined for the natural rainfall periods at the FG site, already shown in the Figure 1.6a.

At the FG site, the sprinkling experiment (rainfall intensity = 60 mm h^{-1}) was carried out on initially wet soil and while the tile line was slowly draining. The drain took about 20 minutes to respond to the rainfall input. The outflow increased for 15 minutes, until it reached

a steady rate of about 0.08 l s^{-1} m^{-1} (Figure 1.7). The maximum surface runoff rate was 0.08 l $s^{-1}m^{-1}$. The total subsurface flow and surface runoff volumes were of about 2 m^3, representing the 83% of the supplied water volume. The $K_{s,l}$ value estimated during the steady outflow phase was 3200 mm h^{-1} and in this case the soil was almost completely saturated (Figure 1.8d). For a given water table depth, less outflow was measured at the FG site than the HM site one (Figure 1.8c). An abrupt change of the outflow rate vs. water table level relationship was observed for *WTD* of about 0.20 m.

4. Discussion

Two years of continuous monitoring highlighted that the land use had a primary role in controlling the hydrological response to rainfall of the sampled hillslope. At the FG site water table and lateral subsurface flow developed and persisted for long periods throughout the rainy seasons. At this site, even small water inputs were enough to increase lateral saturated subsurface flow when the soil was wet and the water table was close to the soil surface. A similar finding was reported by McDaniel et al. (2008). At the adjacent HM site, the groundwater response was weak, and both the peaks and the volumes of the generated outflow were very low throughout the study period. Weaker piezometer responses to rainfall in forested than grassed hillslopes have also been signalled by Germer et al. (2010) and Rockefeller et al. (2004). This result was also in line with other investigations showing an increase in water yield in catchments where forest was partially cleared (Brown et al. 2005; Molina et al. 2012; Sahin and Hall, 1996). At the HM site Pirastru et al. (2014) observed that 30% of the annual gross rainfall was intercepted by the canopy. This result was in line with the canopy interception values observed by other authors under shrubs and trees in other natural semi-arid Mediterranean environments (Gallart et al. 2002; Llorenz and Domingo, 2007). The canopy interception and the water retained by the thick litter on the soil surface create additional water storage that needs to be replenished by the rainfall. This may contribute to delay the beginning of the perched water table formation, to a point that soil saturation does not occur in years with low rainfall. At the HM site, we cannot exclude the possibility that the high canopy interception was the main cause of the almost absent saturated subsurface flow and water table rises during the natural rainfall events, also considering that annual rainfall was slightly below the average on both 2014 and 2015. For this site, a longer

period of observation is probably necessary to adequately characterize the lateral subsurface flow of the soil under natural rainfall conditions. Wilcox et al. (1997) also stated that hydrological monitoring in forested semi-arid environments normally requires long periods of observation because runoff-producing events are rare and of short duration, and they only occur under infrequent conditions, such as high rainfall and high antecedent soil moisture conditions.

In both the FG and HM sites, the relationship between the lateral saturated subsurface flow and the water table level was highly non-linear, and abruptly changed for small *WTDs*. Abrupt changes in the relationships between subsurface storage indicators (e.g., soil moisture or groundwater levels) and the subsurface flow have been reported for different hydrological processes and spatial scales of observation (Latron and Gallart, 2008; Penna et al., 2011; Peters et al., 2003). This investigation showed that the change in the *q(WTD)* relationship was linked to $K_{s,l}$, which increased sharply when the water table level was higher than 0.17-0.2 m at the FG site and about 0.25 m at the HM site. This behaviour plausibly reflected the increased density of macropores near the surface, due to roots and micro-fauna activity. Moreover, the increase of the water levels increased the possibility of a spatial connection between isolated patches of permeable soil or macropore network, thus increasing the lateral hydraulic connectivity of the soil pore system as a whole. The increase of $K_{s,l}$ near the surface was most apparent at the HM site compared to the FG site (Figures 1.8b and 1.8d). Plausibly, this result was expressive of the more developed and effective macroporosity in the soil under the maquis compared to the grassed soil, in line with other studies comparing forest and cleared land soils (Alaoui et al., 2011). In situ observations of the distribution of tree and shrub roots in the maquis indicated that fine roots were abundant close to the surface and that many coarse roots developed more in depth, spreading both laterally and vertically. This root structure contributed to increase the hydraulic conductivity of the maquis to a depth greater than that observed at the grassed site.

At the FG site, a minimum water table depth (largest saturated layer) of 0.1 m was observed during the natural rainfall periods, and the corresponding $K_{s,l}$ value was of 3000 mm h^{-1}. During the steady outflow phase of the sprinkling experiment, the water table was on average 0.03 m below the soil surface and a $K_{s,l}$ value of 3200 mm h^{-1} was estimated. In Figure 1.8d, this last $K_{s,l}$ value appears shifted to the left as compared with the exponential

$K_{s,l}(WTD)$ relationship obtained for the natural rainfall periods. Therefore, the results of the sprinkling experiment suggested that, for water table depths smaller than those observed during the natural rainfall periods, there was a stabilization of the $K_{s,l}$ values, thus resulting in a flattening of the $K_{s,l}(WTD)$ relationship close to the soil surface. An analysis of the relationships between $K_{s,l}$ and the subsurface flow rates observed with both the natural and artificial rainfall at the FG site (Figure 1.9a) better clarified this finding. The increases of $K_{s,l}$ with q was less than proportional and a power function with an exponent of 0.82 well described this behaviour. In the range of the outflow rates observed during the natural rainfall, there was a good agreement between the $K_{s,l}(q)$ data points obtained for these periods and those corresponding to the sprinkling experiment. However, beyond this range, the highest $K_{s,l}(q)$ values that were estimated with the sprinkling experiment exhibited a less steep pattern, indicating that the increase of $K_{s,l}$ was slower when the water table was closer to the soil surface. A similar flattening of the $K_{s,l}(q)$ relationship was observed by Montgomery and Dietrich (1995), who found that $K_{s,l}$ increased sharply with q for low discharge values but it was relatively stable at the highest observed discharges. These authors explained the observed behaviour by the progressive filling of macropores that became full of water at the highest discharges. In agreement with Montgomery and Dietrich (1995), Figure 1.9a suggests that the capacity of the soil pore system to transmit flow downslope reached the maximum during the sprinkling experiment. Conversely, the full potential of the system was not reached during the natural rainfall periods.

At the HM site, the saturated conductivity estimated during the steady outflow phase of the sprinkling experiments was in line with the exponential $K_{s,l}(WTD)$ relationship obtained by considering the transient phases of the same experiments (Figure 1.8b). Figure 1.9b also suggests that, despite the high applied rain intensity and the intense drain response, the full potential of the maquis soil in transporting the lateral subsurface flow was only partially explored. For this soil, it is reasonable not to exclude the possibility that $K_{s,l}$ continues to increase up to the soil surface, as observed for example by Brooks et al. (2004).

Brooks et al. (2004) highlighted the need to introduce simplifications in the experimental methodology for estimating $K_{s,l}$ at the hillslope scale, in order to make the method more suitable for routine determinations. A possible simplification could be using the topographic gradient instead of the hydraulic gradient dZ/ds in Eq. (1). This suggestion stems from the

observation that the water table was almost parallel to the surface for most part of the time (Figure 1.3). Figure 1.10 shows that, with the topographic gradient instead of *dZ/ds* in Eq. (1), the absolute errors in $K_{s,l}$ did not exceed 20% and they were smaller than 10% for $K_{s,l} > 500$ mm h^{-1}.

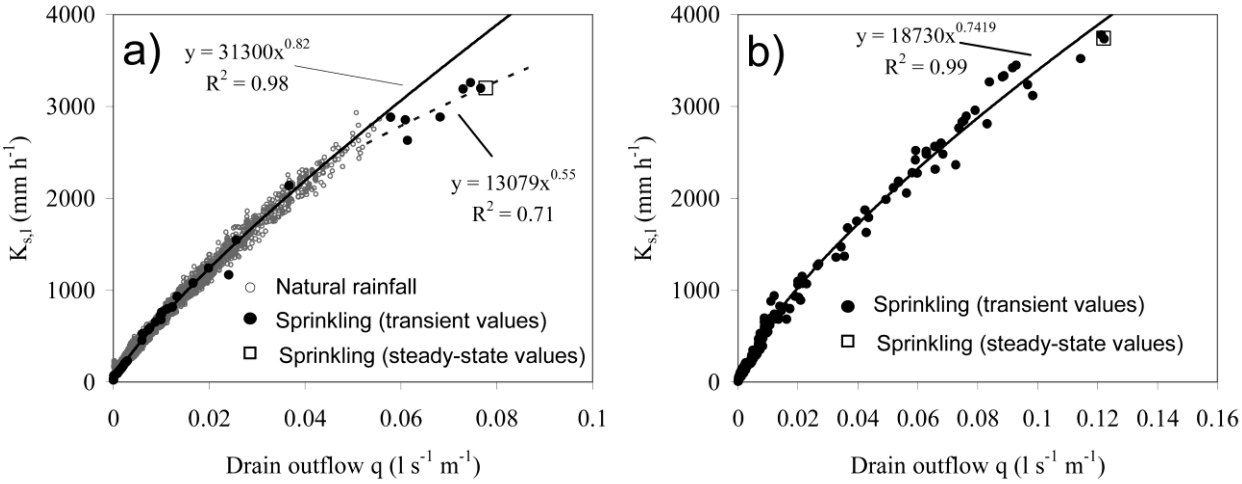

Fig. 1.9. Lateral saturated hydraulic conductivity, $K_{s,l}$, vs. water flow per unit width of drain, q, for (a) the natural rainfall events of years 2014–2015 and the sprinkling experiment in the FG site, and (b) the sprinkling experiments in the HM site.

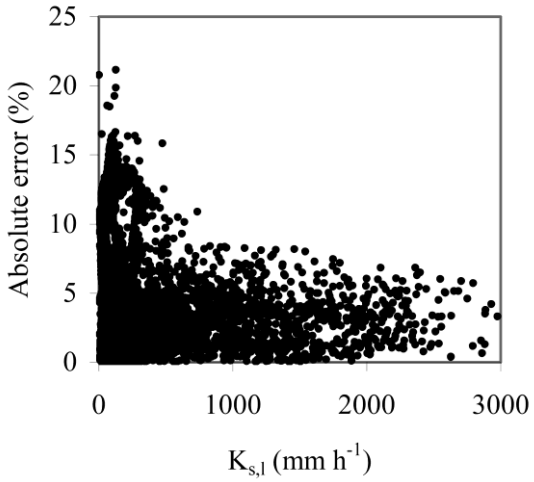

Fig. 1.10. Absolute percentage errors introduced in the estimate of the lateral saturated hydraulic conductivity, $K_{s,l}$, by using the topographic gradient in lieu of the total hydraulic gradient in Eq. (1).

In this investigation, a 2.5 m long drain was used to intercept flow from a non-isolated portion of the hillslope notwithstanding that both sampled sites (HM and FG) were appreciably wider (Figure 1.1). Therefore, the sampling scheme was different from that by Brooks et al. (2004), since these authors used a long drain (18 m) to collect all subsurface flow generated in an isolated hillslope plot. Assuming that flow was perfectly perpendicular to the drain could not be totally exact, since some lateral convergence or divergence of the saturated flow pathways cannot be excluded. However, the results of this investigation were consistent with those by Brooks et al. (2004). In particular, there were signs that macropore contribution to the hydrological response of the hillslope was adequately captured since rapid flow was found to be particularly noticeable when the water table was close to the soil surface. Moreover, the experimental setup used at the HM and FG sites is simpler to replicate in other hillslopes than the one involving hydraulic isolation of the plot and interception of all subsurface flow. Therefore, the experimental methodology used at the Baratz Lake catchment potentially appears a good method to develop other databases in different environments, which is expected to improve our general knowledge of subsurface flow processes. Evidently, further investigations are advisable to test the assumption of perpendicular flow used in this approach, also establishing what happens with drains differing in length.

5. Conclusions

The experimental investigation was carried out to characterize the lateral saturated subsurface flow processes in a hillslope with two plots covered with Mediterranean maquis and grass, respectively. The spatially variable water table levels and the lateral saturated subsurface flows drained at the basis of the hillslope were used for determining relationships between the large-scale lateral saturated soil hydraulic conductivity, $K_{s,l}$, and the thickness of the water table above the impeding layer. The $K_{s,l}$ sharply increased when the water table level was close to the soil surface, where macropores were mostly present. Probably, high water table levels were necessary in the drained area to make large-scale hydraulic connection of the macropore system effective. Further experimental work is need to confirm the role of the macropores in controlling the $K_{s,l}$ at the studied hillslope. For example, near point determinations of the vertical profile of hydraulic conductivity should be carried out to

increase our confidence that a depth-dependent macroporosity was responsible of the detected hydrological response of the hillslope.

In situ experiments for large scale $K_{s,l}$ estimation, such as that illustrated in this paper, are expensive and time consuming. For catchment-scale hydrological studies near-point $K_{s,l}$ determinations remain the only feasible way to obtain spatially distributed $K_{s,l}$ data. In the studied hillslope it would be interesting to carry out a distributed point sampling of the hydraulic conductivity and compare the results with the large scale $K_{s,l}$. In fact, using $K_{s,l}$ resulting from this study as a benchmark, may increase knowledge on the way a distributed point sampling should be planned to obtain useful information for interpreting and simulating subsurface hydrological processes at the hillslope scale.

6. References

Alaoui, A., Caduff, U., Gerke, H. H., Weingartner, R., 2011. A Preferential Flow Effects on Infiltration and Runoff in Grassland and Forest Soils. Vadose Zone Journal, 10(1), 367–377.

Ambroise, B., Beven, K., Freer, J., 1996. Toward a generalization of the TOPMODEL concepts: Topographic indices of hydrological similarity. Water Resources Research, 32(7), 2135–2145.

Anderson, A. E., Weiler, M., Alila, Y., Hudson, R. O., 2009. Subsurface flow velocities in a hillslope with lateral preferential flow. Water Resources Research, 45(11).

Bathke, G. R., Cassel, D. K.,1991. Anisotropic variation of profile characteristics and saturated hydraulic conductivity in an Ultisol landscape. Soil Science Society of America Journal, 55(2), 333–339.

Baxter, C., Hauer, F. R., Woessner, W. W., 2003. Measuring groundwater–stream water exchange: new techniques for installing minipiezometers and estimating hydraulic conductivity. Transactions of the American Fisheries Society, 132(3), 493–502.

Beckwith, C. W., Baird, A. J., Heathwaite, A. L., 2003. Anisotropy and depth-related heterogeneity of hydraulic conductivity in a bog peat. II: modelling the effects on groundwater flow. Hydrological Processes, 17(1), 103–113.

Beven, K., Germann, P., 2013. Macropores and water flow in soils revisited. Water Resources Research, 49(6), 3071–3092.

Blain, C. A., Milly, P. C. D., 1991. Development and application of a hillslope hydrologic model, Adv. Water Resour., 14(4), 168–174.

Blanco-Canqui, H., Gantzer, C. J., Anderson, S. H., Alberts, E. E., Ghidey, F., 2002. Saturated hydraulic conductivity and its impact on simulated runoff for claypan soils. Soil Science Society of America Journal, 66(5), 1596–1602.

Bouma, J., Dekker, L. W., 1981. A method for measuring the vertical and horizontal Ksat of clay soils with macropores. Soil Science Society of America Journal, 45(3), 662–663.

Brooks, E. S., Boll, J., McDaniel, P. A., 2004. A hillslope-scale experiment to measure lateral saturated hydraulic conductivity. Water Resources Research, 40(4).

Brown, A. E., Zhang, L., McMahon, T. A., Western, A. W., Vertessy, R. A., 2005. A review of paired catchment studies for determining changes in water yield resulting from alterations in vegetation. Journal of Hydrology, 310(1), 28–61.

Castellini, M., Iovino, M., Pirastru, M., Niedda, M., Bagarello, V., 2016. Use of BEST Procedure to Assess Soil Physical Quality in the Baratz Lake Catchment (Sardinia, Italy). Soil Science Society America Journal, 80, 742–755.

Chappell, N. A., 2010. Soil pipe distribution and hydrological functioning within the humid tropics: a synthesis. Hydrological Processes, 24(12), 1567–1581.

Chappell, N. A., Franks, S. W., Larenus J., 1998. Multi-scale permeability estimation for a tropical catchment, Hydrological Processes, 12, 1507–1523.

Chappell, N. A., Lancaster, J. W., 2007. Comparison of methodological uncertainties within permeability measurements. Hydrological Processes, 21(18), 2504–2514.

Childs, E. C., 1971. Drainage of groundwater resting on a sloping bed. Water Resources Research, 7(5), 1256–1263.

Dabney, S. M., Selim, H. M.,1987. Anisotropy of a fragipan soil: vertical vs. horizontal hydraulic conductivity. Soil Science Society of America Journal, 51(1), 3–6.

Dusek, J., Vogel, T., 2016. Hillslope-storage and rainfall-amount thresholds as controls of preferential stormflow. Journal of Hydrology, 534, 590–605.

Dusek, J., Vogel, T., Dohnal, M., Gerke, H. H., 2012. Combining dual-continuum approach with diffusion wave model to include a preferential flow component in hillslope scale modeling of shallow subsurface runoff. Advances in Water Resources, 44, 113–125.

Gallart, F., Llorens, P., Latron, J., Regüés, D., 2002. Hydrological processes and their seasonal controls in a small Mediterranean mountain catchment in the Pyrenees. Hydrology and Earth System Sciences Discussions, 6(3), 527–537.

Germer, S., Neill, C., Krusche, A. V., Elsenbeer, H., 2010. Influence of land-use change on near-surface hydrological processes: undisturbed forest to pasture. Journal of Hydrology, 380(3), 473–480.

Giadrossich, F., Niedda, M., Cohen, D., Pirastru, M., 2015. Evaporation in a Mediterranean environment by energy budget and Penman methods, Lake Baratz, Sardinia, Italy. Hydrology and Earth System Sciences, 19(5), 2451–2468.

Grayson, R. B., Moore, I. D., McMahon, T. A., 1992. Physically based hydrologic modeling: 2. Is the concept realistic?. Water Resources Research, 28(10), 2659–2666.

Hilberts, A. G. J., Troch, P. A., Paniconi, C., 2005. Storage-dependent drainable porosity for complex hillslopes. Water Resources Research, 41(6).

Jost, G., Schume, H., Hager, H., Markart, G., Kohl, B., 2012. A hillslope scale comparison of tree species influence on soil moisture dynamics and runoff processes during intense rainfall. Journal of Hydrology, 420, 112–124.

Latron, J., Gallart, F., 2008. Runoff generation processes in a small Mediterranean research catchment (Vallcebre, Eastern Pyrenees). Journal of Hydrology, 358(3), 206–220.

Llorens, P., Domingo, F., 2007. Rainfall partitioning by vegetation under Mediterranean conditions. A review of studies in Europe. Journal of Hydrology, 335(1), 37–54.

Maneta, M., Schnabel, S., Jetten, V., 2008. Continuous spatially distributed simulation of surface and subsurface hydrological processes in a small semiarid catchment. Hydrological Processes, 22(13), 2196–2214.

Matonse, A. H., Kroll, C. N., 2013. Applying hillslope-storage models to improve low flow estimates with limited streamflow data at a watershed scale. Journal of Hydrology, 494, 20–31.

McDaniel, P. A., Regan, M. P., Brooks, E., Boll, J., Barndt, S., Falen, A., Young, S.K., Hammel, J. E., 2008. Linking fragipans, perched water tables, and catchment-scale hydrological processes. Catena, 73(2), 166–173.

Molina, A., Vanacker, V., Balthazar, V., Mora, D., Govers, G., 2012. Complex land cover change, water and sediment yield in a degraded Andean environment. Journal of Hydrology, 472, 25–35.

Montgomery, D. R., Dietrich, W. E., 1995. Hydrologic processes in a low-gradient source area. Water Resources Research, 31(1), 1–10.

Morgan, R. P. C., Duzant, J. H., 2008. Modified MMF (Morgan–Morgan–Finney) model for evaluating effects of crops and vegetation cover on soil erosion. Earth Surface Processes and Landforms, 33(1), 90–106.

Newman, B. D., Campbell, A. R., Wilcox, B. P., 1998. Lateral subsurface flow pathways in a semiarid ponderosa pine hillslope. Water Resources Research, 34(12), 3485–3496.

Niedda, M., Pirastru, M., 2013. Hydrological processes of a closed catchment-lake system in a semi-arid Mediterranean environment. Hydrological Processes, 27(25), 3617–3626.

Niedda, M., Pirastru, M., 2015. Field investigation and modelling of coupled stream discharge and shallow water-table dynamics in a small mediterranean catchment (Sardinia). Hydrological Processes, 28(21), 5423–5435. doi:10.1002/hyp.10016

Niedda, M., Pirastru, M., Castellini, M., Giadrossich, F., 2014. Simulating the hydrological response of a closed catchment-lake system to recent climate and land-use changes in semi-arid Mediterranean environment. Journal of Hydrology, 517, 732–745.

Penna, D., Tromp-van Meerveld, H. J., Gobbi, A., Borga, M., Dalla Fontana, G., 2011. The influence of soil moisture on threshold runoff generation processes in an alpine headwater catchment. Hydrology and Earth System Sciences, 15(3), 689–702.

Peters, N. E., Freer, J., Aulenbach, B. T., 2003. Hydrological dynamics of the Panola Mountain research watershed, Georgia. Ground Water, 41(7), 973–988.

Pirastru, M., Niedda, M., 2013. Evaluation of the soil water balance in an alluvial flood plain with a shallow groundwater table. Hydrological Sciences Journal, 58(4), 898–911.

Pirastru, M., Niedda, M., Castellini, M., 2014. Effects of maquis clearing on the properties of the soil and on the near-surface hydrological processes in a semi-arid Mediterranean environment. Journal of Agricultural Engineering, 45(4), 176–187.

Reynolds, W. D., 2010. Measuring soil hydraulic properties using a cased borehole permeameter: steady flow analyses. Vadose Zone Journal, 9(3), 637–652.

Reynolds, W. D., 2011. Measuring soil hydraulic properties using a cased borehole permeameter: falling-head analysis. Vadose Zone Journal, 10(3), 999–1015.

Rockefeller, S.L., McDaniel P.A., Falen A.L., 2004. Perched water table responses to forest clearing in northern Idaho. Soil Science Society of America Journal, 68, 168–174.

Sahin, V., Hall, M. J., 1996. The effects of afforestation and deforestation on water yields. Journal of Hydrology, 178(1), 293–309.

Sherlock, M. D., Chappell, N. A., J. J. McDonnell, 2000. Effects of experimental uncertainty on the calculation of hillslope flow paths, Hydrological Processes, 14, 2457–2471.

Uchida, T., Asano, Y., Mizuyama, T., McDonnell, J. J., 2004. Role of upslope soil pore pressure on lateral subsurface storm flow dynamics. Water Resources Research, 40(12).

van Schaik, N. L. M. B., Schnabel, S., Jetten, V. G., 2008. The influence of preferential flow on hillslope hydrology in a semi-arid watershed (in the Spanish Dehesas). Hydrological Processes, 22(18), 3844–3855.

van Schaik, N. L. M. B., Bronstert, A., Jong, S. M., Jetten, V. G., Dam, J. C., Ritsema, C. J., & Schnabel, S., 2014. Process-based modelling of a headwater catchment in a semi-arid area: the influence of macropore flow. Hydrological Processes, 28(24), 5805–5816.

Weiler, M., McDonnell, J.J., Tromp-van Meerveld, H.J., Uchida, T., 2005. Subsurface stormflow. In Encyclopedia of Hydrological Sciences, vol. 3, Anderson MG, McDonnell JJ (eds). Wiley: Chichester; 1719–1732.

Wilcox, B. P., Newman, B. D., Brandes, D., Davenport, D. W., Reid, K., 1997. Runoff from a semiarid ponderosa pine hillslope in New Mexico. Water Resources Research, 33(10), 2301–2314.

CHAPTER 2

Lateral saturated hydraulic conductivity of soil horizons evaluated in large-volume soil monoliths

Mario Pirastru [1,*], Roberto Marrosu [1], Simone Di Prima [1], Saskia Keesstra [2], Filippo Giadrossich [1] and Marcello Niedda [1]

[1] Agricultural Department, University of Sassari, Viale Italia, 39, 07100 Sassari, Italy; rmarrosu@uniss.it (R.M.); simoedg@gmail.com (S.D.P.); fgiadrossich@uniss.it (F.G.); niedda@uniss.it (M.N.)
[2] Soil Physics and Land Management Group, Wageningen University, Droevendaalsesteeg 4, 6708PB Wageningen, The Netherlands; saskia.keesstra@gmail.com

Published in: *Water. 2017, 9(11), 862.*

https://doi.org/10.3390/w9110862

Abstract. Evaluating the lateral saturated hydraulic conductivity, $K_{s,l}$, of soil horizons is crucial for understanding and modelling the subsurface flow dynamics in many shallow hill soils. A $K_{s,l}$ measurement method should be able to catch the effects of soil heterogeneities governing hydrological processes at the scale of interest, in order to yield $K_{s,l}$ representative values over large spatial scales. This study aims to develop a field technique to determine spatially representative $K_{s,l}$ values of soil horizons of an experimental hillslope. Drainage experiments were performed on soil monoliths of about 0.12 m^3 volume, encased in situ with polyurethane foam. Median $K_{s,l}$ of 2450 mm h^{-1} and 552 mm h^{-1} were estimated in the A and B horizon, respectively. In the upper part of the B horizon, the median $K_{s,l}$ was 490 mm h^{-1}, whereas it mostly halved near the underlying restricting layer. The decline of $K_{s,l}$ values with depth was consistent with the water-table dynamics observed at the same site in previous studies. Moreover, the $K_{s,l}$ from the monoliths were in line with large spatial-scale $K_{s,l}$ values reported from the hillslope in a prior investigation based on drain data analysis. This indicated that the large-scale hydrological effects of the macropore network were well represented in the investigated soil blocks. Our findings suggest that performing drainage experiments on large-volume monoliths is a promising method for characterizing lateral conductivities over large spatial scales. This information could improve our understanding of hydrological processes and can be used to parameterize runoff-generation models at hillslope and catchment scale.

Keywords: soil block; subsurface flow; macropore network; spatial scale; polyurethane foam; hillslope.

1. Introduction

In many hillslopes with shallow steep soils, the spatial and temporal dynamics of the perched water table are dominated by the lateral (namely slope-parallel) saturated subsurface flow. These water tables often originate from infiltrated precipitation that is hindered from further downwards percolation by restrictive layers beneath soils, e.g., fragipan in (McDaniel et al., 2008), argillic Bt horizon in (Du et al., 2016), and weathered granite in (Dusek et al., 2012). Then, the water flows towards the footslope, where it can reach the surface once again and produces runoff (Alaoui et al., 2011; van Schaik et al., 2008; Wienhöfer and Zehe, 2014). In most cases, the preferential flow via macropores controls this runoff-generation process (Dusek et al., 2012; McDaniel et al., 2008; Schmocker-Fackel et al., 2007; Weiler et al., 2006). The lateral saturated hydraulic conductivity, $K_{s,l}$, is the soil property that influences transmission rate of the lateral subsurface water flow (Brooks et al., 2004; Montgomery and Dietrich, 1995).

In layered soils on hillslopes, soil horizons can differ in hydraulic conductivity by orders of magnitude (Brooks et al., 2004; McGuire and McDonnell, 2010; Montgomery and Dietrich, 1995). Evaluating the hydraulic conductivity of each soil horizon is fundamental to understanding the subsurface flow dynamics of these hillslopes. Moreover, it is necessary to characterize the vertical variability of the hydraulic conductivity in order to model consistently the spatial and temporal soil hydrological dynamics. The vertical architecture of the permeability also controls the dynamics of nutrients and pollutants, as revealed by a number of tracer experiments in natural and agricultural landscapes (Starr et al., 2005; Stutter et al., 2005; van Verseveld et al., 2009). Many modelling applications assume saturated hydraulic conductivities exponentially declining with depth (Ambroise et al., 1996). As reported by Ameli et al. (2016) changing the rate of the exponential $K_{s,l}$ decline significantly affects model simulation of soil water and solute storage, mixing, and releasing in hillslopes. Hence, the lack of information about the vertical variability of the hydraulic conductivity in soils can be one of the major limitations in the numerical modelling of the hydrological behaviour of hillslopes.

Despite the acknowledged importance of a detailed hydraulic characterization of the soils, few methods have been specifically developed to assess $K_{s,l}$ values in the field,

particularly for steep soils. Therefore, in most cases only laboratory-derived conductivity values are available. Furthermore, it is difficult to obtain $K_{s,l}$ data that can be representative of large spatial scales, from tens to hundreds of square meters, as the typical cell extents of the grid-based hydrological models. Consequently, some modelers consider the $K_{s,l}$ as a calibration parameter, without any experimental evaluation (as for example in Matonse and Kroll (2013)). In other cases (e.g., Maneta et al. (2008); van Schaik et al. (2014)) runoff-generation models use $K_{s,l}$ values obtained through methodologies inducing flow processes mainly vertically oriented. Instead, the hydraulic conductivity should be determined in agreement with the modelled flow direction. In fact, anisotropy can cause saturated conductivity to greatly differ with flow direction (e.g., Bathke and Cassel (1991); Beckwith et al.(2003)).

A useful approach for determining representative $K_{s,l}$ values of macroporous soil is to perform drainage experiments in large-volume soil blocks, or monoliths, encased in situ with impermeable material. These experiments constrain the water flow along a prescribed direction through the soil, in order to define unambiguously the terms of Darcy's law (Mendoza and Steenhuis, 2002; Vepraskas and Williams, 1995). Field procedures for evaluating the $K_{s,l}$ in large soil samples are reported, among others, by Blanco-Canqui et al. (2002) and Mendoza and Steenhuis (2002). The latter described a device called a "hillslope infiltrometer" by which the lateral drainage from each horizon of a layered soil was collected. The drainage rates were used to compute specific $K_{s,l}$ values of the soil horizons.

Both Blanco-Canqui et al. (2002) and Mendoza and Steenhuis (2002) in their field applications used steel plates to enclose and hydraulically isolate the soil blocks. In some cases, metal-sheet insertion may be too cumbersome, especially in stony soils. Expandable polyurethane foam can be more conveniently used in situ as material encasing the soil blocks. The foam is used as waterproof material to obtain soil bulk density data with the excavation method (Brye et al., 2004; Muller and Hamilton, 1992; Page-Dumroese et al., 1999), and to study the hydraulic soil anisotropy by measuring hydraulic conductivities in the laboratory on small cubes (Bagarello et al., 2009; Bagarello and Sgroi, 2008) or on large soil cores (Germer and Braun, 2015). To our knowledge, the suitability of the expandable polyurethane foam for support in situ $K_{s,l}$ experimental investigations has not been tested until now. The foam is purchased in pressurized cans, which are easy to transport to the field. It is waterproof, fast to

apply, and it adheres to the irregular soil surfaces preventing bypass flow at the edges of the samples.

This paper focuses on field experiments aimed at evaluating the $K_{s,l}$ of the shallow soil of a steep hillslope. The measurements were carried out on monoliths encased in situ with expandable polyurethane foam. The soil surface and volume of the monoliths were on average about 0.4 m^2 and 0.12 m^3, respectively. Hence, the sample soil sizes were larger than the commonly sampled sizes through laboratory and field methods, with the exception of studies based on either drain or trench measurements. By saturating decreasing soil thicknesses during each experiment, the $K_{s,l}$ for each soil horizon was detected. Using the method illustrated in this paper, we aim to obtain, with a sustainable effort, field soil data that are useful for interpreting the hydrological response of hillslopes, and that can be used to parameterize hydrological models. The specific objectives of the research are: (1) to design a method to determine in field soil $K_{s,l}$ values; (2) to assess the $K_{s,l}$ variability in the soil vertical profile, in order to obtain $K_{s,l}$ values for each soil horizon; (3) to evaluate spatially representative $K_{s,l}$ values for the soil horizons in the studied hillslope.

2. Material and Methods

2.1. Location

The experiments were carried out in the Baratz Lake watershed, in north-west Sardinia, Italy. The study site (Figure 2.1a) is the steep side of a hill (40°41′53.36″ N, 8°14′4.15″ E) with elevations ranging from 50 to 65 m a.s.l. and mean slope of 30%. The area is a firebreak about 60 m long and 15 m wide with a mainly herbaceous coverage, bounded by Mediterranean maquis (Castellini et al., 2016). The soil is a sandy loam Lithic Haploxerepts, ranging in depth from 30 cm to 40 cm. The soil horizons are Ap (0–15 cm), BW and C (Pirastru et al., 2014). The latter is a dense altered Permian sandstone acting as restrictive layer. In the remainder of the text, A, B and "restrictive layer" are substituted for the Ap, BW and "C horizon", respectively. The climate is semiarid Mediterranean, with mild winters, warm summers and high water deficit from April to September. The average annual precipitation is about 600 mm, mainly falling from autumn to spring. The potential evapotranspiration is around 1000 mm per year (Giadrossich et al., 2015).

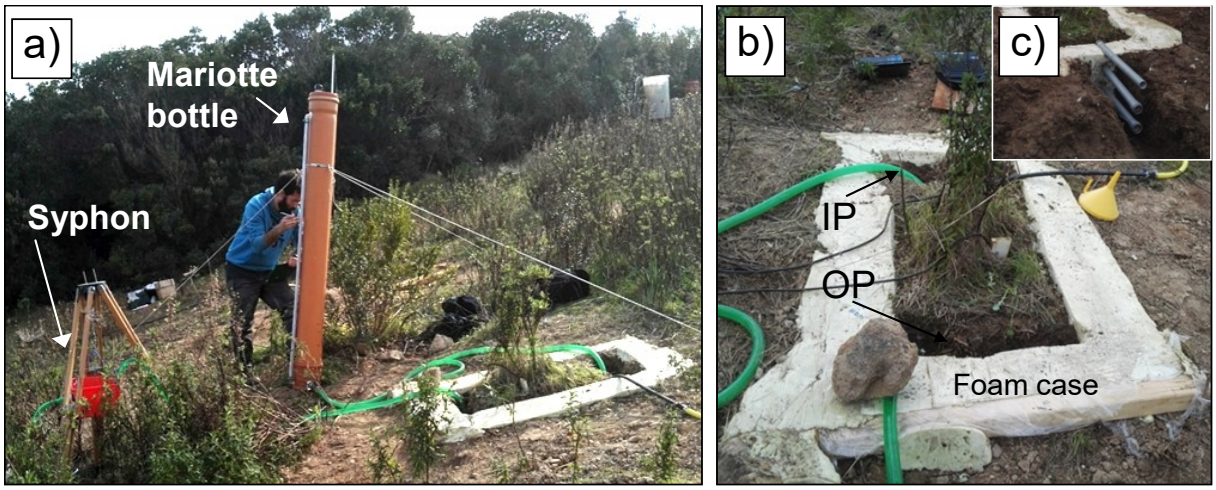

Fig. 2.1. Field equipment to determine lateral saturated soil hydraulic conductivities in the monoliths MA, MB and MC; (b) soil monolith encased with polyurethane foam, with signed inflow (IP) and outflow (OP) pits; (c) spillway pipes inserted in the OP foam of the monolith MD to set the water level and collect the drainage.

2.2. Soil monolith preparation

In winter 2017 four soil monoliths, represented by letters MA, MB, MC and MD, were carved out on selected locations on the hillslope. Soil blocks, each approximately 50 cm wide, 105 cm long and 70 cm deep (Figure 2.1b), extending for about 40 cm within the restrictive layer, were obtained by hand digging 20 cm-wide enclosing trenches. Vegetation at the monolith surfaces was preserved and the roots spreading out from the exposed faces were gently cut. Expandable polyurethane foam was injected to fill about 70% of the trench volume. Pressurized cans of 750 mL, each providing 0.05 m^3 of expanded foam, were used. Wooden boards were placed on top of the trenches to constrain the foam expansion.

The boards forced the foam expansion towards the trench and monolith sides in order to achieve a tight contact between the foam and the irregular block surfaces. This was essential for minimizing leakages between the soil and the foam at the monolith edges during the drainage experiments. After 24 h, the expanded foam completely backfilled the trenches, and any foam excess was cut off. Consequently, two 16 cm-wide pits were excavated to the depth of the restrictive layer at the uphill and downhill internal sides of the foam barriers. Inflow and outflow pits were, therefore, created, hereby noted as IP and OP respectively (Figure 2.1b). At the end, the resulting monoliths had soil volumes ranging from 0.1 m^3 to 0.16 m^3. Table 2.1 reports the dimensions of each sampled monolith.

Table 2.1. Dimensions of the soil monoliths sampled in the drainage experiments.

Monolith	Length (cm)	Width (cm)	Soil Depth (cm)	Soil Volume (m^3)	Surface Slope
MA	80	52.5	31	0.13	0.27
MB	69	50.0	29	0.10	0.35
MC	68	50.0	30	0.10	0.42
MD	85	54.0	35	0.16	0.36

2.3. Instrumentation

A custom-built Mariotte bottle supplied water and regulated the water level in the IP during the experiments (Figures 2.1a and 2.2). It was a 2 m-high PVC pipe with the capacity of about 0.06 m^3. The water level in the IP was set by adjusting in height the air-entry tube inlet of the bottle. The bottle discharged into the IP within a fissured PVC pipe wrapped with geotextile to minimize flow turbulence when the bottle outlet-tap was turned on. The discharged volume was computed from the lowering water level measured in the transparent level gauge of the bottle, which had a resolution of 1 mm (28.6 $mL \cdot mm^{-1}$). Accuracy of the Mariotte device was tested for several discharge rates (from 0.6–4.1 $L \cdot min^{-1}$, the maximum discharge allowed by the bottle) by measuring the water volumes flowing from the bottle outlet. The mean relative error among the collected volumes and the estimated ones with the readings taken at the bottle was 0.6%, which was considered acceptable for the purposes of this study. At the MA, MB and MC monoliths, a syphon system was used both to maintain the prescribed water levels into the OP and to measure the outgoing drainage. The syphon system consisted of a vacuum tube connecting the pit to a small water tank with spillway. The tank hung from a tripod by a rope and pulley, so as to finely tune the reservoir elevation and the water level within the OP accordingly. For a prescribed elevation, the outflow from the spillway was the drainage through the soil monoliths. The outgoing flow discharged into a bucket and was weighted with a scale (5 g of resolution). In monolith MD, the system was slightly different as for the water level control and the collection of the drainage, since pipes through the foam were inserted as spillways in OP (Figure 2.1c). This was done by removing the resting soil from the outside-down foam wall of the OP. The foam was holed in order to place three spillway pipes at prescribed levels, then any gap between the pipes and foam was resealed.

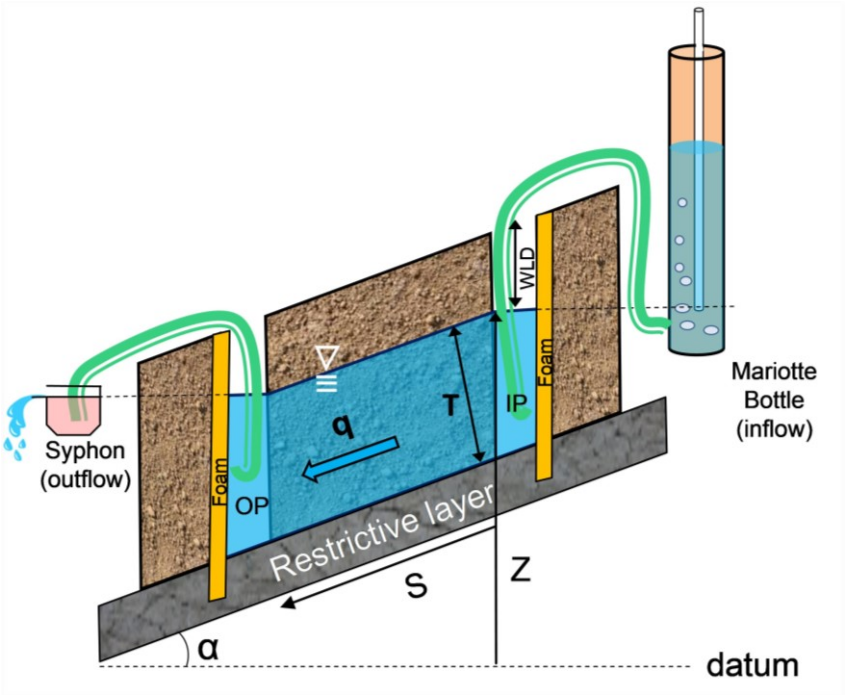

Fig. 2.2. Experimental design to estimate the lateral saturated hydraulic conductivity of soil horizons from drainage of large-volume soil monoliths. The sketch represents the syphon system used in the MA, MB and MC monoliths to set the water levels and collect the drainage.

2.4. Drainage experiments

At first, water was poured into the IP from a storage reservoir located at the top of the hillslope. The water level was slowly increased until it reached the depth of 5 cm below the soil surface. The same water-level depth (WLD) was achieved in the OP by the water that flowed through the soil monolith. At the WLD of 5 cm in the OP, water started flowing in the vacuum tube of the syphon system (monoliths MA to MC), or through the spillway inserted in the foam at that depth (MD). At that moment, we started to feed the IP through the Mariotte bottle and to measure the flow rates. This procedure of soil saturation from below was chosen because it was similar to the bottom-up saturation process that took place during the natural rainfall events, as reported in Pirastru et al. (2014) for the same area. Moreover, visual inspection of the exposed seepage soil face in the OP at the beginning of the drainage reveals the dominant flow processes, i.e., preferential or uniform flows, which helps data interpretation.

For each monolith, the WLDs of 5 cm, 15 cm and 25 cm in both inflow and outflow pits were sequentially imposed. The top 5 cm of soil was excluded to avoid water-table cross depressions at the soil surface. The water levels were changed when either the flows became steady or the time of the stage with a prescribed level lasted over 1.5 h. The inflows and outflows were considered steady once the rate variations were below the instrumental resolutions for more than at least 30 min. The WLD transitions were achieved by first lowering the level in the OP, then waiting for equilibration in the IP until the prescribed depth, over which the bottle restarted supplying water. To measure the low flow rates accurately, the inflows and outflows were monitored by increasing time intervals, namely every 5 min, 10 min and 15 min for WLDs of 5 cm, 15 cm and 25 cm.

2.5. $K_{s,l}$ calculation

The $K_{s,l}$ of the saturated soil layers were estimated by Darcy's formula:

$$K_{s,l} = -\frac{q}{T\ grad\ \phi} \tag{1}$$

where q [$L^2 \cdot T^{-1}$] was the outflow rate per unit width of the monoliths, computed as the mean of the rates over the last half-hour of a stage with a prescribed water level; T was the thickness of the saturated layers, measured perpendicularly to the sloping restrictive layer; and $grad\ \phi$ was the total hydraulic gradient, negative along the flow direction.

The $K_{s,l}$ value determined by Equation (1) represented the average value of lateral saturated hydraulic conductivities, $K_s(z)$, at a specific elevation z within the soil profile that was saturated (Brooks et al., 2004). By definition, $K_{s,l}$ is related to $K_s(z)$ by the following relation:

$$K_{s,l} = \frac{\int_{z_0}^{Z} K_s(z)dz}{Z - z_0} \tag{2}$$

where z_0 and Z are, respectively, the elevation of the restrictive layer and of the water table above an arbitrary datum. The numerator of Equation (2) is the transmissivity of the saturated layer above the restrictive layer, and the denominator is the saturated thickness.

By imposing decreasing water levels in the monolith pits during the drainage experiments, the $K_{s,l}$ values of three decreasing saturated soil thicknesses on the restrictive layer were computed for each monolith by using Equation (1). These values are denoted by $K_{s,l\ WLD5}$, $K_{s,l\ WLD15}$ and $K_{s,l\ WLD25}$ with reference to the water-level depths sequentially applied. These $K_{s,l}$ values are then used to calculate the specific $K_{s,l}$ values of the individual soil layers in each monolith: (i) A horizon, approximately as large as the root zone, from 5 to 15 cm of depth; (ii) upper layer of the B horizon, from 15 to 25 cm of soil depth; (iii) lower layer of the B horizon profile, from 25 cm to the depth of the restrictive layer. Differentiation in the B horizon was done in order to detect the $K_{s,l}$ changes in proximity of the restrictive layer. For computing the specific $K_{s,l}$ of the A horizon, both $K_{s,l\ WLD5}$ and $K_{s,l\ WLD15}$ were used. By denoting with z_{WLD5} and z_{WLD15} the elevations above the datum of the water levels 5 cm and 15 cm deep, respectively, the $K_{s,l}$ of the A horizon was:

$$K_{s,l}(A) = \frac{\int_{z_{WLD15}}^{z_{WLD5}} K_s(z)dz}{z_{WLD5} - z_{WLD15}} = \frac{K_{s,l_{WLD5}} \cdot (z_{\mathrm{WLD5}} - z_0) - K_{s,l_{WLD15}} \cdot (z_{\mathrm{WLD15}} - z_0)}{z_{WLD5} - z_{WLD15}} \quad (3)$$

The same procedure was applied to compute the specific $K_{s,l}$ for the upper part of the B profile, but for this layer the $K_{s,l\ WLD15}$ and $K_{s,l\ WLD25}$ values and the proper water-level elevations were used. Finally, the specific $K_{s,l}$ for the lower part of the B horizon profile was $K_{s,l\ WLD25}$.

3. Results

3.1. Observed inflow and outflow rates

The mean inflow and outflow rates computed over the last 30 min of stages with the three prescribed water levels are shown in Table 2.2. The greatest decrease in drainage rates with depth was recorded in MC, varying by about two orders of magnitude when it was going from a WLD of 5 cm to 25 cm. For this monolith in particular, we observed quick flow through macropores at the seepage face in the OP when the water level was near the soil surface during the saturation stage, whereas uniform matrix flow dominated the drainage for small saturated soil thicknesses on the restrictive layer (WLD > 15 cm). This was different in MB, where for the same water level variation the outflow decreased by 79%. This monolith gave

the highest outflow rates among the monoliths for each set WLD. During the saturation stage, we observed a macropore gushing copiously at the interface between the soil and the restrictive layer. This contributed to sustaining a high soil water transmissivity, despite the lowering of water level.

Table 2.2. Arithmetic means of the outflow and inflow rates calculated over the last 30 min of the stages for each prescribed water-level depth. Inflows are in parentheses. The rates are in $mL \cdot min^{-1} \cdot m^{-1}$.

Monolith	Water-Level Depth (WLD)		
	5 cm	15 cm	25 cm
MA	810 (838)	218 (236)	42 (47)
MB	2660 (2671)	851 (864)	565 (565)
MC	1581 (1595)	273 (272)	21 (15)
MD	307 (2308)	98 (867)	23 (286)

In the monolith MD, the removal of soil from the downhill foam wall of the outflow pit to permit the spillways insertion caused water leakage below the lower end of the foam, from the OP reservoir towards the surrounding soil. This resulted in a poor outflow collection, although the leakage did not hinder setting of the prescribed water levels throughout the experiment time. At the end of the run, the soil resting against the external walls of the foam was removed, in order to check for traces of leakages around the monolith. Signs of water leakage were not found along the external sides, except for the lower foam edge of the OP. This suggested that the supplied water flowed unaffected through the whole soil sample. Therefore, in the monolith MD the measured inflow was used in place of the outflow in Equation (1) for computing $K_{s,l}$.

Figure 2.3a,b show two representative examples of the temporal dynamics of the inflow and outflow rates measured during the drainage experiments. In MA (Figure 2.3a), the inflows for the water-level depths of 5 cm, 15 cm and 25 cm were almost immediately stable at the beginning of the measurement. The same was true for the outflow rates, except for the imposed WLD of 25 cm. In MC (Figure 2.3b), for WLD = 5 cm the flows were nearly stable at the start of the measurement, but approximately 140 min after the start of the experiment linearly decreased, and became 3% lower than the initial values after half an hour. A decreasing rate was observed with WLD set to 15 cm as well. Declining flow rates were also observed in MB and MD monoliths when WLD was 5 cm, and in the MD trough at the stage

with WLD set to 15 cm. In this last case, a steady-state condition was reached at the end of the stage.

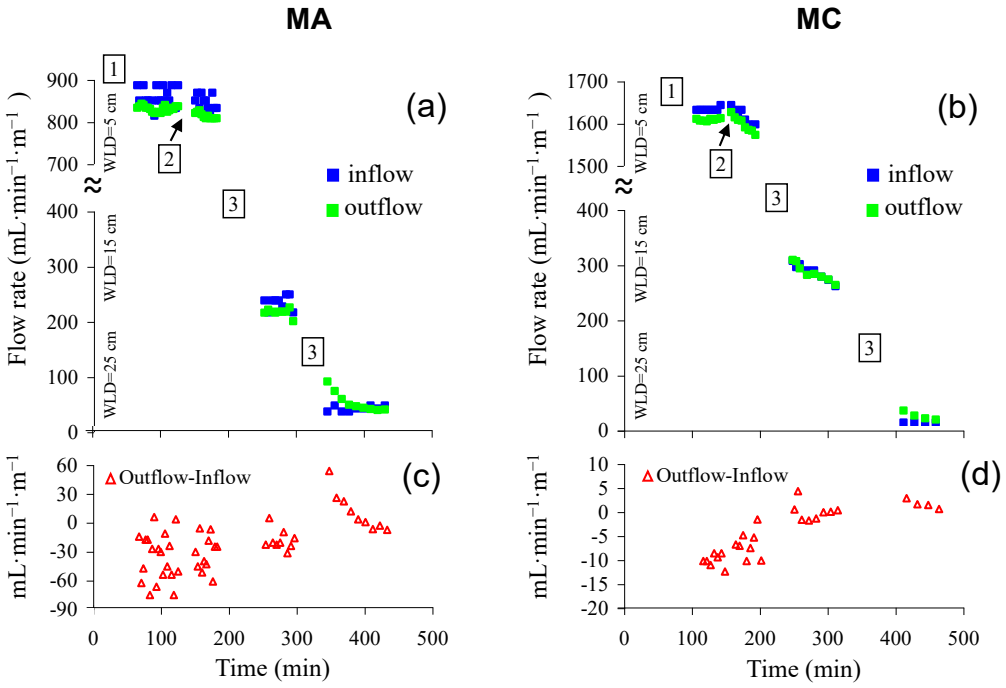

Fig. 2.3. (a,b) Time series of the inflow and outflow rates measured during the experiments in the soil monoliths MA and MC; (c,d) computed differences between outflows and inflows. Note the difference in flow rate scale in the graphics. Numbers in squares indicate the following experiment stages: (1) soil saturation; (2) Mariotte bottle refilling; (3) water-level depth transition.

Initially in all the drainage experiment stages with WLD set to 25 cm, the outflow was observed to be in excess of inflow and progressively was converging towards these latter, as shown in Figure 2.3a,b for MA and MC. This was because the outflow included inflow and vertical drainage from the upper unsaturated soil. The vertical drainage decreased over time due to the progressive desaturating of the unsaturated zone until this approached the hydrostatic equilibrium state.

The differences between the mean rates of outflows and inflows at each end stage of the drainage runs and for the three imposed water levels (Table 2.2) were on average 11 $mL \cdot min^{-1} \cdot m^{-1}$ for monoliths MA, MB and MC. The partials of the differences between outflows and inflows through drainage experiments were at the maximum at the start of the runs, and decreased with time, as illustrated in Figure 2.3c,d for MA and MC, respectively.

The scattering of the outflow/inflow difference data points was caused by measuring errors due to both the instrument resolutions and the difficulty of taking accurate readings at the bottle level gauge, particularly when high water rates were supplied.

3.2. Lateral saturated soil hydraulic conductivities

The estimated $K_{s,l}$ values in the soil monoliths for WLD of 5 cm, 15 cm and 25 cm are reported in Table 2.3. In MC the $K_{s,l}$ decreased by 15 times in the passage from WLD of 5 cm to 25 cm. Smaller reductions with depth were found in the other monoliths, with the exception of MB, where at 25 cm the $K_{s,l}$ increased to 2750 mm·h^{-1}. This was the highest value found among all the experiments. The variability of the $K_{s,l}$ estimates (Table 2.3) increased with depth, because soil heterogeneity effects were averaged over progressively smaller soil volumes. The median values roughly halved going from 5 cm to 15 cm. At WLD of 25 cm, the median $K_{s,l}$ value reduced further, and was 40% lower than the median determined at 15 cm of depth. However, this result was largely affected by very high $K_{s,l}$ found in MB. As can be seen in Table 2.3 and in Figure 2.4, it clearly appeared as an outlier in comparison to the rest of the $K_{s,l}$ assessments. Without considering this monolith, the median $K_{s,l}$ at WLD = 25 cm became about 70% lower than that estimated at the depth of 15 cm.

Table 2.3. Lateral saturated soil hydraulic conductivities, $K_{s,l}$ (mm·h^{-1}), estimated from the drainage experiments in the four soil monoliths for the water-level depths (WLD) of 5 cm, 15 cm and 25 cm from the soil surface.

Monolith	Water-Level Depth		
	5 cm	15 cm	25 cm
MA	724	313	153
MB	2157	1184	2750
MC	1066	307	70
MD	1416	791	509
Median	1241	552	331

The specific $K_{s,l}$ values calculated for the A horizon in the soil monoliths, and for the upper and lower layers of the B horizon, are shown in Figure 2.4. The median value of the specific $K_{s,l}$ was around 2450 mm h^{-1} in the A horizon. This value reduced by 80% in the upper layer of the B horizon. The ratio of the median $K_{s,l}$ of the lower and upper B layers was 0.67 or 0.31, depending on whether or not the monolith MB was included in the calculation.

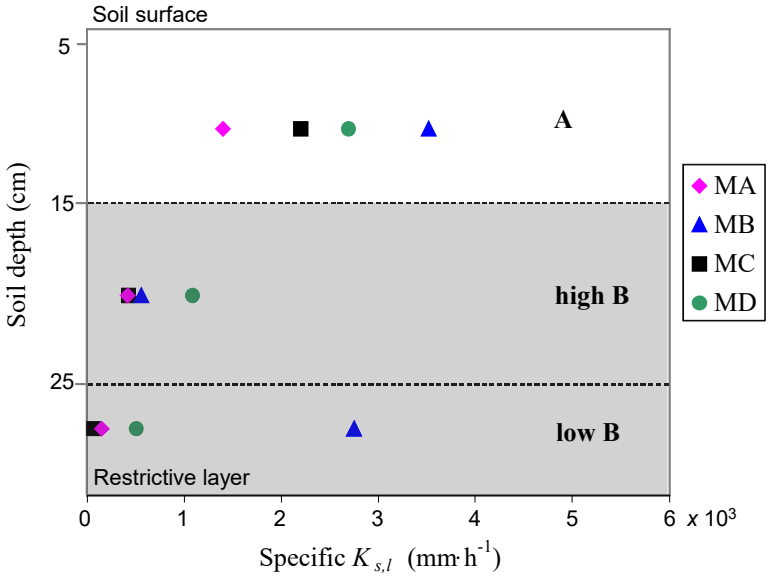

Fig. 2.4. Computed specific $K_{s,l}$ values in the A horizon and in the upper and lower layers of the B horizon. The shaded area is the soil B horizon.

4. Discussion

4.1. Benefits of the proposed field soil $K_{s,l}$ assessment tool

The soil block methodology employed by Blanco et al. (2002) to assess the soil $K_{s,l}$ was modified in order to obtain accurate conductivity values of individual layers in a vertical soil profile, as well as to simplify field procedures. The self-built Mariotte bottle and the syphon system allowed easy and accurate setting of the sequence of descending water levels within the inflow and outflow pits, respectively. The developed procedure appeared simpler than lateral flow collectors embedded in the soil profile in order to yield separately the drainage from each horizon, as undertaken, for instance, by Mendoza and Steenhuis (2002). The procedure illustrated is certainly more practical for investigations in soils with widespread stoniness, where the rock fragments could prevent the collectors from being placed correctly (e.g., in Day et al. (1998)).

The water heads overlying the restrictive layer in both up and downhill pits of the monoliths defined first-type, or Dirichlet, boundary conditions to the flow spatial domain. The positive pressure diagrams at the monolith faces were like those determined by groundwater that built up on the restrictive layer when the soil was saturated by rainfall. Mainly for the

downhill seepage face of the monoliths, digging pits to store water has advantages in comparison with other drainage-collecting systems, such as the aforementioned insertion of lateral flow collectors in the soil profile. In fact, from the latter, water had to be quickly removed to allow measurement, in this way establishing an atmospheric pressure boundary condition at the exfiltration surface.

All the hydrological processes of water leakage, vertical unsaturated flow and air spilling determined the temporal dynamics of the differences between outflows and inflows observed during the drainage experiments. Water leakages were due to percolation in the low-permeable subsoil and leakage at the bottom foam edges. These two processes were expected to decrease sharply over time with progressive subsoil saturation and for the lowering of the hydraulic head settings throughout the experiments. For WLDs set to 5 cm leakages in particular, we expected to account for the greatest part of the differences between outflows and inflows. Water movement from the unsaturated soil zone towards the water table in the monoliths increased the lateral saturated flow. The rates of vertical flow were related to the unsaturated zone thicknesses, and thus were lower at the starting WLD of 5 cm as compared to the other WLDs. Furthermore, at a prescribed WLD, the decrease over time of unsaturated drainage was due to unsaturated zone depletion, as can be deduced from Figure 2.3a,b for WLDs of 25 cm. The soil-air spill process, which was caused by the air-water dissolution and by the drag forces induced by the lateral water flow, contributed to reducing the differences between outflow and inflow during the experiments. However, this process was expected to have the least effect as compared with the water leakages and unsaturated vertical flow. In fact, the initial procedure of soil saturation by slowly increasing the water table level from below, without water ponding on the soil surface, should have facilitated the upward spilling of most entrapped soil air.

The q term of Equation (1) was the flow that perpendicularly was crossing the saturated soil sections throughout the monolith's extent. Hence, in order to obtain reliable estimates of q, the groundwater equipotential lines had to be kept as parallel as possible in the flow spatial domain. First, this was done by imposing equal water-level depths in the pits, which also allowed evaluation with sufficient certainty the flow cross sections and hydraulic gradients to be used in Equation (1). However, within the monoliths, water leakages and unsaturated vertical drainages could have caused deviations from the right conditions, so that both

processes had to be minimized in order to apply Darcy's law properly. In the monoliths MA, MB and MC for the WLDs of 5 cm and 15 cm, and in MB for WLD = 25 cm, at the end of the stages outflows differed negligibly from inflows (Table 2.2). This indicated that the restrictive layer limited the deep-water percolation in a satisfactory way and the polyurethane expandable foam sufficiently sealed all sides of the monoliths. Furthermore, at the end of the stage, the unsaturated vertical drainage rates were negligible in comparison with the high lateral saturated flow rates. Consequently, the q flow terms were evaluated accurately in all the cases we referred to above. The recorded outflows in monolith MD, which were much lower than inflows (Table 2.2), did not account for a fair picture of the flow dynamics within the monolith. In this case, there was field evidence of localized water leakage at the bottom foam edge at the OP, while the hydraulic sealing was preserved in the inflow pit and at the lateral sides of the monolith. Furthermore, the encouraging results from the experiments in MA, MB and MC provided more weight to the idea that, in MD also, the restrictive layer and the undisturbed polyurethane foam efficiently encased the soil block. In addition, the unsaturated vertical flow was also expected to be a negligible fraction of the outflow rate in this monolith at all the investigated WLDs. Therefore, to use inflow instead of outflow in Equation (1) was a reasonable assumption in order to obtain reliable determinations of $K_{s,l}$. Very slow lateral flows were measured in monoliths A and C during the experimental stages with a WLD of 25 cm. In these cases, it could not be excluded that both leakages and unsaturated vertical flows had affected the final outflow values. Therefore, in these experiments, the $K_{s,l}$ evaluations for the highest imposed WLD should be less certain in percentage terms compared to the remaining cases.

Steady-state flows were not achieved in some stages of the experiments with WLD set to 5 cm and 15 cm. In the illustrated case of the MC monolith for WLD = 5 cm (Figure 2.3b), transient ending flows were measured despite the fact that in an early stage of the process steady-state conditions were detected. Similar circumstances were reported in Alagna et al. (2016) for the recorded infiltration rates during prolonged runs. The same behavior also was pointed out by Bagarello et al. (2009) in long-time drainage experiments on small (0.001 m^3) undisturbed soil samples. Dikinya et al. (2008) observed that when water moved in two repacked soil columns, the hydraulic conductivities decreased up to one order of magnitude from the start until the shutdown of the flow experiments. These authors argued that this was

due to particle mobilization and pore-clogging processes. It is probable that in the monoliths, the observed decline of flow rates revealed pore-structure rearrangements, as plausibly caused by the high drainage rates in the soil layers close to the surface. In fact, the fast flow in macropores might have weakened the bonds of fine soil particles. This resulted in the detachment and delivery of particles through the soil, and clogging in the flow path. The choice to vary the water level, despite the fact that the steady-state flow was not always reached, was made in order to limit the ongoing soil rearrangement processes during the experiments. The $K_{s,l}$ values computed for the WLDs of 5 cm and 15 cm by the mean flow measurements from the first half-hour of the experiment stages were on average 12% greater than $K_{s,l}$ calculated from the final mean flow measurements (Table 2.2). This suggested that the soil rearrangement processes did not have significant impacts on the results of the experiments.

4.2. $K_{s,l}$ values of individual soil horizons

Median $K_{s,l}$ of 2450 mm·h^{-1} was computed for the A soil horizon averaging the specific $K_{s,l}$ values determined through Equation (3) for each soil monolith (Figure 2.4). The high median $K_{s,l}$ indicated that macropores governed the lateral drainage processes in this horizon. Decayed roots and micro- and mesofauna activities were probably most responsible for the slope-parallel macropore network, which was observed close to the soil surface. Similar findings were reported by Brooks et al. (2004), which estimated $K_{s,l}$ values up to 600 mm·h^{-1} in the macro-porous A horizon of their study site. Also Appels et al. (2015) measured topsoil $K_{s,l}$ values over 1900 mm·h^{-1}. Dusek et al. (2012) used $K_{s,l}$ values of several thousands of mm·h^{-1} to simulate water flow in macropores in the superficial soil layers in an experimental hillslope. The median $K_{s,l}$ value, 552 mm·h^{-1} (Table 2.3), of the B horizon of the monoliths (from 15 cm of depth to the restrictive layer), was about 78% lower than that of the A horizon. In particular, in the upper layer of the B horizon (15–25 cm of depth) specific $K_{s,l}$ values spanning from around 400–1000 mm·h^{-1} indicated that macropores here dominated the flow processes. In the lower B layer, estimated specific $K_{s,l}$ values ranging from tens to thousands of mm·h^{-1} suggested that, in some cases, the flow was dominated by the soil matrix and in the rest by macropore flow. Overall, median specific values of $K_{s,l}$ were reduced by a factor of 0.20 passing from the A to the upper B layer, and further decreased in the lower B

horizon compared to the upper B. This indicated that there was a vertical gradient of macropore density. Instead, the increase of matrix porosity with depth could be excluded, based on a previous investigation in the same site (2014) reporting the invariance of the bulk density along the vertical soil profile.

Pirastru et al. (2014) determined average soil vertical hydraulic conductivities of 139 $mm \cdot h^{-1}$ and 94 $mm \cdot h^{-1}$ in the A and B horizons, respectively, with a single-ring infiltrometer (see Table 2 in Pirastru et al. (2014), winter measurements). Therefore, the saturated soil hydraulic conductivities were much greater in the sub-horizontal direction compared to the vertical conductivity. Pirastru et al. (2014) and Pirastru et al. (2017) observed, in piezometers augered to the restrictive layer, the water table rapidly depleted when it rose in the A horizon. Even under the heaviest rainfall, the water table never reached the soil surface, with the exception of the wells located at the foot slope, close to the stream. Conversely, the water table persisted in the lower part of the B soil profile throughout the inter-storm periods during the rainy winters, and completely ran out from the hillslope only at the beginning of the dry periods in spring. The hydromorphic signs as greyish, brown and reddish soil color anomalies, commonly found in this part of the profile, also confirm that here the soil is prone to waterlogging. The very high $K_{s,l}$ values computed for the near soil surface in the monoliths can explain the reported groundwater hydrological dynamics in the A horizon of the hill. In fact, the high lateral permeability of this horizon caused the swift downslope delivery of the soil water, resulting in the rapid depletion of the water table when it approached the soil surface. This hindered the saturation of the whole soil profile, even during intense precipitation. In the lower B horizon, the persistence of the water table for long periods across the hillslope indicated the lower permeability of the soil near the restrictive layer. This hydrological behavior, which was in contrast to that observed in the A horizon, was consistent with the remarkable decreasing of the median $K_{s,l}$ value along the vertical soil profile, as determined through the drainage experiments in the soil monoliths.

Another objective of the research was to investigate the effectiveness of the drainage experiments in large soil-volume monoliths in order to evaluate spatially representative $K_{s,l}$ values for the soil horizons in the analysed hillslope. For this reason, we took the relationship between $K_{s,l}$ and water-table depths reported in Pirastru et al. (2017) for the same site as a benchmark. The authors estimated soil average $K_{s,l}$ by combining measurements of drainage

rates from a 2.5 m-long drain and water-table levels from two well transects extending 10 m upslope of the drain. Therefore, this relationship was considered representative for the soil over a large area of the hillslope. Although specific $K_{s,l}$ values for soil horizons are not shown in Pirastru et al. (2017), these can easily be gathered by applying Equation (3) with the $K_{s,l}$ values of the large-scale relationship coupled with the prescribed soil depths and the corresponding water-table elevations. Having done this, mean specific large-scale $K_{s,l}$ values of 8000 mm·h^{-1}, 780 mm·h^{-1} and 180 mm·h^{-1} were calculated for the A, upper B and lower B soil layers, respectively. Compared to these values, the median $K_{s,l}$ values of the same soil layers in the monoliths differed by factors of 0.3, 0.6 and 1.8, respectively. Hence, the $K_{s,l}$ values in the soil monoliths were similar in magnitude to the large-scale $K_{s,l}$ determinations. Brooks et al. (2004) reported hillslope-scale estimations in soil horizons within one and two orders of magnitude greater than the available values from Guelph permeameter measurements. Montgomery and Dietrich (1995) evaluated the $K_{s,l}$ of an A horizon both by falling-head tests in wells and by yielding discharge from a gully cut, which had shown evidence of macropore flow. They estimated $K_{s,l}$ values from the falling-head tests ranging between 10^{-1} cm·s^{-1} to 10^{-2} cm·s^{-1}, and large-scale $K_{s,l}$ values comparable only with the high end of the range of conductivities obtained in the wells. Chappell and Lancaster (2007) reported large-scale $K_{s,l}$ values by trench percolation tests on average 37 times larger than the mean conductivity obtained by slug tests made in piezometers adjacent to their trenches. Therefore, in comparison to these studies, in our investigation we detected a more satisfactory agreement between the estimated $K_{s,l}$ in the monoliths and the values available from the large spatial scale investigation.

For the lower B soil layer, the median $K_{s,l}$ value measured in soil monoliths is more consistent with the large-scale value from the drain when the high $K_{s,l}$ value estimated in MB (2750 mm·h^{-1}) is excluded from the computation. In fact, in this case the median $K_{s,l}$ value of the lower B layer was just 15% lower than the large-scale value. This result suggested that in the monolith MB the characteristics of lateral drainage for small-saturated soil thicknesses of the hillslope were probably not fairly represented. Also, the water-table dynamics reported for the B horizon of this site by Pirastru et al. (2014) and Pirastru et al. (Pirastru et al., 2017) further supported the idea that in MB the characteristics of soil lateral drainage were misrepresented. During the saturation phase of the experiment, we observed that an isolated,

large pore located at the soil-restrictive layer interface quickly drained when water was initially supplied to the inflow pit. We assume that this macropore ran thought the entire length of the sample. Instead, such macropores in the field are commonly constrained in their extent by the surrounding soil matrix. By converting this macropore into a continuous pipe within the sample, the soil $K_{s,l}$ may have been significantly overestimated.

In a modeling study assessing the climate and land-use change effects in the water balance at the Baratz lake catchment, Niedda et al. (Niedda et al., 2014) used a maximum value of the $K_{s,l}$ parameter of 1000 mm·h^{-1} at the soil surface, then it decreased in depth. They efficiently simulated the discharge at the catchment outlet. The median $K_{s,l}$ values (Table 2.3) found in the soil monoliths were in line with the parameter values used in simulations. This suggests that drainage experiments in large-volume soil monoliths can potentially be used to obtain parameter values for the hydrological models, in order to simulate the runoff-generation processes at catchment scale.

5. Conclusions

The lateral saturated hydraulic conductivities in the soil horizons of the shallow steep soil of a hillslope was evaluated in situ by drainage experiments in monoliths ranging in volume from 0.1 m^3 to 0.16 m^3. The expandable polyurethane foam used to encase the samples on the field made the hydraulic isolation of the soil blocks easy. Moreover, the removal of the foam from the field was easy, allowing a reduction of the impact on the experimental area. Minimizing leakages along the sides of the foam barriers allowed evaluation of the flow rate, cross-section area and hydraulic gradient terms of Darcy's law, in order to obtain reliable $K_{s,l}$ values. Thanks to the large volume sampled in each experiment, soil macropores were included in the measurements and sufficiently characterized. The information about the lateral permeability of the soil horizons that was obtained was consistent with the groundwater dynamics observed during previous investigations in the hillslope studied. Likewise, the median values of the $K_{s,l}$ obtained in the soil horizons of monoliths were comparable with large spatial-scale $K_{s,l}$ values computed through drain flow measurements in the same site. This indicated that the hydrological large-scale effects of the soil macropore network of the hillslope were sufficiently represented in the large-volume soil samples. Currently, drainage measurements are ongoing at an 8.5 m-long drain, in order to yield $K_{s,l}$ values that could be

more representative for the hillslope scale. A future comparison with these values will give us further indications about the suitability of the drainage experiments in the soil monoliths for characterizing hydrological processes and determining hydraulic conductivities at the hillslope-scale.

It took four days to prepare the setup and perform the drainage experiment on each soil monolith in order to determine the $K_{s,l}$. Considering the effort required and the need to maintain a field campaign of reasonable duration, a limited number of samples were investigated. Despite this, $K_{s,l}$ values sufficiently representative for the soil in the hillslope were achieved. The $K_{s,l}$ discrepancies between the monoliths and the drain were smaller in comparison with those reported by other authors who have compared small- and large-scale $K_{s,l}$ values. Therefore, the methodology described in this study appears to represent a step forward in the possibility of detecting, through a low number of experiments, representative hydraulic conductivities of soil horizons over large spatial scales. Hence, such experimentation will allow, through a sustainable effort, valuable information for interpreting hydrological processes and parameterizing runoff-generation models both at the hillslope and catchment scale to be obtained.

Acknowledgments: This research was funded by the program**:** "Promotion of the scientific research and technological innovation in Sardinia (IT), RL7/2007", specific project "Anthropogenic and climate impacts in the hydrologic cycle at basin and hillslope scales".

Author Contributions: M.P., R.M. and S.D.P. carried out the experimental work and write the paper. All authors designed the work and analyzed the results.

6. References

Alagna, V., Bagarello, V., Di Prima, S., Giordano, G., Iovino, M., 2016. Testing infiltration run effects on the estimated water transmission properties of a sandy-loam soil. Geoderma 267, 24–33. https://doi.org/10.1016/j.geoderma.2015.12.029

Alaoui, A., Caduff, U., Gerke, H.H., Weingartner, R., 2011. A Preferential Flow Effects on Infiltration and Runoff in Grassland and Forest Soils. Vadose Zone Journal 10, 367. https://doi.org/10.2136/vzj2010.0076

Ambroise, B., Beven, K., Freer, J., 1996. Toward a Generalization of the TOPMODEL Concepts: Topographic Indices of Hydrological Similarity. Water Resources Research 32, 2135–2145. https://doi.org/10.1029/95WR03716

Ameli, A.A., Amvrosiadi, N., Grabs, T., Laudon, H., Creed, I.F., McDonnell, J.J., Bishop, K., 2016. Hillslope permeability architecture controls on subsurface transit time distribution and flow paths. Journal of Hydrology 543, 17–30. https://doi.org/10.1016/j.jhydrol.2016.04.071

Appels, W.M., Graham, C.B., Freer, J.E., McDonnell, J.J., 2015. Factors affecting the spatial pattern of bedrock groundwater recharge at the hillslope scale: Spatial Patterns of Bedrock Groundwater Recharge. Hydrological Processes 29, 4594–4610. https://doi.org/10.1002/hyp.10481

Bagarello, V., Sferlazza, S., Sgroi, A., 2009. Testing laboratory methods to determine the anisotropy of saturated hydraulic conductivity in a sandy-loam soil. Geoderma 154, 52–58. https://doi.org/10.1016/j.geoderma.2009.09.012

Bagarello, V., Sgroi, A., 2008. Testing Soil Encasing Materials for Measuring Hydraulic Conductivity of a Sandy-Loam Soil by the Cube Methods. Soil Science Society of America Journal 72, 1048. https://doi.org/10.2136/sssaj2007.0022

Bathke, G.R., Cassel, D.K., 1991. Anisotropic Variation of Profile Characteristics and Saturated Hydraulic Conductivity in an Ultisol Landscape. Soil Science Society of America Journal 55, 333. https://doi.org/10.2136/sssaj1991.03615995005500020005x

Beckwith, C.W., Baird, A.J., Heathwaite, A.L., 2003. Anisotropy and depth-related heterogeneity of hydraulic conductivity in a bog peat. II: modelling the effects on groundwater flow. Hydrological Processes 17, 103–113. https://doi.org/10.1002/hyp.1117

Blanco-Canqui, H., Gantzer, C.J., Anderson, S.H., Alberts, E.E., Ghidey, F., 2002. Saturated Hydraulic Conductivity and Its Impact on Simulated Runoff for Claypan Soils. Soil Science Society of America Journal 66, 1596–1062. https://doi.org/10.2136/sssaj2002.1596

Brooks, E.S., Boll, J., McDaniel, P.A., 2004. A hillslope-scale experiment to measure lateral saturated hydraulic conductivity. Water Resour. Res. 40, W04208. https://doi.org/10.1029/2003WR002858

Brye, K.R., Morris, T.L., Miller, D.M., Formica, S.J., Van Eps, M.A., 2004. Estimating Bulk Density in Vertically Exposed Stoney Alluvium Using a Modified Excavation Method. Journal of Environment Quality 33, 1937. https://doi.org/10.2134/jeq2004.1937

Castellini, M., Iovino, M., Pirastru, M., Niedda, M., Bagarello, V., 2016. Use of BEST Procedure to Assess Soil Physical Quality in the Baratz Lake Catchment (Sardinia, Italy). Soil Science Society of America Journal 80, 742. https://doi.org/10.2136/sssaj2015.11.0389

Chappell, N.A., Lancaster, J.W., 2007. Comparison of methodological uncertainties within permeability measurements. Hydrological Processes 21, 2504–2514. https://doi.org/10.1002/hyp.6416

Day, R.L., Calmon, M.A., Stiteler, J.M., Jabro, J.D., Cunningham, R.L., 1998. Water balance and flow patterns in a fragipan using in situ soil block. Soil science 163, 517–528.

Dikinya, O., Hinz, C., Aylmore, G., 2008. Decrease in hydraulic conductivity and particle release associated with self-filtration in saturated soil columns. Geoderma 146, 192–200. https://doi.org/10.1016/j.geoderma.2008.05.014

Du, E., Rhett Jackson, C., Klaus, J., McDonnell, J.J., Griffiths, N.A., Williamson, M.F., Greco, J.L., Bitew, M., 2016. Interflow dynamics on a low relief forested hillslope: Lots of fill, little spill. Journal of Hydrology 534, 648–658. https://doi.org/10.1016/j.jhydrol.2016.01.039

Dusek, J., Vogel, T., Dohnal, M., Gerke, H.H., 2012. Combining dual-continuum approach with diffusion wave model to include a preferential flow component in hillslope scale modeling of shallow subsurface runoff. Advances in Water Resources 44, 113–125. https://doi.org/10.1016/j.advwatres.2012.05.006

Germer, K., Braun, J., 2015. Determination of Anisotropic Saturated Hydraulic Conductivity of a Macroporous Slope Soil. Soil Science Society of America Journal 79, 1528. https://doi.org/10.2136/sssaj2015.02.0071

Giadrossich, F., Niedda, M., Cohen, D., Pirastru, M., 2015. Evaporation in a Mediterranean environment by energy budget and Penman methods, Lake Baratz, Sardinia, Italy. Hydrology and Earth System Sciences 19, 2451–2468. https://doi.org/10.5194/hess-19-2451-2015

Maneta, M., Schnabel, S., Jetten, V., 2008. Continuous spatially distributed simulation of surface and subsurface hydrological processes in a small semiarid catchment. Hydrological Processes 22, 2196–2214. https://doi.org/10.1002/hyp.6817

Matonse, A.H., Kroll, C.N., 2013. Applying hillslope-storage models to improve low flow estimates with limited streamflow data at a watershed scale. Journal of Hydrology 494, 20–31. https://doi.org/10.1016/j.jhydrol.2013.04.032

McDaniel, P.A., Regan, M.P., Brooks, E., Boll, J., Barndt, S., Falen, A., Young, S.K., Hammel, J.E., 2008. Linking fragipans, perched water tables, and catchment-scale hydrological processes. CATENA 73, 166–173. https://doi.org/10.1016/j.catena.2007.05.011

McGuire, K.J., McDonnell, J.J., 2010. Hydrological connectivity of hillslopes and streams: Characteristic time scales and nonlinearities. Water Resources Research 46. https://doi.org/10.1029/2010WR009341

Mendoza, G., Steenhuis, T.S., 2002. Determination of hydraulic behavior of hillsides with a hillslope infiltrometer. Soil Science Society of America Journal 66, 1501. https://doi.org/10.2136/sssaj2002.1501

Montgomery, D.R., Dietrich, W.E., 1995. Hydrologic Processes in a Low-Gradient Source Area. Water Resources Research 31, 1–10. https://doi.org/10.1029/94WR02270

Muller, R.N., Hamilton, M.E., 1992. A simple, effective method for determining the bulk density of stony soils[1]. Communications in Soil Science and Plant Analysis 23, 313–319. https://doi.org/10.1080/00103629209368590

Niedda, M., Pirastru, M., Castellini, M., Giadrossich, F., 2014. Simulating the hydrological response of a closed catchment-lake system to recent climate and land-use changes in semi-arid Mediterranean environment. Journal of Hydrology 517, 732–745. https://doi.org/10.1016/j.jhydrol.2014.06.008

Page-Dumroese, D.S., Brown, R.E., Jurgensen, M.F., Mroz, G.D., 1999. Comparison of Methods for Determining Bulk Densities of Rocky Forest Soils. Soil Science Society of America Journal 63, 379–383. https://doi.org/10.2136/sssaj1999.03615995006300020016x

Pirastru, M., Bagarello, V., Iovino, M., Marrosu, R., Castellini, M., Giadrossich, F., Niedda, M., 2017. Subsurface flow and large-scale lateral saturated soil hydraulic conductivity in a Mediterranean hillslope with contrasting land uses. Journal of Hydrology and Hydromechanics 65. https://doi.org/10.1515/johh-2017-0006

Pirastru, M., Niedda, M., Castellini, M., 2014. Effects of maquis clearing on the properties of the soil and on the near-surface hydrological processes in a semi-arid Mediterranean environment. Journal of Agricultural Engineering 45, 176. https://doi.org/10.4081/jae.2014.428

Schmocker-Fackel, P., Naef, F., Scherrer, S., 2007. Identifying runoff processes on the plot and catchment scale. Hydrology and Earth System Sciences 11, 891–906. https://doi.org/10.5194/hess-11-891-2007

Starr, J.L., Sadeghi, A.M., Pachepsky, Y.A., 2005. Monitoring and Modeling Lateral Transport through a Large In Situ Chamber. Soil Science Society of America Journal 69, 1871. https://doi.org/10.2136/sssaj2004.0162

Stutter, M.I., Deeks, L.K., Billett, M.F., 2005. Transport of conservative and reactive tracers through a naturally structured upland podzol field lysimeter. Journal of Hydrology 300, 1–19. https://doi.org/10.1016/j.jhydrol.2004.04.026

van Schaik, N.L.M.B., Bronstert, A., Jong, S.M. de, Jetten, V.G., Dam, J.C. van, Ritsema, C.J., Schnabel, S., 2014. Process-based modelling of a headwater catchment in a semi-arid area: the influence of macropore flow. Hydrological Processes 28, 5805–5816. https://doi.org/10.1002/hyp.10086

van Schaik, N.L.M.B., Schnabel, S., Jetten, V.G., 2008. The influence of preferential flow on hillslope hydrology in a semi-arid watershed (in the Spanish Dehesas). Hydrological Processes 22, 3844–3855. https://doi.org/10.1002/hyp.6998

van Verseveld, W.J., McDonnell, J.J., Lajtha, K., 2009. The role of hillslope hydrology in controlling nutrient loss. Journal of Hydrology 367, 177–187. https://doi.org/10.1016/j.jhydrol.2008.11.002

Vepraskas, M.J., Williams, J.P., 1995. Hydraulic Conductivity of Saprolite as a Function of Sample Dimensions and Measurement Technique. Soil Science Society of America Journal 59, 975. https://doi.org/10.2136/sssaj1995.03615995005900040003x

Weiler, M., McDonnell, J.J., Tromp-van Meerveld, I., Uchida, T., 2006. Subsurface Stormflow, in: Anderson, M.G., McDonnell, J.J. (Eds.), Encyclopedia of Hydrological Sciences. John Wiley & Sons, Ltd, Chichester, UK.

Wienhöfer, J., Zehe, E., 2014. Predicting subsurface stormflow response of a forested hillslope – the role of connected flow paths. Hydrology and Earth System Sciences 18, 121–138. https://doi.org/10.5194/hess-18-121-2014

CHAPTER 3

In situ characterization of preferential flow by combining plot- and point-scale infiltration experiments on a hillslope

S. Di Prima[1,*], R. Marrosu[1], L. Lassabatere[2], R. Angulo-Jaramillo[2], M. Pirastru[1]

[1] Agricultural Department, University of Sassari, Viale Italia, 39, 07100 Sassari, Italy
[2] Université de Lyon; UMR5023 Ecologie des Hydrosystèmes Naturels et Anthropisés, CNRS, ENTPE, Université Lyon 1, 3 rue Maurice Audin, 69518 Vaulx-en-Velin, France

Published in: *Journal of Hydrology 2018, 563, 633-642.*

https://doi.org/10.1016/j.jhydrol.2018.06.033

Abstract. This study focuses on the identification of the lateral preferential flow at the hillslope scale and the estimation of the saturated hydraulic conductivity for the fast-flow region, $K_{s,f}$, based on infiltration experiments carried out at different spatial scales (point- and plot-scales), and at different soil depths. The discrepancies between the considered scales were mainly attributed to macropore flow and the difficulty in adequately embodying the macropore network on small sampled soil volumes. Conversely, at the plot-scale, the sampled volume was sufficient to activate the macropore network. This information helped establish the usability of a given technique to determine the parameters describing the hydraulic properties of the soil in the matrix and fast-flow regions. While Ks data obtained from the Beerkan method with the Beerkan Estimation of soil Transfer (BEST) parameter algorithm (point-scale) were used to describe the matrix ($K_{s,m}$), the saturated hydraulic conductivity for the fast-flow region was estimated using the soil block method (plot-scale). Estimated $K_{s,f}$ values were one to three orders of magnitude higher than $K_{s,m}$. The overall decrease of $K_{s,f}$ with the soil depth supported the hypothesis that the macropore density decreased as a function of depth, yielding higher macropore flow variability. The soil block method, in association with the Beerkan infiltration runs, allowed the estimation of the saturated hydraulic conductivity for the fast-flow region based on a relatively simple field procedure.

Keywords: Beerkan, BEST algorithm, in situ soil block method, cube method, lateral preferential flow, macropore.

1. Introduction

Scarcity of water has been universally recognized as a global issue (Vörösmarty et al., 2000). Climatic changes have profound effects on the hydrological cycle, thus reducing the availability of water resources in many environments (Groppelli et al., 2011). In semiarid and arid regions, increasing demands on limited water supplies require urgent efforts to improve water quality and quantity by preserving and improving the groundwater recharge of surface water bodies (Scanlon et al., 2006). Recharge processes can be classified as uniform downward movements of water through the unsaturated zone (piston flow), and nonuniform downward water movement along more active pathways, also referred to as preferential flow (Sukhija et al., 2003). Preferential flow can contribute to the rapid transport of contaminants from the soil surface into receiving streams, bypassing the filtering capacity of the soil (e.g., Lamy et al., 2009; Lassabatere et al., 2007; Prédélus et al., 2017). Water flow may mainly occur via preferential flow paths (Blöschl and Sivapalan, 1995), especially at the hillslope scale. Therefore, there is an urgent need to assess procedures and techniques for characterizing water transport in hillslopes especially when this transport appears to be affected by preferential flow paths, which may be induced by structural cracks, faunal activity or roots, specific pedological conditions, and soil management practices (Angulo-Jaramillo et al., 2016).

The saturated soil hydraulic conductivity, K_s, exerts a dominating influence on the partitioning of rainfall in vertical and lateral flow paths (Dusek et al., 2012). Therefore, estimates of K_s are essential for describing and modeling hydrological processes (Niedda and Pirastru, 2013; Zimmermann et al., 2013). However, this soil property may be scale-dependent mainly owing to the soil structure, preferential flow paths, and heterogeneities, whose effects cannot be observed and quantified in measurements conducted on small soil volumes. In addition, the scale dependence of flow and transport parameters essentially makes the use of parameters estimated through pedotransfer functions for numerical simulations impossible (Pachepsky et al., 2014). The saturated hydraulic conductivity must be measured in the laboratory or field. Several studies have shown that the saturated soil hydraulic conductivity values, K_s, measured on macroporous soils, can vary over several orders of magnitude depending on the sampled soil volume (Chapuis et

al., 2005). For instance, Vepraskas and Williams (1995) compared K_s values using sample volumes equal to 3.5×10^{-4}, 6.3×10^{-3}, and 6.8×10^{-1} m^3, concluding that the minimum sample size needed in situ for K_s measurements ought to be approximately equal to at least 5×10^{-3} m^3. Experiments used to determine K_s values at different spatial scales were performed by Chappell and Lancaster (2007). These authors applied six field methods, namely slug tests, constant- and falling-head borehole permeameters, a ring permeameter and two types of trench tests. The K_s values determined by the larger scale experiments, i.e., the trench percolation tests were, on average, 37 times larger than the mean conductivity obtained by slug tests conducted using piezometers positioned near the trenches (Chappell and Lancaster, 2007). Brooks et al. (2004) discussed different reasons to explicate such a discrepancy. For instance, small samples may not adequately represent water transmission, since smaller sampled volumes imply a smaller opportunity to include macropores (Zobeck et al., 1985). In particular, the extent of the macropores in the porous medium was considered as the main factor in determining the gap between measurements.

Hillslope-scale measurements overcome the lack of representativeness commonly encountered in small-scale measurements and allow process characterization at the appropriate scale. These types of measurements are therefore recommended for model calibration. However, the number of studies that have focused on the assessment of large-scale experiments and their comparisons with smaller-scale experiments have been limited. Among the studies that focused on large-scale experiments, those that have addressed preferential or macropore flows are particularly few. Montgomery and Dietrich (1995) compared the hydraulic conductivity calculated from a gully head cut with those observed in falling head tests. Only the higher values obtained from this latter experiment approached the bulk conductivity measured from the gully head cut by integrating through- and macropore flows. Brooks et al. (2004) proposed a methodology to measure the lateral K_s values at the top of an impeding layer at the hillslope scale. Their measurements yielded K_s values from one to two orders of magnitude larger than those measured at small-scales on small soil cores and by using the Guelph permeameter. The discrepancy between measurements at different spatial scales was greatest near the surface and was attributed to the effect of the macropores. Furthermore, according to these authors, more economical methods are needed to obtain spatially distributed K_s data, or for routine measurements (Brooks et al., 2004). Reliable K_s

values should be measured on a soil volume similar to the minimum representative elementary volume (REV) to incorporate the natural heterogeneity of the soil (Mendoza and Steenhuis, 2002). The REV is the smallest volume over which a measurement can be made to yield a representative value of the entire porous medium (Pachepsky and Hill, 2017). Its size depends on the soil structural characteristics and it is expected to increase for decreasing macropore spatial densities. Thus, in order to adequately represent the hydrological effects of the macropore network, the REV should include a sufficient number of nodes and branches in such a way to representatively embody the macropore network topology since it may control scale dependencies.

The in situ block method (Day et al., 1998) has proven to be a useful tool for saturated soil hydraulic conductivity measurements. This technique consists of measuring water flow in situ on a large, undisturbed soil block that seals the exposed sides in order to confine water flow. For example, Day et al. (1998) measured water flow on a 3.38 m^3 soil block. The block's vertical faces were sealed using bentonite, sand, and lumber. Blanco-Canqui et al. (2002) evaluated K_s on three, in situ, 0.029 m^3 soil blocks enclosed by steel plates, and inserted approximately 35 cm below the soil surface and on bentonite-slurry to seal the soil-steel plate interfaces. Mendoza and Steenhuis (2002) developed and tested a hillslope infiltrometer to measure in situ vertical and lateral saturated soil hydraulic conductivity. The hillslope infiltrometer is a metal box installed around an undisturbed 0.045 m^3 soil block slightly smaller than the infiltrometer. Starr et al. (2005) designed an in situ steel chamber for studying water flow under shallow water table and riparian zone conditions. The chamber was lowered over a 0.97 m^3 soil block. However, K_s measurements on the soil block remain rare for the following reasons: i) the need for a sloping impermeable bed to avoid deep-water percolation, ii) the need to encase a large soil volume with impermeable materials so that all terms of Darcy's law can be unambiguously defined, iii) the need for a number of operators over the entire duration of the experiment, and the iv) the need of a large displacement of liquid to reach steady state conditions during flow measurements.

Several studies have considered small-scale measurements on macroporous soils including both laboratory and in situ tests (Akay et al., 2008). These approaches are generally simpler and parsimonious in terms of the experimental devices and required measurements. However, small-scale measurements may not adequately represent K_s depending on whether

water flows through a small fraction of the soil along preferential flow paths (Bouma et al., 1977) or only through the matrix. In fact, at this scale, macropores are hardly intercepted, while their continuity at the larger scale is unknown (Beven and Germann, 1982; Zobeck et al., 1985). Moreover, the presence of aggregates, stones, fissures, fractures, tension cracks, and root holes, commonly encountered in unsaturated soil profiles, is difficult to represent in small samples (Haverkamp et al., 1999). The dual permeability approach has been developed for modeling and for quantifying preferential flow (Gerke et al., 2015; Šimůnek et al., 2003). The dual-permeability approach assumes that soils encompass two regions, including the matrix and the fast-flow regions that respectively host the smallest and the larger pores. Lassabatere et al. (2014b) used the dual-permeability approach to model water infiltration below ponded and tension infiltrometers in heterogeneous soils. At the hillslope scale, Dusek et al. (2012) studied the preferential flow effects on the subsurface runoff by combining a one-dimensional (1D) vertical dual-continuum approach with a 1D lateral flow equation. More recently, different innovative approaches were proposed for dual- and multiple-permeability medium characterizations. For instance, Abou Najm and Atallah (2016) proposed a new method to experimentally characterize porous media by using Newtonian and non-Newtonian fluids. Lassabatere et al. (2014a) proposed the BEST–2K method for hydraulic characterization of dual permeability media on the infiltration data acquired on the field. However, all these methods need to be further developed and tested to address processes at the small scale (i.e., maximum meter scale).

The objective of this research was to characterize and quantify a lateral preferential flow at the hillslope scale. For this purpose, we considered the double permeability approach (concomitancy of fast-flow and matrix regions) and estimated the saturated hydraulic conductivities of both fast-flow and matrix regions, $K_{s,f}$ and $K_{s,m}$, by coupling data from the infiltration experiments carried out at different spatial scales, namely, at point- and plot-scales. Specifically, we combined the following experiments: (i) in situ, small scale measures of soil vertical hydraulic conductivity using the Beerkan method, (ii) laboratory small scale measures of vertical and horizontal hydraulic conductivity using the modified cube method, and (iii) plot-scale measure of lateral hydraulic conductivity using in situ soil blocks. We assumed that Beerkan runs would help the determination of the saturated hydraulic conductivity of the matrix and the modified cube method in the determination of the vertical

and horizontal hydraulic conductivity of the soil. These measures are then used to analyze the observed flow through the soil blocks and to identify and quantify the contribution of the matrix and the macropore network to the total lateral flux as a function of the volume of the soil block that is submitted to lateral flow.

2. Material and Methods

2.1. Study site description

The study area consists of a north-facing steep slope side located in the Baratz Lake basin (Niedda et al., 2014) on Sardinia's North-West coast in Italy (40.69825 N, 8.2346 E, WGS84). The site features a semiarid Mediterranean climate with a mild winter, warm summer, and a high water deficit between April and September. The mean annual temperature is 15.8°C. The average annual precipitation is approximately 600 mm, mainly concentrated from autumn to spring. The potential evapotranspiration is approximately 1000 mm $year^{-1}$. The experimental hillslope has elevations ranging from 51 to 65 m a.s.l., and it is approximately 60 m long, and with an average slope of 30%. While the incoming surface and subsurface flows are diverted by the ditches on both sides of a road at the upper end, the hillslope is drained by the main stream channel of the catchment at the toe. The hillslope soil was classified as a Lithic Haploxerepts (Soil Survey Staff, 2006). Its profile is approximately 0.3–0.4 m deep. The soil horizons include A, Bw, and C (Pirastru et al., 2014). The latter is a dense altered substratum of Permian sandstone which exhibits very low permeability (Castellini et al., 2016). During the rainy season, a perched water table and lateral subsurface flow were observed owing to the presence of this restrictive layer. In terms of vegetation, the experimental area is covered with spontaneous grass grown after the clearing of the Mediterranean maquis and deep moldboard ploughing. The conversion into grassland took place approximately 15 years ago in order to create a 15 m wide firebreak. The area has remained almost unmanaged ever since.

2.2. Soil sampling

Soil samples were collected at depths of 0, 5, 10, 20 cm. In particular, undisturbed soil cores (0.05 m in height and 0.05 m in diameter) were collected at randomly sampled points and were used to determine both the soil bulk density, ρ_b (g cm^{-3}), and the initial volumetric soil water content, θ_i ($cm^3 cm^{-3}$). The soil porosity was calculated from the ρ_b data, assuming a

soil particle density of 2.65 g cm^{-3}. According to other investigations, the field's saturated soil water content, θ_s (cm^3cm^{-3}), was equal to the porosity (Di Prima et al., 2018; Mubarak et al., 2009).

Disturbed soil samples were also collected inside the confined soil after each ponding infiltration runs and was used (50 g for each sample) to determine the particle size distribution based on conventional methods following H_2O_2 pretreatment to eliminate organic matter and clay deflocculation using sodium metaphosphate and mechanical agitation (Gee and Bauder, 1986). In particular, fine size fractions were determined using the hydrometer method, whereas the coarse fractions were obtained by mechanical dry sieving. According to USDA standards, the soil of the studied area was classified as sandy loam. According to Shirazi and Boersma (1984), the geometric mean particle diameter was also estimated. Table 3.1 summarizes the physical parameters of the soil at the studied hillslope.

Table 3.1. Clay (%), silt (%) and sand (%) content (U.S. Department of Agriculture classification), geometric mean particle diameter, d_g (mm), dry soil bulk density, ρ_b (g cm^{-3}), initial soil water content, θ_i (cm^3 cm^{-3}), and saturated soil water content, θ_s (cm^3 cm^{-3}), for the four sampled soil depths. The coefficients of variation (%) are listed in parentheses.

Soil depth (cm)	**0**	**5**	**10**	**20**
Sample size	10	10	10	9
Clay	17.4 (28.6)	19.5 (18.6)	20.2 (25.1)	23.2 (20.7)
Silt	28.8 (8.9)	29.2 (10.2)	28.3 (7.7)	27.9 (9.2)
Sand	53.8 (12.6)	51.4 (9.8)	51.5 (13.3)	48.9 (14.4)
d_g	0.114 (37.1)	0.095 (30.7)	0.096 (37.3)	0.080 (43.7)
Sample size	3	3	3	3
ρ_b	1.56 (3.0)	1.66 (7.1)	1.55 (6.2)	1.52 (3.0)
θ_i	0.23 (18.3)	0.25 (4.1)	0.18 (15.0)	0.18 (10.3)
θ_s	0.41 (4.3)	0.37 (11.9)	0.42 (8.7)	0.43 (4.0)

2.3. In-situ block method

The soil block method aimed at including the lateral component of the preferential flow at the plot scale for lateral K_s measurements. More details on the soil block preparation can be found in Di Prima et al. (2017b) and Pirastru et al. (2017). At first, four soil blocks with dimensions of 50 cm (width) by 105 cm (length) by 70 cm (depth) were obtained by careful hand digging of trenches with widths of 20 cm surrounding each soil block. Since the interface between the upper horizons and the restrictive substratum was located at a depth of approximately 38 cm, the excavated soil blocks consisted of layered blocks, and included the upper A and Bw horizons, and approximately 32 cm of impeding substratum. No evidence of man-made cracks was observed during the excavation process. Expandable polyurethane foam was then injected into the trench volumes in order to encase the exposed soil blocks. This inert material is not expected to alter the chemical (Lewis et al., 1990) and physical (Bagarello and Sgroi, 2008) characteristics of the soil, and it concurrently prevents edge flows (Germer and Braun, 2015). After the foam was completely dried, two pits were excavated up to the depth of the soil-substratum interface in order to expose the up- and downhill faces of the soil block and to create inflow (IP) and outflow pits (OP), respectively. At the end, the resulting soil blocks, hereafter referred to as SBs, were associated with a geometrically calculated volume above the impeding layer that ranged from 0.100 to 0.163 m^3. Each drainage experiment consisted of four stages. After a first satiation stage, three water table depths (WTDs, Figure 3.1) were sequentially settled at 5, 15, and 25 cm below the soil surface in the IP with a custom-built Mariotte bottle. The large 50 L capacity of the bottle avoided the need of frequent refilling throughout the duration of the executed stages. Each imposed water table depth was maintained until the achievement of quasi-steady-state conditions. A syphon system was used to impose from time to time the same water table depths in the OP. During these processing stages, visual readings of the water level in the bottle were used to calculate the inflow rates, as obtained through a liquid-level gauge. The excess water flowing from the OP through the syphon system was measured by weighting the collected water volumes. Figure 3.2 depicts the experimental setup. The total run duration varied between 260 and 460 min, depending on the run.

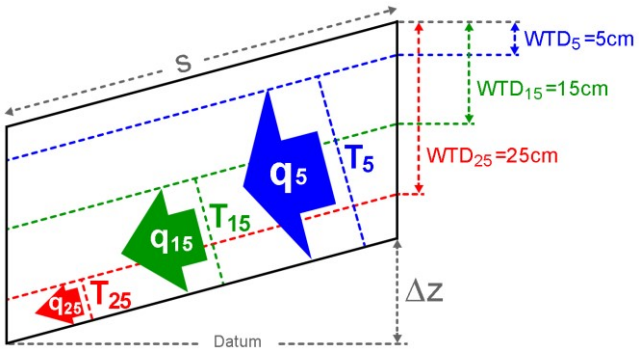

Fig. 3.1. Schematic diagram of a drainage experiment carried out on a soil block. Measured flows per unit width of the block (q_{WTD}) and thickness of the flow zones (T_{WTD}) for different water table depths (WTDs), distances along the sloping bed (s), and water table elevation from an arbitrary datum (ΔZ).

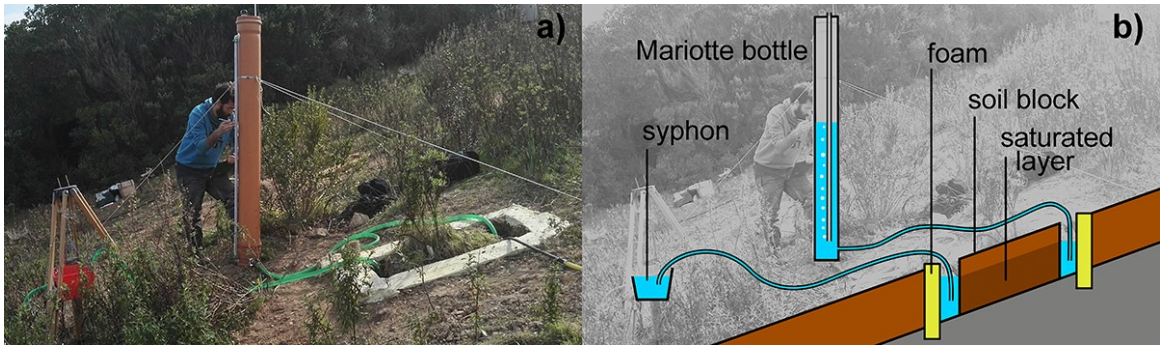

Fig. 3.2. (a) Photo and (b) schematic view of the experimental setup of a drainage experiment carried out on a soil block.

A first attempt to measure outflow from the OP was carried out using a 4 cm diameter PVC pipe used as a spillway. At the downhill side, the pipes were inserted in the dried foam at a smooth slope in order to maintain a constant water level and to divert the excess volume for collection. This procedure was applied only on the SB1 because field observations revealed that the pipe installations produced a slight discontinuity between soil and foam, thus resulting in leakages. To avoid such a problem, the syphon system was used for the other soil blocks (Figure 3.2). Therefore, for these latter experiments, the water loss was small, thus yielding similar inflow and outflow measurements (Figure 3.3). However, in the third and fourth SBs, the same differences between inflow and outflow rates were detected for WTD_{25}. In particular, water draining from progressive desaturation of the upper soil volume (i.e., the layer that had a depth that ranged between 15 and 25 cm) initially contributed to yield higher

outflows. During this stage, the desaturation of the upper soil volume did not affect the inflow rates since the flow zone was already saturated during the previous stages of the experiment. This difference was not observed in the SB2 experiment probably owing to the higher measured flow rates (Figure 3.3). Therefore, for the 2nd, 3rd, and 4th drainage experiments, the outflows measured under quasi-steady-state conditions were used to estimate the lateral saturated soil hydraulic conductivity of the soil blocks, K_{s-SB} (mm h^{-1}), according to Darcy's formula, as follows:

$$K_{s-SB} = -\frac{q}{T}\frac{s}{\Delta Z} \quad (1)$$

where q (L^2T^{-1}) is the flow of water per unit width of the block, T (L) is the thickness of the flow zone measured perpendicular to the bed, Z (L) is the water table elevation from an arbitrary datum, and s (L) is the distance measured on a straight line in the direction of the sloping bed. In this investigation, q, T, s, and ΔZ, were measured during the field experiment, or were determined using a simple geometry (Figure 3.1). We decided to use measured inflows rather than outflows only for the first SB1 experiment because: i) field observations during this experiment revealed localized water leakages from the OP and the measured inflow was thus completely infiltrated through the SB1, and ii) the measured inflow of the first experiment was consistent with the other ones.

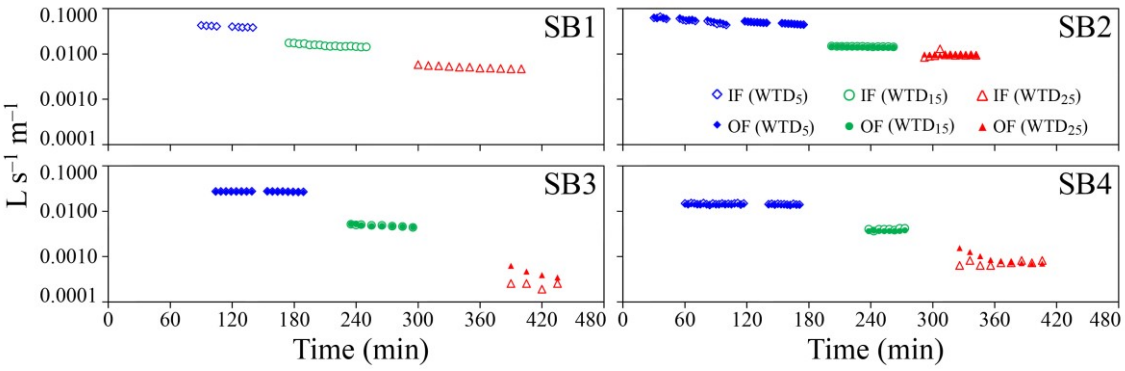

Fig. 3.3. Inflow (IF, open symbols) and outflow (OF, solid symbols) rates vs. time measured on the four soil blocks (SBs) at a water table depth (WTD) of 5 (blue rhombus), 15 (green circles) and 25 cm (red triangles).

2.4. Modified cube method

The horizontal and vertical hydraulic conductivities of the saturated soil, K_s, were determined based on the modified cube method (MCM) (Beckwith et al., 2003) to gain insight on the potential effects of anisotropic conditions on the comparison between the K_s measurements (Blanco-Canqui et al., 2002). In fact, the presence of layers parallel to the soil surface is expected to induce effective horizontal K_s values that are greater than the vertical ones (Zaslavsky and Rogowski, 1969).

According to the procedure described by Bagarello and Sgroi (2008) and Bagarello et al. (2009), a total of 20 soil cubes were collected at depths that ranged between 0 and 11 cm by carefully carving out 11 cm (width) by 11 cm (length) by 14 cm (depth) soil prisms (Figure 3.4a). A wooden box (side length = 17 cm) that was open at the bottom and top sides, was placed around each exposed soil prism (Figure 3.4b). Expandable polyurethane foam was injected between the box and the exposed soil and on the soil surface (Figure 3.4c). To avoid foam adhesion and to facilitate reusing, the box was wrapped with plastic wrap. In order to confine the foam expansion, a wood was positioned on the top of the box (Figure 3.4d). After the total expansion of the foam, the excess was cut off with a knife and the cube was marked to preserve direction. A layer of soil with a 3 cm thickness was removed from the bottom of the prism to obtain a cubic soil sample. Finally, the sample was completely encased by applying the foam at the bottom side.

In the laboratory, the vertical conductivity, $K_{s,v-MCM}$, was measured for ten randomly chosen cubes. The cubes were taken from the wooden box and the foam was removed from the top and bottom faces using a knife. The horizontal conductivity, $K_{s,h-MCM}$, was measured for the remaining soil cubes. In this latter case, the foam was removed from the up and downhill faces of the cube. For each cube, a single measurement was carried out given that the first measurement may affect the second when bidirectional measurements are performed on a single soil cube (Bagarello et al., 2009). A wire net was placed at the bottom face of the cube to support the weight of the soil. The soil samples were then slowly saturated from the bottom for 24 h. The constant-head laboratory permeameter method (Klute and Dirksen, 1986), with an established ponding depth of 1 cm was applied to measure K_s according to Darcy's law. A syphon was used to maintain the constant depth of ponding on the soil surface. The use of a Mariotte bottle with small ponding depths was avoided since it

may promote turbulence close to the soil's surface, potentially resulting in clogging the exposed pores (Bagarello et al., 2009). The constant-head permeameter used for measuring $K_{s,v–MCM}$ and $K_{s,h–MCM}$ was operated with water that flowed from the top and the uphill cube faces, respectively. The experiments were carried out until steady state conditions were established (i.e., at approximately 30 to 95 min). Depending on the run, the last 10–35 minutes of the measured flow rate data were used to calculate K_s. Finally, for each measurement direction, the ten determinations of K_s were averaged, and the ratio $K_{s,h\text{-}MCM}/K_{s,v\text{-}MCM}$ was evaluated to check the occurrence of anisotropy, i.e., the prevalence of the vertical ($K_{s,h–MCM}/K_{s,v–MCM} \leq 1$) or horizontal ($K_{s,h–MCM}/K_{s,v–MCM} \geq 1$) flow directions (Beckwith et al., 2003). The chosen sample size ($N = 10$) was expected to yield representative mean $K_{s,v}$ and $K_{s,l}$ values at the scale considered in this investigation (Reynolds et al., 2002).

Fig. 3.4. Successive steps during the in situ extraction of the soil cube: (a) carving out the soil prism, (b) placing the wooden box to contain lateral foam expansion, (c) injecting polyurethane expandable foam between the box and the exposed soil and on the soil surface, and (d) positioning wood and a weight to prevent top foam expansion.

2.5. BEST method

The Beerkan estimation of the soil transfer (BEST) parameter method for soil hydraulic characterization introduced by Lassabatere et al. (2006) was chosen for this investigation to yield an estimate for the saturated hydraulic conductivity of the matrix since it constitutes a practical alternative to more cumbersome and time-consuming methods (Bagarello et al., 2014a). Indeed, this method needs simple equipment and minimal field work, and it is gaining popularity in soil science.

A total of 40 ponding infiltration runs of the Beerkan type were carried out at the depths of 0, 5, 10, and 20 cm (ten for each soil depth) at randomly selected points of the hillslope. A small diameter ring (i.e., 8 cm) inserted at a depth of 1 cm was used. The soil disturbance was minimized by the limited ring insertion depth (Alagna et al., 2013). A relatively small ring diameter was chosen since the total sampled area cannot be too large given that the ring had to be inserted on a sloping surface (Angulo-Jaramillo et al., 2016) and to avoid the sampling of the macropore network. For each run, 15 water volumes, each equal to 43 mL, were successively poured on the confined infiltration surface. The number of infiltrated volumes was sufficient to reach steady state, as required by the Beerkan methods (Lassabatere et al., 2006). The energy of the falling water was dissipated with the hand fingers to minimize the soil disturbance owing to water pouring, as commonly suggested (e.g., Alagna et al., 2017; Castellini et al., 2018; Di Prima et al., 2017a; Reynolds, 1993). For each water volume, the time needed for the water to infiltrate was logged, and the cumulative infiltration, I (mm) was plotted against time, t (s). A regression line was then fitted to the last data points to describe the steady-state conditions, to estimate the experimental steady-state infiltration rate, i_s (mm h^{-1}), and the associated intercept, b_s (mm). The steady algorithm of BEST (Bagarello et al., 2014b) was then applied to estimate the saturated soil hydraulic conductivity, K_{s-BEST} (mm h^{-1}) based on the following equation (Di Prima et al., 2016):

$$K_{s-BEST} = \frac{C\, i_s}{A\, b_s + C} \tag{2}$$

where the constants A (mm^{-1}) and C are defined as follows (Haverkamp et al., 1994),

$$A = \frac{\gamma}{r\left(\theta_s - \theta_i\right)} \tag{3a}$$

$$C = \frac{1}{2\left[1 - \left(\frac{\theta_i}{\theta_s}\right)^{\eta}\right](1-\beta)} \ln\left(\frac{1}{\beta}\right) \tag{3b}$$

where θ_i and θ_s refer to the initial and saturated water contents, respectively, γ (parameter for geometrical correction of the infiltration front shape), and β are the coefficients that are commonly set at 0.75 and 0.6, r (mm) is the radius of the disk source, and η is a shape parameter that is estimated from the analysis of the particle size data with the pedotransfer function included in the BEST procedure (Lassabatere et al., 2006). More details on the methods and the validation of equations based on fitted experimental data can be found in Di Prima et al. (2016) and Lassabatere et al. (2009).

In this investigation, the BEST-steady algorithm was chosen since it yields higher percentage of success (i.e., positive K_s values) on the infiltration runs, and allows simple calculation of K_s as compared to other BEST algorithms, namely BEST-intercept (Yilmaz et al., 2010) and BEST-slope (Lassabatere et al., 2006).

2.6. Dual-permeability approach

On the basis of the measures obtained from the Beerkan runs and the block method, it was expected that the hydraulic conductivity of macropores would be efficiently computed. For dual permeability systems, it is considered that the global hydraulic conductivity, $K_{s,2K}$ (mm h^{-1}), can be decoupled in terms of its contributions to the matrix and to the fast-flow region (Gerke and van Genuchten, 1993),

$$K_{s,2K} = w_f K_{s,f} + \left(1 - w_f\right) K_{s,m} \tag{4}$$

where w_f is the void ratio occupied by the fast-flow region (dimensionless), i.e., the ratio of the volumes of the macropore and total-flow regions, and $K_{s,f}$ and $K_{s,m}$ (mm h^{-1}) are the saturated hydraulic conductivities for the fast-flow and the matrix regions, respectively. In this investigation, we assumed that we had an estimate for the saturated hydraulic conductivity of the matrix from the Beerkan runs. If we also assume that $K_{s,2K}$ can be

estimated by the bulk values obtained based on drainage experiments, we can deduce the hydraulic conductivity of the fast-flow region using equation (4), and its solution for $K_{s,f}$, which leads to,

$$K_{s,f} = \frac{K_{s,2K} - (1 - w_f)K_{s,m}}{w_f} \quad (5)$$

Since the void ratio occupied by the fast-flow region was unknown, we have evaluated multiple scenarios with w_f values ranging from 0.05 to 0.1, i.e., the fast-flow region was considered to occupy 5 to 10% of the entire region. This range was adopted since the fast-flow fraction generally occupied a very small fraction of the soil's porosity (Bouma et al., 1977). Moreover, these values were selected to agree with those reported by many dual-permeability applications. For instance, Dusek et al. (2012) settled the w_f values to 7% and 5% at the soil surface and at a 75 cm depth, respectively, in a hillslope covered with grass (*Calamagrostis villosa*) and spruce (*Picea abies*). For numerical simulations, Lassabatere et al. (2014b) considered a value of 10% for w_f.

2.7. Data analyses

K_s data were assumed to be log-normally distributed since the statistical distribution of these data is generally log-normal (Lee et al., 1985; Warrick, 1998). Therefore, the geometric mean, m_G, and the associated standard deviation, SD, and coefficient of variation, CV, were calculated using the appropriate "log-normal Equations" (Lee et al., 1985). The arithmetic mean, m_A, was calculated for ρ_b, θ_i, and θ_s. Statistical comparison between the two sets of data was conducted using two-tailed Student's *t*-tests, whereas the Tukey's honestly significant test was applied to compare three or more datasets. The ln(K_s) data were considered for comparative purposes since K_s was better described by the log-normal distribution than the normal distribution. An updated version of the workbook by Di Prima (2013) was used to analyze the Beerkan infiltration runs by the BEST-steady algorithm. All statistical analyses were carried out using the Minitab© computer program (Minitab Inc., State College, PA, USA).

3. Results and discussion

3.1. In-situ and laboratory small-scale measurements

Our results show that the K_s values estimated with the Beerkan method ($K_{s–BEST}$) progressively decreased with soil depth (Figure 3.5a and Table 3.2). From a statistical point of view, results of the Tukey's honestly significant difference test showed significant differences between the K_s values measured at different soil depths. The dry soil bulk density, ρ_b, ranged between 1.44 and 1.78 g cm^{-3} (N = 12). No differences were detected along the soil profile in terms of ρ_b (Table 3.1). Conversely, the $K_{s–BEST}$ values increased with the sand content (Pearson's correlation coefficients, r = 0.471; p = 0.002) and decreased with the clay content (r = –0.606; p < 0.001, Figure 3.5b). The higher percentage of coarse particles in the upper soil layer could suggest a certain rigidity of the porous medium (Table 3.1). On the contrary, the increase in clay particles with soil depth implies more opportunities for clogging the largest pores, and thus, lower K_s values. In the upper soil, these values were very close to the prediction of saturated conductivity from soil textural characteristics (e.g., K_s = 44.2 mm h^{-1} for a sandy-loam soil according to Carsel and Parrish (1988)). Therefore, the macroporosity did not likely influence the measured infiltration process. In general, isolated macropores are physically difficult to include in the sampled volume (Brooks et al., 2004). Using small rings in the soils with macropores (with ring inner diameters of 8 cm in this investigation) implies a relatively high probability to sample only the soil matrix. This yields a measurement of K_s that is representative only of the matrix instead of the entire system of macropores (Angulo-Jaramillo et al., 2016). In addition, using small rings also implies fewer opportunities of inclusion of continuous macropores intersecting the confined soil surface. Large rings appear more appropriate than small rings in eliciting a signal associated with the occurrence of soil macropores or fast-flow regions in the field since smaller soil volumes are functionally more homogeneous than larger volumes (Bagarello et al., 2013). Castellini et al. (2016) applied the Beerkan method using a ring with an inner diameter of 15 cm to assess the physical quality of the upper soil of the same experimental hillslope. These authors obtained similar results for K_s (mean = 24.1 mm h^{-1}, coefficient of variation, CV = 118). The mean K_s values collected during the two sampling campaigns differed by a factor of 1.8. This could be

considered practically negligible for many hydrological applications (Elrick and Reynolds, 1992).

Table 3.2. Sample size, N, minimum, Min, maximum, Max, geometric mean, m_G, standard deviation, SD, and coefficient of variation, CV (%) of the saturated soil hydraulic conductivity, $K_{s–BEST}$ (mm h^{-1}). All values were obtained using the Beerkan method at the depths of 0, 5, 10, and 20 cm.

Statistic	**Depth (cm)**			
	0	5	10	20
N	10	10	10	10
Min	12.4	3.2	1.5	1.3
Max	171.1	58.3	25.2	13.2
m_G	43.3 A	13.4 B	6.7 BC	4.0 C
SD	2.3	2.7	2.5	2.5
CV	101.8	130.7	118.8	116.3

The values followed by the same letter were not significantly different according to the Tukey's honest significant difference test ($P < 0.05$). The values followed by a different letter were significantly different.

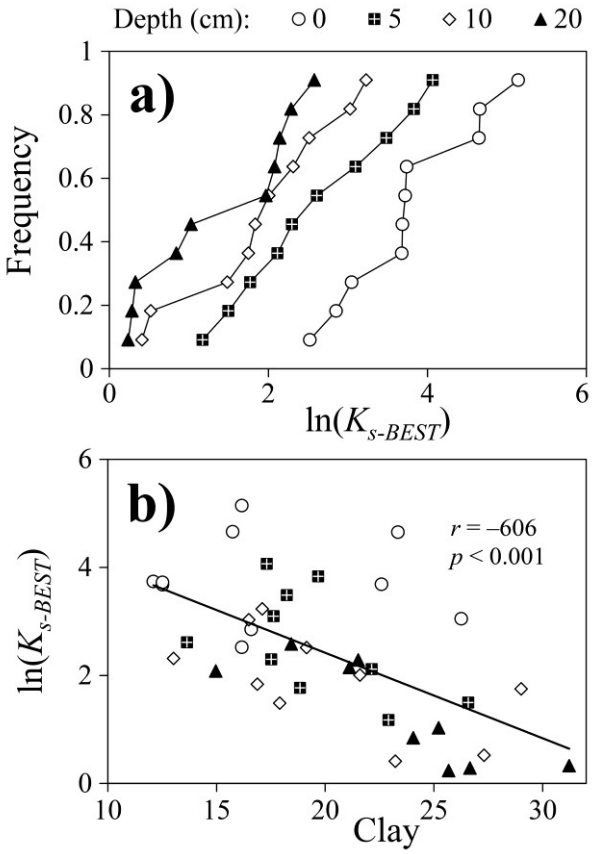

Fig. 3.5. (a) Cumulative empirical frequency distributions of the log-transformed saturated soil hydraulic conductivity data, ln($K_{s–BEST}$), obtained by the Beerkan method at the depths of 0, 5, 10, and 20 cm, and (b) ln($K_{s–BEST}$) values plotted against the clay content (in %). The Pearson correlation coefficient, *r*, is also reported.

Table 3.3 summarizes the parameters obtained by the modified cube method (MCM). The means of K_s were equal to 173.0 and 167.1 mm h^{-1} for the vertical and horizontal directions, respectively. The MCM yielded statistically different and higher K_s estimates than Beerkan. The comparison between these methods requires additional considerations that are discussed below. In-situ K_s measurements allow the maintenance of the functional connections of the sampled volumes with the surrounding matrix (e.g., Bagarello et al., 2017; Bouma, 1982; Di Prima, 2015; Lauren et al., 1988). In comparison, in the laboratory, the overall connection of extracted soil samples is expected to be higher because of the increased probability of their impact by macropores and the interception of the edges of the extracted samples. We thus conclude that the higher values of saturated hydraulic conductivity for the MCM method results from a partial activation of the largest pores in the soil samples. This increase in connectivity was discussed in detail in a review article by Pachepsky and Hill (2017). To explain this effect, these authors considered data from one-dimensional vertical water flow experiments. In these experiments, K_s decreased with increases of the soil column length L according to the following power law $K_s \propto L^{-m}$. Anderson and Bouma (1973) attributed this effect to the increasing probability that pores will remain connected throughout the length of a core as a function of decreasing core lengths. In particular, for longer samples, the water flux appears to be controlled by a more homogeneous soil matrix with lower hydraulic conductivity values. The process discussed above essentially mimics what happens during the Beerkan infiltration runs, which allow the preservation of the functional connection of the sampled volume with the surrounding matrix, thus yielding lower K_s values than those obtained with the MCM (samples biased by pores).

Table 3.3. Sample size, N, minimum, Min, maximum, Max, geometric mean, m_G, standard deviation, SD, and coefficient of variation, CV (%) of the vertical, $K_{s,v-MCM}$ (mm h^{-1}) and horizontal, $K_{s,h-MCM}$ (mm h^{-1}) saturated soil hydraulic conductivity values obtained by the constant-head laboratory permeameter method on soil cubes (Klute and Dirksen, 1986).

$m_G(K_{s,h-MCM})/m_G(K_{s,v-MCM})$	Statistic	$K_{s,v-MCM}$	$K_{s,h-MCM}$
0.97	N	10	10
	Min	51.7	52.6
	Max	480.7	341.4
	m_G	173.0 A	167.1 A
	SD	2.1	1.9
	CV	87.5	71.9

The two K_s values followed by the same letter are not significantly different according to a Student's two-tailed t-test ($P < 0.05$).

Several examples of the overestimation of K_s on extracted soil samples can be found in the literature. For instance, the increase in K_s owing to open-ended pores on undisturbed soil samples was assessed by Blanco-Canqui et al. (2002). These authors measured K_s on 180 soil cores (with 76 mm (diameter) × 76 mm (height)) with and without bentonite to seal the macropores. These authors found that K_s values without bentonite were approximately four times higher than the corresponding K_s values with bentonite. Kanwar et al. (1989) compared the K_s values determined in situ using the Guelph permeameter device (Reynolds and Elrick, 2005) and the velocity permeameter (Merva, 1979) with those obtained in the laboratory based on the constant head permeameter method on undisturbed soil cores (75 mm (diameter) × 75 mm (height)). The in situ methods yielded values that were 10–800 times lower than the laboratory method. Young (1998) and Regan (2000) measured K_s values using vertical soil cores and the Guelph permeameter, respectively. The in situ methods yielded values that were three to four times lower than the soil core K_s measurements. Differences were attributed to continuous pores connecting the exposed surfaces of the cores for the laboratory method.

In this investigation, the soil cube method provided further insight on the potential effect of anisotropic conditions on the comparison between K_s measurements (Blanco-Canqui et al., 2002). The anisotropy of K_s was not substantial given that the difference between the $K_{s,v–MCM}$ and $K_{s,h–MCM}$ values was not statistically significant, according to a two-tailed Student's *t*-test ($P < 0.05$) (Dabney and Selim, 1987). The ratio between the mean values of $K_{s,v–MCM}$ and $K_{s,h–MCM}$ was equal to 0.97 (Table 3.3). In general, the effect of allowing only one-dimensional flow into the soil leads to an important "error" when the anisotropy is large and when no attempt is made to measure separately the horizontal and vertical components of permeability (Chappell and Lancaster, 2007). However, the biasing problem on small soil cubes and the impossibility to sample all the macropores probably precluded the detection of the effect that macropores may exert on a specific flow direction. Indeed, even if we explained the higher values of the MCM method in comparison to Beerkan estimates obtained on the field based on the hypothesis of the activation of the macropore network, we are not sure that this activation is complete. In addition, the size of the soil samples may not be large enough to sample the largest macropores encountered in the field. In other words, the measurement of the vertical and horizontal flow on small soil cubes may

not be representative of the real anisotropic behavior of the macropore network that may occur at a larger scale in the field. However, we can consider that for the matrix alone, the runs are representative of the field conditions. Therefore, the result of a substantial isotropic behavior of the soil at the point scale suggested that the direction of the flow measurements, i.e., vertical or horizontal, did not play a role on K_s estimation for the matrix at the small scale.

3.2. Comparing plot- and point-scale measurements

Figure 3.3 shows the subsurface flows measured for three different water table depths (WTDs) for the four soil blocks. The steady flow rates ranged from 3.4×10^{-4} to 4.4×10^{-2} L s^{-1} m^{-1} (sample size, $N = 12$), thus yielding $K_{s–SB}$ values that equaled 70 and 2157 mm h^{-1} (Table 3.4) for WTD_{25} and WTD_5, respectively. For WTD_5, the mean $K_{s–SB}$ value (1239 mm h^{-1}, sample size, $N = 4$) was an order of magnitude higher than that elicited by the MCM. Therefore, a smaller soil volume was found to be more homogeneous than a larger volume (Lai and Ren, 2007). Macropore flow likely occurred at the sampled site since even the lowest mean of $K_{s–SB}$ (724 mm h^{-1}) was 4.3 times higher than those of the MCM, known to overestimate the saturated hydraulic conductivity of the matrix (see discussion above). The discrepancy between the two spatial scales is even greater for the case of the Beerkan runs. Therefore, both laboratory and small-scale field measurements yielded consistently lower values than those of the plot-scale. Small-scale measurements also yielded higher standard deviations (SDs) and coefficient of variations (CVs) than those obtained on the soil blocks for WTD_5, thus suggesting the degradation of sample representativeness at smaller scales. In fact, the variability of the data is expected to decrease as the size of the sampled soil volume increases (Angulo-Jaramillo et al., 2016). Conversely, large soil volumes allowed the determination of representative $K_{s–SB}$ values that account for soil heterogeneity and the contribution of the macropore network. This result is also consistent with the suggestion of Pachepsky and Hill (2017) who stated that the macropore flow cannot be seen at the small scale but emerges and becomes of interest at the plot scale. In other words, the large volume of soil adequately embodied the macropore network (Blanco-Canqui et al., 2002; Day et al., 1998; Mendoza and Steenhuis, 2002). The relatively low variability of the data (CV = 48.6%) also suggested the replicability of the measurements.

Table 3.4. Geometrical dimensions and estimated saturated hydraulic conductivity, K_{s-SB} (mm h^{-1}) values for the four soil blocks.

	Depth (cm)	Length (cm)	Width (cm)	Volume (m^3)	K_{s-SB}		
					WTD_5	**WTD_{15}**	**WTD_{25}**
Soil block 1	35.5	85	54.0	0.163	1.4×10^3	7.9×10^2	5.1×10^2
Soil block 2	29.0	69	50.0	0.100	2.2×10^3	1.2×10^3	2.8×10^3
Soil block 3	30.0	68	50.0	0.102	1.1×10^3	3.1×10^2	7.0×10^1
Soil block 4	31.5	80	52.5	0.132	7.2×10^2	3.1×10^2	1.5×10^2
m_G					1.2×10^3	5.5×10^2	3.5×10^2
Mean	31.5	75.5	51.6	0.124			
SD	2.9	8.3	2.0	0.030	1.6	2.0	5.0
CV (%)	9.1	11.1	3.8	23.9	48.6	76.3	345.8

3.3. Lateral preferential flow

The results from the comparison between plot- and point-scale measurements suggested that the studied soil was clearly made of two components, namely, the matrix and the macropore network that constituted a fast-flow region. In the following subsection, we attempt to fully characterize both regions. The matrix could be characterized by the values of saturated hydraulic conductivity obtained with Beerkan runs. The Beerkan runs along with the four drainage experiments were used to estimate the saturated hydraulic conductivity of the fast-flow region, $K_{s,f}$ (mm h^{-1}) using Eq. (5). The values of $K_{s,f}$ ranged from 6.0×10^2 to 5.5×10^4 mm h^{-1}, depending on the WTD and w_f values (Table 3.5). For the lower (0.05) and upper (0.1) range values of w_f, the $K_{s,f}$ estimates were in the range of two to three and one to three orders of magnitude higher than $K_{s,m}$, respectively. Conversely, differences never exceeding a factor of two were encountered for the $K_{s,f}$ estimates within the selected w_f ranges, which may be considered within the natural range of spatial heterogeneity for the saturated hydraulic conductivity (Kodešová et al., 2010). Therefore, because larger discrepancies occurred between the fast-flow and the matrix regions, it can be argued that the selected w_f values had a lesser impact on the comparison between the K_m and K_f values.

Figure 3.6 shows the impact of w_f on the $K_{s,f}$ values estimated at different water table depths (WTDs) for the four soil blocks. Firstly, it should be taken into account that the global hydraulic conductivity was measured in the field, and thus Eq. (5) was applied constraining $K_{s,2k}$ values. As shown in Figure 3.6, $K_{s,f}$ estimates decreased for higher w_f values. To explain this general trend, we should consider that with the constrained $K_{s,2k}$ value, the increase of w_f should correspond to a decrease in $K_{s,f}$ estimates. Indeed, the product of w_f $K_{s,f}$ that quantifies

the contribution of the macropore network to the bulk hydraulic conductivity $K_{s,2K}$ (Eq.(4)) must remain constant irrespective of the value of w_f. This condition is representative of a larger volume occupied by macropores, which are in turn less connected, and/or with a smaller diameter corresponding to lower hydraulic conductivities. On the contrary, when w_f decreases, the increase in $K_{s,f}$ is representative of a smaller volume occupied by more connected and/or larger diameter macropores and a higher hydraulic conductivity. In any case, the contribution of the macropore network system remains constant. Moreover, $K_{s,f}$ estimates decreased for higher WTDs, i.e., for a thinner saturated soil layer, with the exception of soil block 2. In this case, a higher $K_{s,f}$ value was estimated for WTD_{25} because of the effect of an open-ended macropore biasing the matrix that was located at the bottom of the soil block. This hypothesis was supported by field observations. In particular, during the saturation stage, we observed water copiously flowing from a deep macropore. This contributed to a higher $K_{s,f}$ value than those obtained for lower WTDs. However, as shown in Figure 3.6, the overall decrease of $K_{s,f}$ supported the hypothesis that the macropore density decreased with depth. It can be argued that the sampled volume should be increased for lower horizons in order to adequately represent the macropore network. In contrast, the increase in WTD from 5 to 15 and to 25 cm resulted in a reduction of the sampled soil volume. Under such conditions, the sampled volumes may have not been sufficient to activate the macropore networks located in the deeper horizons. Moreover, the $K_{s,f}$ variability increased abruptly for thinner saturated layers. A smaller macropore density was noted as a function of depth that increased the macropore flow variability, which may ultimately contribute to the explanation of the smaller transfer rates in the deeper horizons (Köhne et al., 2009).

These results implied that the proper scale to study macropore flow for small thickness of the saturated layer may be the hillslope-scale on the studied hillslope. This effect likely had a certain impact on the measurements for lower WTDs, thus resulting in a minor $K_{s,f}$ overestimation in some circumstances owing to the occasional presence of deep, open-ended macropores (soil block 2). Notwithstanding this finding, considering the entire volume of the soil blocks, the water flow was mainly controlled by the dense macropore network which characterized the porous medium in proximity of the soil surface. Thus, in these cases, the effect of deep, open-ended macropores, was less noticeable.

Table 3.5. Estimated values of the saturated hydraulic conductivity for the fast-flow region, $K_{s,f}$ (mm h^{-1}), for the lower (0.05) and upper (0.1) range values of the void ratio occupied by the fast-flow region, w_f (-), for the four soil blocks.

	$K_{s,f}$ (w_f = 0.05)			$K_{s,f}$ (w_f = 0.1)		
	WTD_5	**WTD_{15}**	**WTD_{25}**	**WTD_5**	**WTD_{15}**	**WTD_{25}**
Soil block 1	2.8×10^4	1.6×10^4	10.0×10^3	1.4×10^4	7.8×10^3	5.0×10^3
Soil block 2	4.3×10^4	2.3×10^4	5.5×10^4	2.1×10^4	1.2×10^4	2.7×10^4
Soil block 3	2.1×10^4	5.9×10^3	1.2×10^3	1.1×10^4	3.0×10^3	6.0×10^2
Soil block 4	1.4×10^4	6.0×10^3	2.8×10^3	7.1×10^3	3.0×10^3	1.4×10^3
m_G	2.5×10^4	1.1×10^4	6.5×10^3	1.2×10^4	5.4×10^3	3.3×10^3
SD	1.6	2.0	5.3	1.6	2.0	5.3
CV (%)	49.1	78.3	387.5	49.1	78.2	385.0

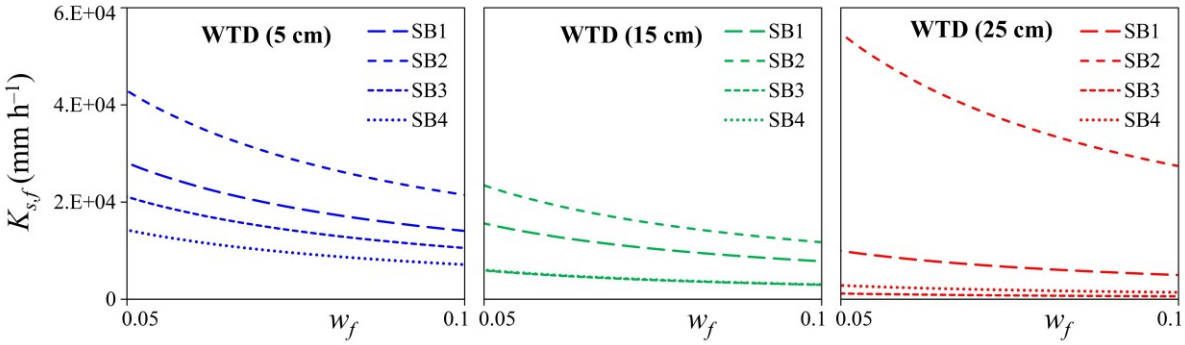

Fig. 3.6. Impact of the fast-flow fraction, w_f (-), on the saturated hydraulic conductivity for the fast-flow region, $K_{s,f}$ (mm h^{-1}), estimated at different water table depths (WTDs) on the four soil blocks (SBs). The reported w_f values range from 0.05 to 0.1.

4. Conclusions

This investigation was carried out to characterize the subsurface flow processes in a hillslope at different spatial scales, namely at point- and plot-scale using the Beerkan method with the BEST algorithm, the MCM, and the soil block method. The differences between the considered scales were attributed mainly to the effect of the macropore flow and the impossibility to adequately embody the macropore network on small sampled soil volumes. The comparison of K_s measurement techniques allowed us to establish the peculiarity of each K_s data obtained at a particular spatial scale. This information helped establish the usability of a given technique to interpret or simulate a particular hydrological process. In particular, the scale dependence of K_s essentially precluded the use of small-scale measurements for detecting a dual-permeability behavior. Otherwise, plot-scale measurements allowed us to obtain reliable estimates accounting for macropore flow. In our study, we clearly proved the advantage of experimental protocols based on multiscale experiments. Our results yielded encouraging evidence for the applicability of the soil block method (at the plot-scale) along the Beerkan infiltration runs (at the point-scale) for a plausible estimation of the saturated hydraulic conductivities for the matrix and the fast-flow region, $K_{s,m}$ and $K_{s,f}$, using a relatively simple field procedure. The use of expandable polyurethane foam as a suitable material to encase soil blocks for hydraulic conductivity measurements was successfully tested. It closely adhered to the irregular soil surface (Brye et al., 2004; Germer and Braun, 2015; Muller and Hamilton, 1992), avoided water loss and obtained accurate measurements of K_s. This is a promising result given that researcher studies should constantly focus their efforts to simplify field measurements (Alagna et al., 2016).

In the future, the proposed methodology may be applied to explain saturation excess runoff (i.e., saturation overland flow) or to study subsurface macropore flow. Indeed, these processes constitute the major mechanisms affecting the dynamics of the shallow groundwater perched table above a restrictive layer, which is an integrated process that needs a minimum contributing area to be activated (Blöschl and Sivapalan, 1995). Further experimental work is needed to determine the macropore domain (w_f). Based on this aim, the fraction of the macropore domain in the dual-permeability model could be estimated using micromorphological images (Kodešová et al., 2009). This approach could allow us to estimate w_f as the ratio of the porosity determined by image analysis and the overall porosity of the

sampled soil. The role of the macropores in controlling $K_{s,f}$ at the studied hillslope needs to be further investigated. For example, tracer experiments may be carried out to investigate macroporosity extensions and connectivity (Ahuja et al., 1995; Köhne et al., 2009), which was considered responsible for the detected scale dependence of the studied soil properties.

5. References

Abou Najm, M.R., Atallah, N.M., 2016. Non-Newtonian Fluids in Action: Revisiting Hydraulic Conductivity and Pore Size Distribution of Porous Media. Vadose Zone J. 15. https://doi.org/10.2136/vzj2015.06.0092

Ahuja, L.R., Johnsen, K.E., Heathman, G.C., 1995. Macropore Transport of a Surface-Applied Bromide Tracer: Model Evaluation and Refinement. Soil Science Society of America Journal 59, 1234–1241. https://doi.org/10.2136/sssaj1995.03615995005900050004x

Akay, O., Fox, G.A., Šimůnek, J., 2008. Numerical Simulation of Flow Dynamics during Macropore–Subsurface Drain Interactions Using HYDRUS. Vadose Zone Journal 7, 909. https://doi.org/10.2136/vzj2007.0148

Alagna, V., Bagarello, V., Di Prima, S., Giordano, G., Iovino, M., 2013. A simple field method to measure the hydrodynamic properties of soil surface crust. Journal of Agricultural Engineering 44, 74–79. https://doi.org/10.4081/jae.2013.(s1):e14

Alagna, V., Bagarello, V., Di Prima, S., Iovino, M., 2016. Determining hydraulic properties of a loam soil by alternative infiltrometer techniques. Hydrological Processes 30, 263–275. https://doi.org/10.1002/hyp.10607

Alagna, V., Di Prima, S., Rodrigo-Comino, J., Iovino, M., Pirastru, M., Keesstra, S.D., Novara, A., Cerdà, A., 2017. The Impact of the Age of Vines on Soil Hydraulic Conductivity in Vineyards in Eastern Spain. Water 10, 14. https://doi.org/10.3390/w10010014

Anderson, J.L., Bouma, J., 1973. Relationships Between Saturated Hydraulic Conductivity and Morphometric Data of an Argillic Horizon. Soil Science Society of America Journal 37, 408–413. https://doi.org/10.2136/sssaj1973.03615995003700030029x

Angulo-Jaramillo, R., Bagarello, V., Iovino, M., Lassabatère, L., 2016. Infiltration Measurements for Soil Hydraulic Characterization. Springer International Publishing.

Bagarello, V., Di Prima, S., Giordano, G., Iovino, M., 2014a. A test of the Beerkan Estimation of Soil Transfer parameters (BEST) procedure. Geoderma 221–222, 20–27. https://doi.org/10.1016/j.geoderma.2014.01.017

Bagarello, V., Di Prima, S., Iovino, M., 2017. Estimating saturated soil hydraulic conductivity by the near steady-state phase of a Beerkan infiltration test. Geoderma 303, 70–77. https://doi.org/10.1016/j.geoderma.2017.04.030

Bagarello, V., Di Prima, S., Iovino, M., 2014b. Comparing Alternative Algorithms to Analyze the Beerkan Infiltration Experiment. Soil Science Society of America Journal 78, 724. https://doi.org/10.2136/sssaj2013.06.0231

Bagarello, V., Iovino, M., Lai, J.-B., 2013. Field and Numerical Tests of the Two-Ponding Depth Procedure for Analysis of Single-Ring Pressure Infiltrometer Data. Pedosphere 23, 779–789. https://doi.org/10.1016/S1002-0160(13)60069-7

Bagarello, V., Sferlazza, S., Sgroi, A., 2009. Testing laboratory methods to determine the anisotropy of saturated hydraulic conductivity in a sandy–loam soil. Geoderma 154, 52–58. https://doi.org/10.1016/j.geoderma.2009.09.012

Bagarello, V., Sgroi, A., 2008. Testing Soil Encasing Materials for Measuring Hydraulic Conductivity of a Sandy-Loam Soil by the Cube Methods. Soil Science Society of America Journal 72, 1048. https://doi.org/10.2136/sssaj2007.0022

Beckwith, C.W., Baird, A.J., Heathwaite, A.L., 2003. Anisotropy and depth-related heterogeneity of hydraulic conductivity in a bog peat. I: laboratory measurements. Hydrol. Process. 17, 89–101. https://doi.org/10.1002/hyp.1116

Beven, K., Germann, P., 1982. Macropores and water flow in soils. Water Resour. Res. 18, 1311–1325. https://doi.org/10.1029/WR018i005p01311

Blanco-Canqui, H., Gantzer, C.J., Anderson, S.H., Alberts, E.E., Ghidey, F., 2002. Saturated hydraulic conductivity and its impact on simulated runoff for claypan soils. Soil Science Society of America Journal 66, 1596–1062. https://doi.org/10.2136/sssaj2002.1596

Blöschl, G., Sivapalan, M., 1995. Scale issues in hydrological modelling: a review. Hydrological processes 9, 251–290.

Bouma, J., 1982. Measuring the hydraulic conductivity of soil horizons with continuous macropores. Soil Science Society of America Journal 46, 438. https://doi.org/10.2136/sssaj1982.03615995004600020047x

Bouma, J., Jongerius, A., Boersma, O., Jager, A., Schoonderbeek, D., 1977. The function of different types of macropores during saturated flow through four swelling soil horizons. Soil Science Society of America Journal 41, 945–950.

Brooks, E.S., Boll, J., McDaniel, P.A., 2004. A hillslope-scale experiment to measure lateral saturated hydraulic conductivity. Water Resour. Res. 40, W04208. https://doi.org/10.1029/2003WR002858

Brye, K.R., Morris, T.L., Miller, D.M., Formica, S.J., Eps, V., A, M., 2004. Estimating Bulk Density in Vertically Exposed Stoney Alluvium Using a Modified Excavation Method. Journal of Environmental Quality 33, 1937–1942. https://doi.org/10.2134/jeq2004.1937

Carsel, R.F., Parrish, R.S., 1988. Developing joint probability distributions of soil water retention characteristics. Water Resour. Res. 24, 755–769. https://doi.org/10.1029/WR024i005p00755

Castellini, M., Di Prima, S., Iovino, M., 2018. An assessment of the BEST procedure to estimate the soil water retention curve: A comparison with the evaporation method. Geoderma 320, 82–94. https://doi.org/10.1016/j.geoderma.2018.01.014

Castellini, M., Iovino, M., Pirastru, M., Niedda, M., Bagarello, V., 2016. Use of BEST Procedure to Assess Soil Physical Quality in the Baratz Lake Catchment (Sardinia, Italy). Soil Science Society of America Journal. https://doi.org/10.2136/sssaj2015.11.0389

Chappell, N.A., Lancaster, J.W., 2007. Comparison of methodological uncertainties within permeability measurements. Hydrological Processes 21, 2504–2514. https://doi.org/10.1002/hyp.6416

Chapuis, R.P., Dallaire, V., Marcotte, D., Chouteau, M., Acevedo, N., Gagnon, F., 2005. Evaluating the hydraulic conductivity at three different scales within an unconfined sand aquifer at Lachenaie, Quebec. Canadian Geotechnical Journal 42, 1212–1220. https://doi.org/10.1139/t05-045

Dabney, S.M., Selim, H.M., 1987. Anisotropy of a Fragipan Soil: Vertical vs. Horizontal Hydraulic Conductivity1. Soil Science Society of America Journal 51, 3. https://doi.org/10.2136/sssaj1987.03615995005100010001x

Day, R.L., Calmon, M.A., Stiteler, J.M., Jabro, J.D., Cunningham, R.L., 1998. Water balance and flow patterns in a fragipan using in situ soil block. Soil science 163, 517–528.

Di Prima, S., 2015. Automated single ring infiltrometer with a low-cost microcontroller circuit. Computers and Electronics in Agriculture 118, 390–395. https://doi.org/10.1016/j.compag.2015.09.022

Di Prima, S., 2013. Automatic analysis of multiple Beerkan infiltration experiments for soil Hydraulic Characterization, in: 1st CIGR Inter-Regional Conference on Land and Water Challenges. p. 127. https://doi.org/10.13140/2.1.4112.0324

Di Prima, S., Bagarello, V., Lassabatere, L., Angulo-Jaramillo, R., Bautista, I., Burguet, M., Cerdà, A., Iovino, M., Prosdocimi, M., 2017a. Comparing Beerkan infiltration tests with rainfall simulation experiments for hydraulic characterization of a sandy-loam soil. Hydrological Processes 31, 3520–3532. https://doi.org/10.1002/hyp.11273

Di Prima, S., Lassabatere, L., Bagarello, V., Iovino, M., Angulo-Jaramillo, R., 2016. Testing a new automated single ring infiltrometer for Beerkan infiltration experiments. Geoderma 262, 20–34. https://doi.org/10.1016/j.geoderma.2015.08.006

Di Prima, S., Marrosu, R., Pirastru, M., Bagarello, V., Iovino, M., Niedda, M., 2017b. In situ determination of the lateral soil hydraulic conductivity on a soil monolith, in: 11th AIIA 2017 Conference - Biosystems Engineering Addressing the Human Challenges of the 21st Century, Bari – Italy, 5-8 July 2017.

Di Prima, S., Rodrigo-Comino, J., Novara, A., Iovino, M., Pirastru, M., Keesstra, S., Cerda, A., 2018. Assessing soil physical quality of citrus orchards under tillage, herbicide and organic managements. Pedosphere 28(3).

Dusek, J., Vogel, T., Dohnal, M., Gerke, H.H., 2012. Combining dual-continuum approach with diffusion wave model to include a preferential flow component in hillslope scale modeling of shallow subsurface runoff. Advances in Water Resources 44, 113–125. https://doi.org/10.1016/j.advwatres.2012.05.006

Elrick, D.E., Reynolds, W.D., 1992. Methods for analyzing constant-head well permeameter data. Soil Science Society of America Journal 56, 320. https://doi.org/10.2136/sssaj1992.03615995005600010052x

Gee, G.W., Bauder, J.W., 1986. Particle-size Analysis, in: SSSA Book Series, Klute, A. (Ed.), Methods of Soil Analysis, Part 1: Physical and Mineralogical Methods. Soil Science Society of America, American Society of Agronomy, pp. 383–411.

Gerke, H.H., van Genuchten, M.T., 1993. A dual-porosity model for simulating the preferential movement of water and solutes in structured porous media. Water Resour. Res. 29, 305–319. https://doi.org/10.1029/92WR02339

Germer, K., Braun, J., 2015. Determination of Anisotropic Saturated Hydraulic Conductivity of a Macroporous Slope Soil. Soil Science Society of America Journal 79, 1528–1536. https://doi.org/10.2136/sssaj2015.02.0071

Groppelli, B., Soncini, A., Bocchiola, D., Rosso, R., 2011. Evaluation of future hydrological cycle under climate change scenarios in a mesoscale Alpine watershed of Italy. Nat. Hazards Earth Syst. Sci. 11, 1769–1785. https://doi.org/10.5194/nhess-11-1769-2011

Haverkamp, R., Bouraoui, F., Zammit, C., Angulo-Jaramillo, R., 1999. Soil properties and moisture movement in the unsaturated zone. Handbook of groundwater engineering.

Haverkamp, R., Ross, P.J., Smettem, K.R.J., Parlange, J.Y., 1994. Three-dimensional analysis of infiltration from the disc infiltrometer: 2. Physically based infiltration equation. Water Resour. Res. 30, 2931–2935. https://doi.org/10.1029/94WR01788

Kanwar, R.S., Rizvi, H.A., Ahmed, M., Horton, R., Marley, S.J., 1989. Measurement of field-saturated hydraulic conductivity by using Guelph and velocity permeameters. Transactions of the ASAE 132.

Klute, A., Dirksen, C., 1986. Hydraulic Conductivity and Diffusivity: Laboratory Methods. Methods of Soil Analysis: Part 1—Physical and Mineralogical Methods sssabookseries, 687–734. https://doi.org/10.2136/sssabookser5.1.2ed.c28

Kodešová, R., Šimůnek, J., Nikodem, A., Jirků, V., 2010. Estimation of the Dual-Permeability Model Parameters using Tension Disk Infiltrometer and Guelph Permeameter. Vadose Zone Journal 9, 213. https://doi.org/10.2136/vzj2009.0069

Kodešová, R., Vignozzi, N., Rohošková, M., Hájková, T., Kočárek, M., Pagliai, M., Kozák, J., Šimůnek, J., 2009. Impact of varying soil structure on transport processes in different diagnostic horizons of three soil types. Journal of Contaminant Hydrology 104, 107–125. https://doi.org/10.1016/j.jconhyd.2008.10.008

Köhne, J.M., Köhne, S., Šimůnek, J., 2009. A review of model applications for structured soils: a) Water flow and tracer transport. Journal of Contaminant Hydrology 104, 4–35. https://doi.org/10.1016/j.jconhyd.2008.10.002

Lai, J., Ren, L., 2007. Assessing the Size Dependency of Measured Hydraulic Conductivity Using Double-Ring Infiltrometers and Numerical Simulation. Soil Science Society of America Journal 71, 1667. https://doi.org/10.2136/sssaj2006.0227

Lamy, E., Lassabatere, L., Bechet, B., Andrieu, H., 2009. Modeling the influence of an artificial macropore in sandy columns on flow and solute transfer. Journal of Hydrology 376, 392–402. https://doi.org/10.1016/j.jhydrol.2009.07.048

Lassabatere, L., Angulo-Jaramillo, R., Soria Ugalde, J.M., Cuenca, R., Braud, I., Haverkamp, R., 2006. Beerkan estimation of soil transfer parameters through infiltration experiments—BEST. Soil Science Society of America Journal 70, 521. https://doi.org/10.2136/sssaj2005.0026

Lassabatere, L., Angulo-Jaramillo, R., Soria-Ugalde, J.M., Šimůnek, J., Haverkamp, R., 2009. Numerical evaluation of a set of analytical infiltration equations: EVALUATION INFILTRATION. Water Resources Research 45. https://doi.org/10.1029/2009WR007941

Lassabatere, L., Spadini, L., Delolme, C., Février, L., Galvez Cloutier, R., Winiarski, T., 2007. Concomitant Zn–Cd and Pb retention in a carbonated fluvio-glacial deposit under both static and dynamic conditions. Chemosphere 69, 1499–1508. https://doi.org/10.1016/j.chemosphere.2007.04.053

Lassabatere, L., Yilmaz, D., Peyrard, X., Peyneau, P.E., Lenoir, T., Šimůnek, J., Angulo-Jaramillo, R., 2014. New Analytical Model for Cumulative Infiltration into Dual-Permeability Soils. Vadose Zone Journal 0, 0. https://doi.org/10.2136/vzj2013.10.0181

Lauren, J.G., Wagnet, R., Bouma, J., Wosten, J., 1988. Variability of saturated hydraulic conductivity in a Glossaquic Hapludalf with macropores. Soil Science 145, 20–28.

Lee, D.M., Elrick, D.E., Reynolds, W.D., Clothier, B.E., 1985. A comparison of three field methods for measuring saturated hydraulic conductivity. Canadian journal of soil science 65, 563–573.

Lewis, T.E., Blasdell, B., Blume, L.J., 1990. Collection of Intact Cores from a Rocky Desert and a Glacial Till Soil. Soil Sci. Soc. Am. J. 54, 938–940. https://doi.org/10.2136/sssaj1990.03615995005400030057x

Mendoza, G., Steenhuis, T.S., 2002. Determination of hydraulic behavior of hillsides with a hillslope infiltrometer. Soil Science Society of America Journal 66, 1501–1504.

Merva, G.E., 1979. Falling head permeameter for field investigation of hydraulic conductivity. American Society of Agricultural Engineers.

Montgomery, D.R., Dietrich, W.E., 1995. Hydrologic Processes in a Low-Gradient Source Area. Water Resour. Res. 31, 1–10. https://doi.org/10.1029/94WR02270

Mubarak, I., Mailhol, J.C., Angulo-Jaramillo, R., Ruelle, P., Boivin, P., Khaledian, M., 2009. Temporal variability in soil hydraulic properties under drip irrigation. Geoderma 150, 158–165. https://doi.org/10.1016/j.geoderma.2009.01.022

Muller, R.N., Hamilton, M.E., 1992. A simple, effective method for determining the bulk density of stony soils. Communications in Soil Science and Plant Analysis 23, 313–319. https://doi.org/10.1080/00103629209368590

Niedda, M., Pirastru, M., 2013. Hydrological processes of a closed catchment-lake system in a semi-arid Mediterranean environment. Hydrol. Process. 27, 3617–3626. https://doi.org/10.1002/hyp.9478

Niedda, M., Pirastru, M., Castellini, M., Giadrossich, F., 2014. Simulating the hydrological response of a closed catchment-lake system to recent climate and land-use changes in semi-arid Mediterranean environment. Journal of Hydrology 517, 732–745. https://doi.org/10.1016/j.jhydrol.2014.06.008

Pachepsky, Y., Hill, R.L., 2017. Scale and scaling in soils. Geoderma, Structure and function of soil and soil cover in a changing world: characterization and scaling 287, 4–30. https://doi.org/10.1016/j.geoderma.2016.08.017

Pachepsky, Y.A., Guber, A.K., Yakirevich, A.M., McKee, L., Cady, R.E., Nicholson, T.J., 2014. Scaling and Pedotransfer in Numerical Simulations of Flow and Transport in Soils. Vadose Zone Journal 13. https://doi.org/10.2136/vzj2014.02.0020

Pirastru, M., Marrosu, R., Di Prima, S., Keesstra, S., Giadrossich, F., Niedda, M., 2017. Lateral Saturated Hydraulic Conductivity of Soil Horizons Evaluated in Large-Volume Soil Monoliths. Water 9, 862. https://doi.org/10.3390/w9110862

Pirastru, M., Niedda, M., Castellini, M., 2014. Effects of maquis clearing on the properties of the soil and on the near-surface hydrological processes in a semi-arid Mediterranean environment. Journal of Agricultural Engineering 45, 176. https://doi.org/10.4081/jae.2014.428

Prédélus, D., Lassabatere, L., Louis, C., Gehan, H., Brichart, T., Winiarski, T., Angulo-Jaramillo, R., 2017. Nanoparticle transport in water-unsaturated porous media: effects of solution ionic strength and flow rate. J Nanopart Res 19, 104. https://doi.org/10.1007/s11051-017-3755-4

Regan, M.P., 2000. Perched water table dynamics and hydrologic processes in an eastern Palouse catchment (M.S. thesis). University of Idaho, Moscow.

Reynolds, W., Elrick, D., Youngs, E., 2002. 3.4.3.2.a. Single-ring and double- or concentric-ring infiltrometers. Methods of Soil Analysis, Part 4, Physical Methods, J.H. Dane and G.C. Topp co-editors, Number 5 in the Soil Science Society of America Book Series, Soil Science Society of America, Inc. Madison, Wisconsin, USA, pp. 821-826.

Reynolds, W.D., 1993. Saturated hydraulic conductivity: Field measurement. M.R. Carter, editor, Soil sampling and methods of analysis. Canadian Society of Soil Science, Lewis Publishers, Boca Raton, FL. 599–613.

Reynolds, W.D., Elrick, D.E., 2005. Chapter 6 Measurement and characterization of soil hydraulic properties. In J. Álvarez-Benedí, & R. Muñoz-Carpena (Co-Eds.), Soil-water-solute process characterization – An integrated approach. Boca Raton: CRC Press.

Scanlon, B.R., Keese, K.E., Flint, A.L., Flint, L.E., Gaye, C.B., Edmunds, W.M., Simmers, I., 2006. Global synthesis of groundwater recharge in semiarid and arid regions. Hydrological Processes 20, 3335–3370. https://doi.org/10.1002/hyp.6335

Shirazi, M.A., Boersma, L., 1984. A unifying quantitative analysis of soil texture. Soil Science Society of America Journal 48, 142–147.

Soil Survey Staff, 2006. Keys to Soil Taxonomy, 10th ed. NRCS, Washington, DC.

Starr, J.L., Sadeghi, A.M., Pachepsky, Y.A., 2005. Monitoring and Modeling Lateral Transport through a Large In Situ Chamber. Soil Science Society of America Journal 69, 1871–1880. https://doi.org/10.2136/sssaj2004.0162

Sukhija, B.S., Reddy, D.V., Nagabhushanam, P., Hussain, S., 2003. Recharge processes: piston flow vs preferential flow in semi-arid aquifers of India. Hydrogeology Journal 11, 387–395. https://doi.org/10.1007/s10040-002-0243-3

Šimůnek, J., Jarvis, N.J., van Genuchten, M.T., Gärdenäs, A., 2003. Review and comparison of models for describing non-equilibrium and preferential flow and transport in the vadose zone. J. Hydrol. 272, 14–35. https://doi.org/10.1016/S0022-1694(02)00252-4

Vepraskas, M.J., Williams, J.P., 1995. Hydraulic conductivity of saprolite as a function of sample dimensions and measurement technique. Soil Science Society of America Journal 59, 975–981.

Vörösmarty, C.J., Green, P., Salisbury, J., Lammers, R.B., 2000. Global Water Resources: Vulnerability from Climate Change and Population Growth. Science 289, 284–288. https://doi.org/10.1126/science.289.5477.284

Warrick, A.W., 1998. Spatial variability. In: Hillel, D. (Ed.), Environmental Soil Physics. Academic Press, San Diego, CA, pp. 655–675.

Yilmaz, D., Lassabatere, L., Angulo-Jaramillo, R., Deneele, D., Legret, M., 2010. Hydrodynamic Characterization of Basic Oxygen Furnace Slag through an Adapted BEST Method. Vadose Zone Journal 9, 107. https://doi.org/10.2136/vzj2009.0039

Young, S.K., 1998. Soil hydrology in an eastern Palouse micro-catchment underlain by a fragipan (M.S. thesis). University of Idaho, Moscow.

Zaslavsky, D., Rogowski, A.S., 1969. Hydrologic and Morphologic Implications of Anisotropy and Infiltration in Soil Profile Development. Soil Science Society of America Journal 33, 594–599. https://doi.org/10.2136/sssaj1969.03615995003300040031x

Zimmermann, A., Schinn, D.S., Francke, T., Elsenbeer, H., Zimmermann, B., 2013. Uncovering patterns of near-surface saturated hydraulic conductivity in an overland flow-controlled landscape. Geoderma 195–196, 1–11. https://doi.org/10.1016/j.geoderma.2012.11.002

Zobeck, T.M., Fausey, N.R., Al-Hamdan, N.S., 1985. Effect of Sample Cross-Sectional Area on Saturated Hydraulic Conductivity in Tow Structured Clay Soils. Transactions of the ASAE 28, 791–794. https://doi.org/10.13031/2013.32339

CHAPTER 4

Dependency of lateral saturated soil hydraulic conductivity from the investigation spatial scale

1. Introduction

The chapter addresses the evaluation of the scale dependency relationship of the lateral saturated soil hydraulic conductivity, $K_{s,l}$, which was the main objective of the thesis. This was carried out by comparing the $K_{s,l}$ values obtained by means of all measurement techniques applied in the field and in laboratory, each of them involving a different soil sampled volume. Only the measurements performed in the hillslope part covered with permanent grass were considered, because the most exhaustive hydraulic characterization was available for this area. The results of each measurement technique have already been presented and discussed separately in the previous chapters of the thesis. Herein, all the $K_{s,l}$ data are considered together, in order to detect how the $K_{s,l}$ values changed depending on the dimension of the sampled soil.

The scale dependency of the $K_{s,l}$ was analysed in relation to the soil horizons of the hillslope, i.e., the A horizon (0–15 cm), the upper layer of the B horizon (afterward indicated by B1, ranging from 15 to 25 cm of depth), and the lower layer of the B horizon (hereinafter called B2, from 25 cm to the depth of the restrictive layer).

The following four decreasing observation scales were considered: hillslope scale, sprinkling-parcel scale, plot scale, i.e., determinations on the large-volume soil monolith, and near-point scale. For the latter scale, the laboratory measurements on the small soil cubes by using the modified cube method (Bagarello et al., 2009; Bagarello and Sgroi, 2008; Beckwith et al., 2003) were considered for the A horizon, whereas the Beerkan measurements in the field (Lassabatère et al., 2006) were applied to characterize B1 and B2 soil layers. Although Beerkan experiments mainly allow to explore a vertical direction of water flow rather than the lateral (or sub-horizontal) one, scientific literature reported some examples of hydrological modelling application of lateral subsurface flow that used similar approaches (e.g., constant-head or falling-head methods). Hence, the possibility of obtaining reliable estimates of the lateral saturated hydraulic conductivity through the routinely use and not expensive Beerkan method was tested.

2. Methods

The values of $K_{s,l}$ at the hillslope scale for the A, B1 and B2 horizons were estimated by applying Equation 3 presented in Chapter 2 of the thesis. To determine the hydraulic conductivity value to be inserted in Equation 3 with reference to the depth of 15 or 25 cm, the exponential $K_{s,l}(WTD)$ function (see Figure 1.6a of Chapter 1) was used with these prescribed soil depths. Regarding the $K_{s,l}$ of competence of 5 cm WTD, a hypothesized value had to be used, because this water table depth was not reached during the periods of natural rainfall. Thus, a $K_{s,l}$ equal to 3200 mm h^{-1} was inserted, which was the value found during the stationary phase of the sprinkling experiments in the grass area (see the results of the sprinkling experiments in the *Results* section of Chapter 1). In this case, it was hypothesized that the hydraulic conductivity close to the soil surface did not increase exponentially, but it stabilized as indicated by the applied rainfall experiments in field (see *Discussion* section in Chapter 1).

The values of $K_{s,l}$ at the sprinkling-parcel scale for the considered soil horizons were also estimated by Equation 3 of Chapter 2. With reference to the depth of 15 or 25 cm, the hydraulic conductivities to be inserted into Equation 3 were computed with the exponential $K_{s,l}(WTD)$ function shown in Figure 1.8d (continuous line) of Chapter 1. For the WTD of 5 cm, a $K_{s,l}$ value of 3200 mm h^{-1} was used for computing the $K_{s,l}$ specifically for the A horizon.

The values of $K_{s,l}$ of the soil horizons A, B1 and B2 estimated in MA, MB, MC and MD soil monolith are shown in Figure 2.4 of Chapter 2. The median of these values was considered indicative for the $K_{s,l}$ at plot spatial scale. However, concerning the B2 horizon, the 2750 mm h^{-1} $K_{s,l}$ value detected close to the restrictive layer in the MB monolith, was not considered when calculating the median. In fact, this very high value appeared clearly to be an outlier, when compared to the remaining $K_{s,l}$ values determined in the other monoliths; it was also in contrast with the perceptual model gained during the multiannual monitoring period about the hydrological processes occurring in the lower part of hillslope soil.

Finally, in the A horizon, the representative $K_{s,l}$ at the near-point scale was the median of $K_{s,l}$ values measured in laboratory through the modify cube method, but considering only the ten cubic samples on which the hydraulic conductivity was measured through the uphill-downhill direction (see Table 3.3 of Chapter 3). For the B1 and B2 soil layers, the

median values of the $K_{s,l}$ estimated by the Beerkan method at the soil depths of 10 cm and 20 cm, respectively, were considered (see Table 3.2 of Chapter 3).

3. Results

The values of $K_{s,l}$ determined for the soil horizons A, B1 and B2 at the different spatial scales under study are listed in Table 4.1. The $K_{s,l}$ estimated for both the hillslope and sprinkling-parcel spatial scales decreased by around 80% passing from A horizon to B1. For the same scales, a reduction by approximately one order of magnitude was detected when going from B1 to B2 layer, which overlaid the restrictive layer. At the plot scale (soil monoliths) an average decrease in hydraulic conductivity by 80% occurred passing from A to B1 layer. Hence, this decrease was in line with that determined for the larger spatial scales. However, in the passage from B1 to B2 layer, plot scale lateral hydraulic conductivity decreased by around 75%, which was less than the reduction observed at the larger hillslope and sprinkling-parcel spatial scales.

Table 4.1. Median values of lateral saturated soil hydraulic conductivity, $K_{s,l}$, determined for different spatial scales of investigation for the A soil horizon, and for the upper (B1) and lower part (B2) of B horizon.

Spatial scale of investigation	Characteristic Length (m)	$K_{s,l}$ (mm h^{-1})		
		A	B1	B2
Hillslope	50	8000	1486	180
Sprinkling-parcel	12	8312	1178	114
Small Plot (soil monoliths)	0.76	2450	490	130
Near-point (small cubic samples)	0.11	174	—	—
Near-point (Beerkan)	0.05	—	6.7	4

Noticeable variations in $K_{s,l}$ values for A and B1 soil horizons can be detected when going from the two largest to the two smallest spatial scales (Table 4.1). In those horizons, the median $K_{s,l}$ values determined at hillslope scale and sprinkling-parcel scale were comparable. Differently, the median $K_{s,l}$ values decreased by about 70% when passing from these large scales to the plot scale. A greater reduction in hydraulic conductivities, by roughly one order of magnitude, could be observed in the passage from plot to the near-point spatial scale. For the A horizon, this result was even more striking if we consider that the soil cubes were carved out at a depth from 0 to 0.1 m, thus embodying the permeable topsoil layer, which was only partially explored through the larger scales of investigation. In the B2 soil layer, a

substantial independence of $K_{s,l}$ from the scale of measuring was detected going from the hillslope to the sprinkling-parcel scale. However, in contrast to what observed in the A and B1 soil horizons, the $K_{s,l}$ value determined in the B2 layer at the plot scale was in line with that obtained for the larger spatial scale. Finally, the $K_{s,l}$ values estimated at the near-point scale with the Beerkan method in that layer were about one order of magnitude lower than that obtained with the plot scale.

The $K_{s,l}$ scale dependency can be seen also in Figure 4.1. In Figures 4.1a–4.1c are plotted, for each investigated soil layer (A, B1, B2, respectively), the median $K_{s,l}$ values against the characteristic lengths of the sampled soil, which quantitatively define the scale of measurements. The characteristic size was taken in agreement with the investigated dominant direction of flow, i.e., the lateral or sub-horizontal one, as suggested by Pachepsky et al. (2014). Hence, the lengths of 50, 12 and 0.78 m, i.e., the sizes of the sampled soil computed in the steepest uphill-downhill directions, were considered for the hillslope, sprinkling-parcel and plot spatial scales, respectively (Table 4.1). For the near-point spatial scale in the A horizon, the size of the cube side was the characteristic length. Regarding the Beerkan experiments, because a characteristic length could not be detected with certainty, a size of 0.05 m was used. This is a commonly reported value for the constant-head and falling-head field measurements (Pachepsky et al., 2014). Figure 4.1 shows that the greatest gain of information about a representative $K_{s,l}$ value at the hillslope scale, which is the most interesting for many hydrological applications (such as for modelling purposes), can be obtained by investigating the characteristic soil length of around one meter. In other words, through drainage experiments in the soil monoliths, it was possible to identify, with a relatively acceptable approximation for various practical applications, the "true" $K_{s,l}$ value at hillslope scale. In line with Schulze-Makuch et al. (1999), the relationships between the $K_{s,l}$ values and the characteristic lengths were satisfactory modelled by means of power curves (Figures 4.1a–4.1c). The exponents of these functions, ranging from about 0.5 to 0.75, also were in agreement with Schulze-Makuch et al. (1999).

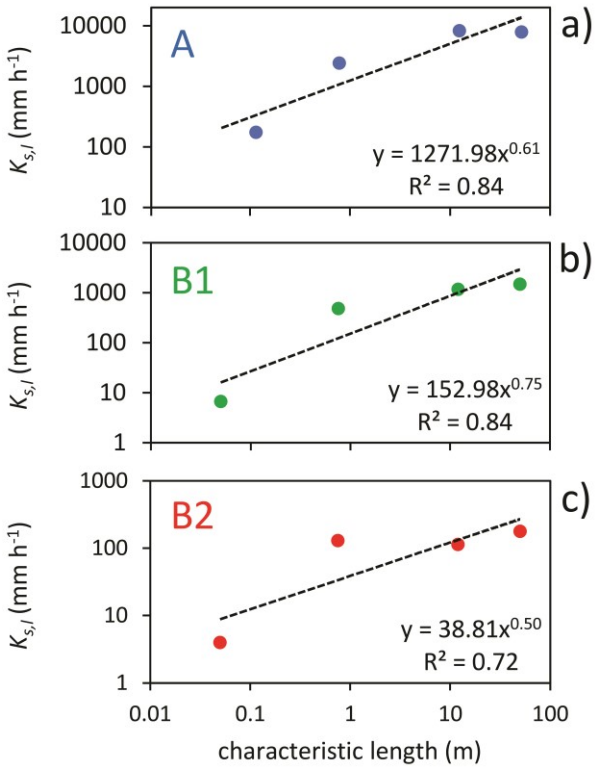

Fig. 4.1. Relationships between the investigated soil characteristic lengths and the median $K_{s,l}$ values for the A, B1 and B2 layers.

4. Discussion

This study showed that the lateral saturated hydraulic conductivity of the soil can vary depending on the size of soil sampled by the different measurement methods. For all the considered soil horizons, the hillslope scale $K_{s,l}$ values, which were taken as benchmark because they are probably the most interesting values for practical applications, were well identified by the drainage experiment with artificially applied rainfall performed in a share of the hillslope (about 25%; see subsection *Sprinkling experiment* in the *Material and Methods* section in Chapter 1). Generally, the plot scale values determined by drainage experiments in the large volume soil monoliths underestimated the $K_{s,l}$ at the hillslope scale. However, the discrepancies found in relation to the values determined at the largest spatial scale can be considered acceptable, considering that the hydraulic conductivity usually exhibits an inherent variability, also of orders of magnitude, over the space (Warrick, 1998). As a consequence, it can be asserted that the experiments performed in the large volume soil monoliths represented

the best compromise between the costs of the experimentation and the representativeness of the obtained $K_{s,l}$ values. Plausibly, in the investigation at the plot scale a sufficient number of macropores were included in the sampled soil volume, leading to adequately characterizing the hydrological behaviour of porous medium also for a greater spatial scale. Moreover, the exploited volume allowed to effectively account for the macropore networks interconnectedness that generally develops over a spatial scale of meters or tens of meters. The scale length at which macropores become fully effective depends on their hydraulic connectivity over a distance of flow path (Anderson et al., 2008; Sidle et al., 2001; van Schaik et al., 2008), a concept which implies that macropores are not necessarily physically continuous over that distance; but rather the connectivity results from a network of macropores embedded in a highly permeable soil matrix. Sidle et al. (2001), in fact, demonstrated that although individual macropores were generally less than 0.5 m in length, they had a tendency to self-organise into a larger preferential flow system whose hydraulic connection expanded upslope as the wetness of the soil matrix increased. Therefore, the minimum size of the sampled soil should be in agreement with the characteristic length of the connectivity process. Brooks et al. (2004) stated that, ideally, the method of investigation of the $K_{s,l}$ should be conducted on a volume comparable to the basic element considered in numerical simulation exercises (i.e., the grid cell dimension) or, at least, on an intermediate size that incorporates the inherent heterogeneities in hillslope soils. At the studied hillslope, plausibly this intermediate size could be close to the size of the investigated soil monoliths.

Concerning the $K_{s,l}$ estimations performed at the smallest spatial scale under study, in all cases the near-point measurements seriously underestimated the hillslope scale values. Sampling a small soil volume as in the modified cube method or using small rings for the in situ Beerkan ponding experiments leaded to a relatively little possibility of including soil macropores, whose spatial disposition in field was not known a priori, in the measures. Consequently, the small $K_{s,l}$ values obtained were considered representative only for the soil matrix. This finding agrees with the results of Brooks et al. (2004), who showed that hillslope-scale estimation of $K_{s,l}$ was 3.2 to 13.7 times greater than the available small-scale measurements from constant and falling head methods as well as from Guelph permeameter gauge. Similarly, Chappell and Lancaster (2007), by applying controlled trench tests and slug tests in piezometers placed close to the trenches, determined large-scale $K_{s,l}$ values on average

37 times larger than the near-point measurements. Finally, Montgomery and Dietrich (1995) estimated the large scale $K_{s,l}$ based on the discharge from a gully cut that showed evidence of macropore flow. Their determinations were comparable with the greatest conductivity obtained by falling-head tests in piezometers.

The detected dependency of the $K_{s,l}$ on the spatial scale under investigation was satisfactorily represented by a power function, implying that $K_{s,l}$ values roughly representative for the hillslope scale can be obtained by sampling in the field soil lengths similar to that of the soil monolith. By investigating larger soil samples, such as in the sprinkling experiment in our case, a small increase in information about the hydraulic conductivity should be expected, despite an increase in experimental costs. The trend in the $K_{s,l}$ scale dependency found in our study was consistent with that reported by Pachepsky et al. (2014). These authors reviewed saturated hydraulic conductivity data reported in literature, for the most part obtained by: i) constant-head or falling-head techniques on support with different size, ii) ponding infiltration experiments by rings with different radius, or iii) measurements through different infiltrometer devices conducted in situ or in laboratory. These authors reported $K_{s,l}$ values that initially increased, by orders of magnitude, with the spatial scale of measurement, until a characteristic size of the investigated support (which they calculated as the radius of the circular area of water application) was reached, beyond which the hydraulic conductivity remained almost constant. Schulze-Makuch et al. (1999) also analysed the relationship between the saturated hydraulic conductivity and the scale of measurement for soil and geologic media (fractured rocks and unconsolidated sediments). Similarly to the findings of the present study on the investigated hillslope soil, these authors showed that the saturated hydraulic conductivity in heterogeneous porous media increased proportionally with the scale of measurement (the volume of the material was used as characteristic size of the spatial scale). Moreover, Schulze-Makuch et al. (1999) also reported that beyond certain values of the characteristic size of the support, which substantially depended on the porous medium type, the hydraulic conductivity did not increase as well.

5. Conclusions of the doctoral thesis

The thesis focused on the lateral saturated hydraulic conductivity of the soil in a hillslope in the semiarid Mediterranean environment. This soil hydraulic property was estimated both in field and in laboratory with reference to spatial scales ranging from the hillslope scale to the near-point spatial scale. Since the knowledge of reliable values, representative for the hillslope scale, is fundamental for the most part of the distributed hydrological modelling application, in this study many efforts were addressed to refine methods to characterize the lateral subsurface flow and the saturated hydraulic conductivity in sampled soil with volumes as large as possible. There was an expected, but not so obvious, proportionality between the exploited soil volume and the experimental efforts. In fact, the experiments based on drainage measurements at the toe of the hillslope are expensive, mainly in terms of field work, and difficult to repeat in many other hillslopes. However, such methodological approach is thought to yield the most reliable values of the lateral saturated soil hydraulic conductivity at the hillslope scale, because the measured drain outflow integrates the heterogeneous hydrological response of the soil in the hillslope, mostly governed by the macropore flow. Although plausible hydraulic conductivity values were obtained, some limitations of this study came from the relatively shortness of the drain. Currently, a new 8.5 m long drain is working in the same hillslope, which is expected to give even more representative values of saturated hydraulic conductivity at the hillslope scale.

The drainage experiments performed in the field on the large volume soil monoliths were probably the best compromise between method expensiveness and representativeness of the resulting values of hydraulic conductivity for the hillslope scale. In fact, thanks to the high soil volume exploited in each soil block, it was possible to obtain, with a relatively low number of runs, values of soil lateral saturated hydraulic conductivity in acceptable correspondence with the values found at the hillslope scale. Even though the method used was not a novelty in scientific research, modifications and simplifications were introduced to the original experimental setup, thus increasing the method usability for routine investigations of the hydraulic conductivity in hillslopes.

Among all methodologies tested, the modified cube and the Beerkan methods used for characterizing the soil hydraulic conductivity at the near-point scale had the lowest

experimental cost. Obviously, this was an advantage, because it allowed the greatest number of replications over the space. However, the hydraulic conductivity values, determined at the near-point scale by these two methods were far from the value identified at the hillslope scale. The study proposed a scale relationship of power-law type that functionally links the values of the lateral saturated hydraulic conductivity to the spatial scale of investigation. These functions could be used for upscaling the near-point scale soil hydraulic conductivity values in order to estimate, with good approximation, representative values also for a larger spatial scale. Such approach could be conveniently adopted also in other hillslopes or basins where near-point scale soil hydraulic conductivity values are already available or can be obtained with low-cost investigations, in order to properly parameterize models applied for large-scale hydrological and environmental studies dealing with soil and water conservation.

6. References

Anderson, A.E., Weiler, M., Alila, Y., Hudson, R.O., 2008. Dye staining and excavation of a lateral preferential flow network. Hydrology and Earth System Sciences Discussions, European Geosciences Union 5, 1043-1065.

Bagarello, V., Sferlazza, S., Sgroi, A., 2009. Testing laboratory methods to determine the anisotropy of saturated hydraulic conductivity in a sandy-loam soil. Geoderma 154, 52–58. https://doi.org/10.1016/j.geoderma.2009.09.012

Bagarello, V., Sgroi, A., 2008. Testing Soil Encasing Materials for Measuring Hydraulic Conductivity of a Sandy-Loam Soil by the Cube Methods. Soil Science Society of America Journal 72, 1048. https://doi.org/10.2136/sssaj2007.0022

Beckwith, C.W., Baird, A.J., Heathwaite, A.L., 2003. Anisotropy and depth-related heterogeneity of hydraulic conductivity in a bog peat. II: modelling the effects on groundwater flow. Hydrological Processes 17, 103–113. https://doi.org/10.1002/hyp.1117

Brooks, E.S., Boll, J., McDaniel, P.A., 2004. A hillslope-scale experiment to measure lateral saturated hydraulic conductivity. Water Resour. Res. 40, W04208. https://doi.org/10.1029/2003WR002858

Chappell, N.A., Lancaster, J.W., 2007. Comparison of methodological uncertainties within permeability measurements. Hydrological Processes 21, 2504–2514. https://doi.org/10.1002/hyp.6416

Lassabatère, L., Angulo-Jaramillo, R., Soria Ugalde, J.M., Cuenca, R., Braud, I., Haverkamp, R., 2006. Beerkan Estimation of Soil Transfer Parameters through Infiltration Experiments—BEST. Soil Science Society of America Journal 70, 521. https://doi.org/10.2136/sssaj2005.0026

Montgomery, D.R., Dietrich, W.E., 1995. Hydrologic Processes in a Low-Gradient Source Area. Water Resources Research 31, 1–10. https://doi.org/10.1029/94WR02270

Pachepsky, Y.A., Guber, A.K., Yakirevich, A.M., McKee, L., Cady, R.E., Nicholson, T.J., 2014. Scaling and Pedotransfer in Numerical Simulations of Flow and Transport in Soils. Vadose Zone Journal 13. https://doi.org/10.2136/vzj2014.02.0020

Schulze-Makuch, D., Carlson, D.A., Cherkauer, D.S., Malik, P., 1999. Scale Dependency of Hydraulic Conductivity in Heterogeneous Media. Groundwater 37, 904–919. https://doi.org/10.1111/j.1745-6584.1999.tb01190.x

Sidle, R.C., Noguchi, S., Tsuboyama, Y., Laursen, K., 2001. A conceptual model of preferential flow systems in forested hillslopes: evidence of self-organization. Hydrological Processes 15, 1675–1692. https://doi.org/10.1002/hyp.233

van Schaik, N.L.M.B., Schnabel, S., Jetten, V.G., 2008. The influence of preferential flow on hillslope hydrology in a semi-arid watershed (in the Spanish Dehesas). Hydrological Processes 22, 3844–3855. https://doi.org/10.1002/hyp.6998

Warrick, A.W., 1998. Spatial variability. In: D. Hillel, Editor. Environmental Soil Physics, San Diego: Academic Press, 655–675.